

Semiconductor detectors

Silvia Masciocchi
GSI Darmstadt and University of Heidelberg

*39th Heidelberg Physics Graduate Days, HGSFP
Heidelberg
October 10, 2017*

Semiconductor detector: basics

IONIZATION as in gas detectors

- Now in semiconductors = solid materials with crystalline structure (Si, Ge, GaAs)
- electron-hole pairs (instead of electron-ion)

+ use microchip technology: structures with few **micrometer** precision can be produced at **low cost**. Read-out electronics can be directly bonded to the detectors

+ only a **few eV** per electron-hole pair → 10 times more charge produced (wrt gas) → better energy resolution

+ high density compared to gases → need only **thin layers** (greater stopping power)

- apart from silicon, the detectors need to be cooled (cryogenics)

- crystal lattices → radiation damage

Applications

Main applications:

- γ spectroscopy with **high energy resolution**
- Energy measurement of charged particles (few MeV) and particle identification (PID) via dE/dx (multiple layers needed)
- Very **high spatial resolution** for tracking and vertexing

A few dates:

1930s – very first crystal detectors

1950s – first serious developments of particle detectors

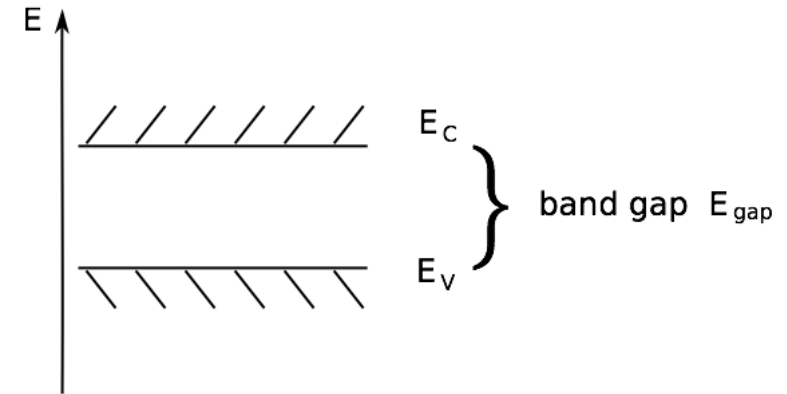
1960s – energy measurement devices in commerce

Semiconductor detectors: outline

- **Principle of operation of semiconductor detectors**
 - **Properties of semiconductors (band structure)**
 - **Intrinsic material**
 - **Extrinsic (doped) semiconductors**
 - **p-n junction**
 - **Signal generation**
- Energy measurement with semiconductor detectors
- Position measurement with semiconductor detectors
- Radiation damage

Principle of operation

- Detector operates as a solid state ionization chamber
- Charged particles create electron-hole pairs
- Place the crystal between two electrodes that set up an electric field → charge carriers drift and induce a signal
- Less than 1/3 of energy deposited goes into ionization. The rest goes into exciting lattice vibrations
- Effect: along track of primary ionizing particle plasma tube of electrons and holes with very high concentration ($10^{15} - 10^{17} \text{ cm}^{-3}$)
- Challenge: need to collect charge carriers before they recombine → very high purity semiconductor materials needed!!



D-tour: band structure of electron levels

Solid → crystalline structure of **atoms in a lattice**, with covalent bonds.

The periodic arrangement of atoms in the crystal causes an overlap of electron wave-functions, which creates a **“band” of energy states allowed** for the outermost shell energy levels.

Electrons are fermions: the Pauli principle forbids to have more than one electron in the same identical state and this produces a degeneracy in the outer atomic shell energy levels. This produces many discrete levels which are very close to each other, which appear as “bands”

The innermost energy levels are not modified, and the electrons remain associated to the respective lattice atoms.

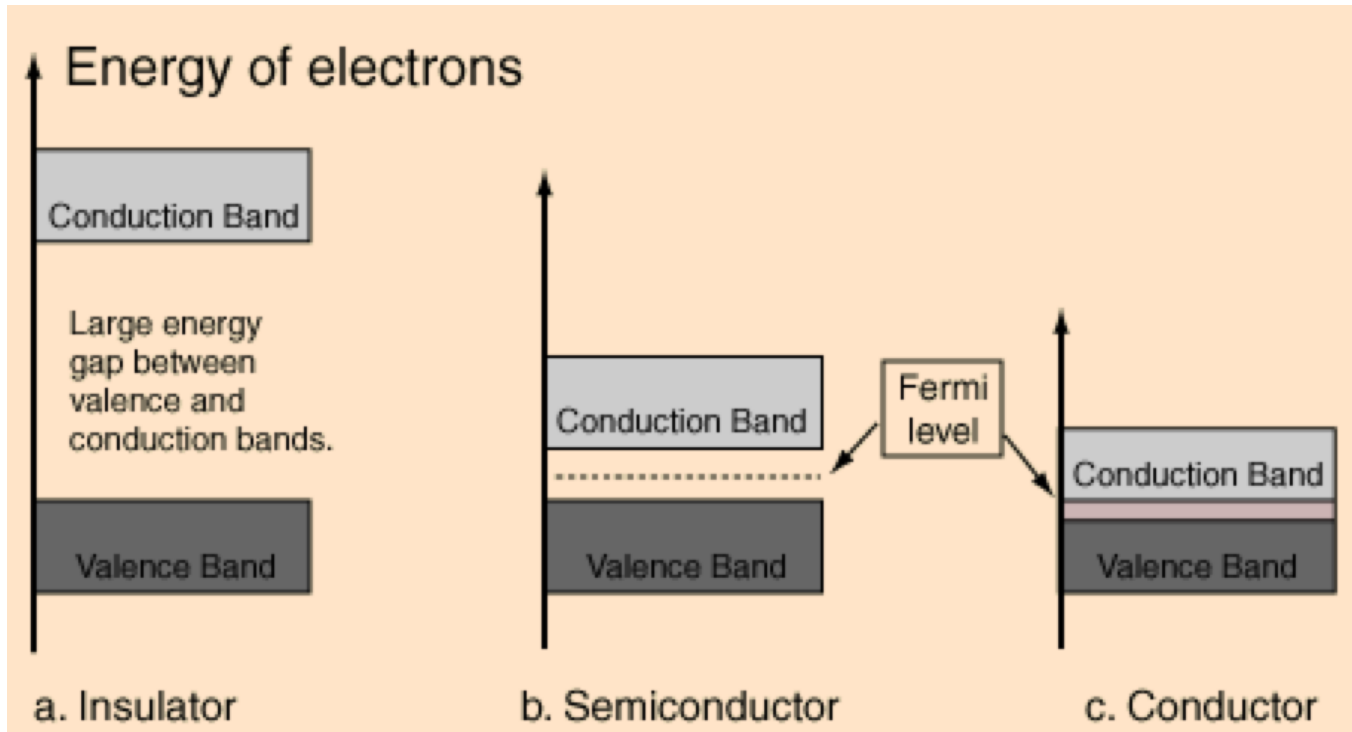
CONDUCTION BAND: electrons are detached from parent atoms and are free to roam about the whole crystal

VALENCE BAND: electrons are more tightly bound and remain associated to the respective lattice atom

FORBIDDEN BAND: in pure crystals, between the two bands above there are NO available energy levels

Band theory of solids

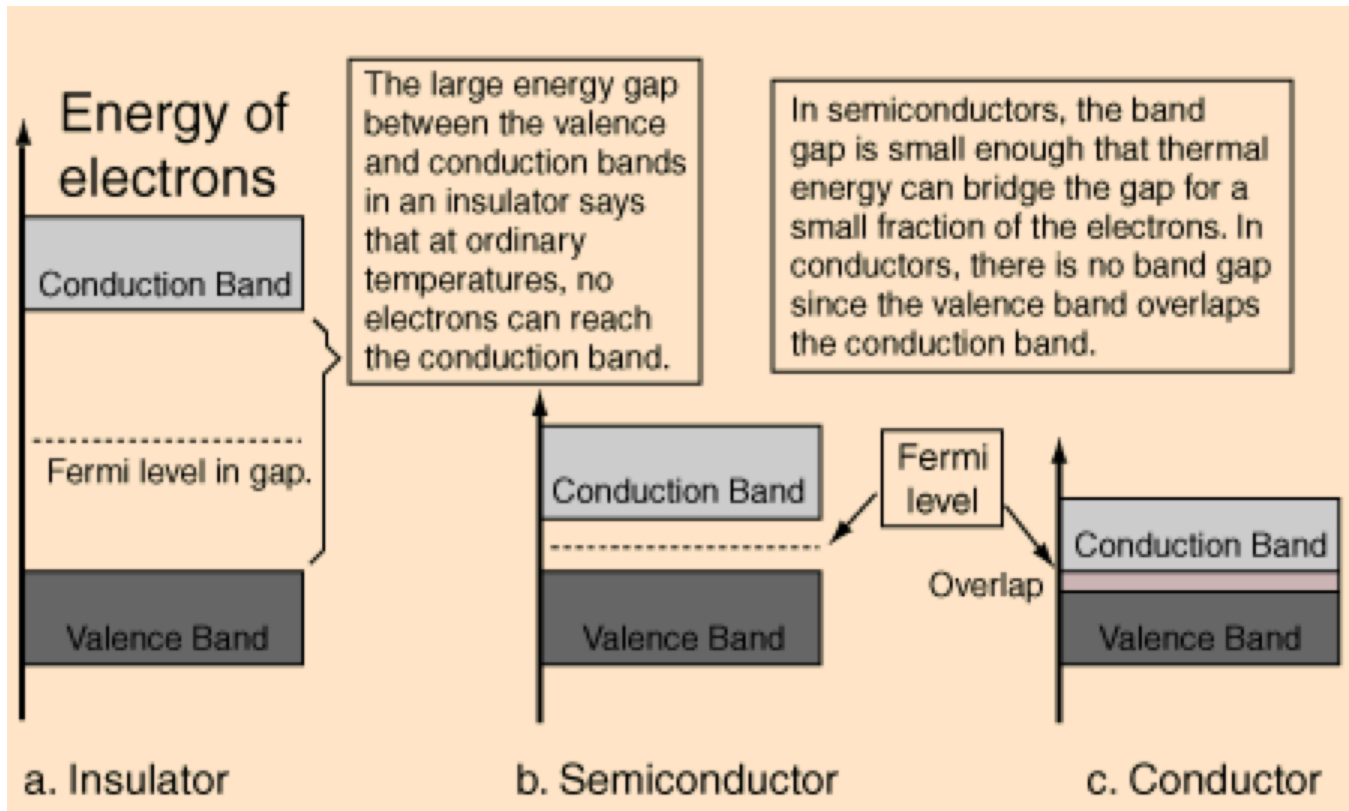
The width of the energy bands and the energy gap is determined by the **inter-atomic spacing**. This depends on **temperature and pressure**.



Bands determine the density of available energy states

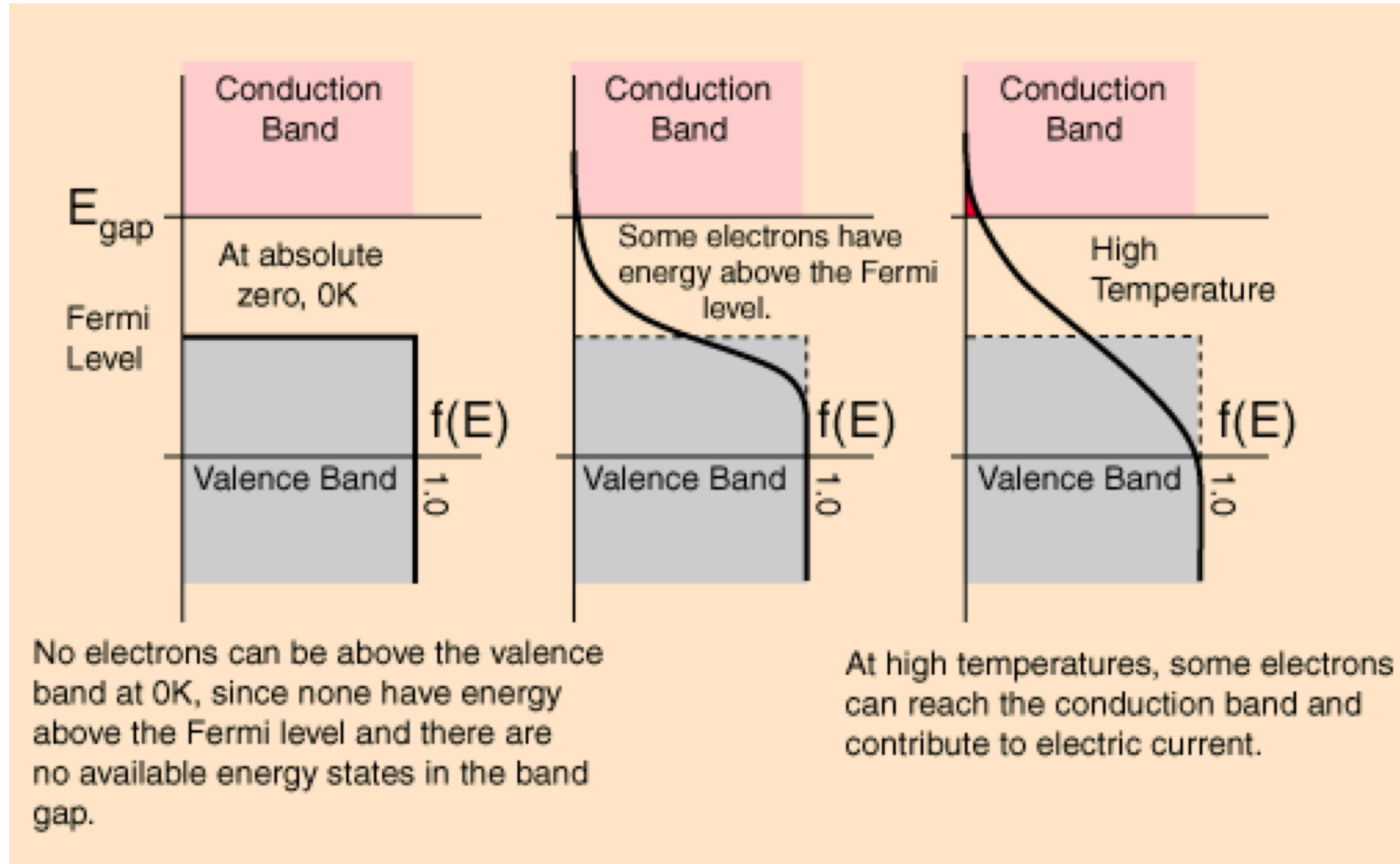
Band theory of solids

The width of the energy bands and the energy gap is determined by the inter-atomic spacing. This depends on temperature and pressure.



Bands determine the density of available energy states

Semiconductors: temperature dependence



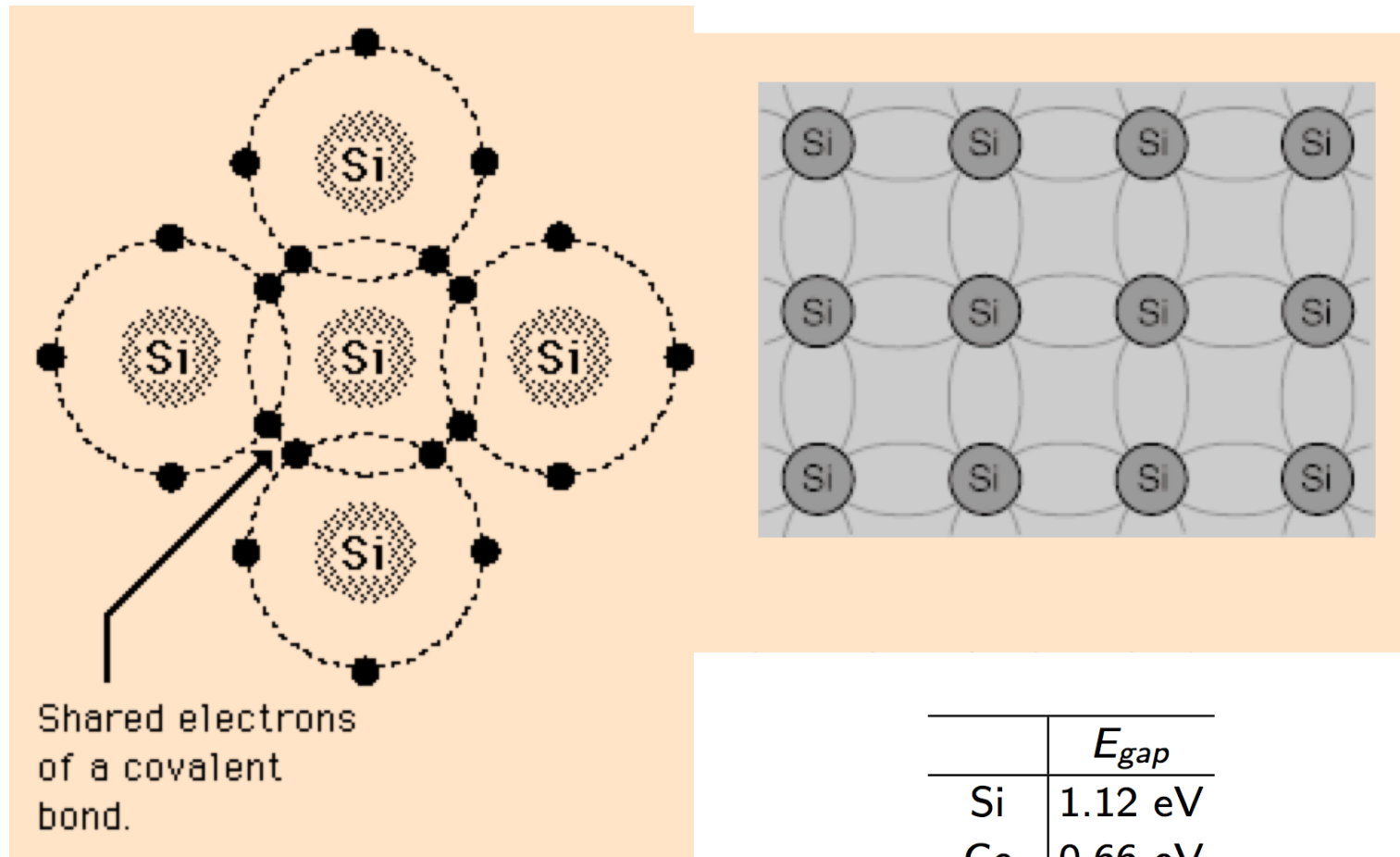
Charge carriers in semiconductors

- **Intrinsic semiconductors:** VERY PURE material, tetravalent
Charge carriers are created by thermal or optical excitation of electrons to the conduction band: $N_- = N_+$
 - Difficult to produce large volumes of so pure materials.
 - Extremely low concentrations of charge carriers

- **Extrinsic or doped semiconductors:**
Majority of charge carriers provided by impurity atoms at lattice sites of the crystal
 - Impurity atoms (pentavalent elements, donors) provide extra electrons → n-type (majority charge carriers: electrons)OR
 - Impurity atoms (trivalent elements, acceptors) have insufficient number of electrons for the covalent bonds, free hole at impurity site, provide extra holes → p-type (majority charge carriers: holes)

Intrinsic semiconductors

Crystalline lattice, of tetravalent elements (Si, Ge)
4 valence electrons → covalent bonds



Intrinsic semiconductors

At zero temperature, all electrons participate in covalent bonds.

At non-zero temperature: thermal energy can excite a valence electron into the conduction band. A hole = positive charge remains in the valence band

Under the action of an E-field: the electron can move in the conduction band. In the valence band, other electrons can fill the hole → effective movement of holes (electric current)

Intrinsic **charge carrier** concentration:

$$n_i = \sqrt{N_C N_V} \cdot \exp\left(-\frac{E_g}{2kT}\right) = A T^{3/2} \exp\left(-\frac{E_g}{2kT}\right)$$

At $T = 300 \text{ K}$, $n_i = 2.5 \times 10^{13} \text{ cm}^{-3}$ in Germanium

$n_i = 1.5 \times 10^{10} \text{ cm}^{-3}$ in Silicon

wrt $10^{22} \text{ atoms cm}^{-3}$

**VERY LOW
CONCENTRATIONS !!!**

Mobility of charge carriers

The electrical behavior is determined by the mobility of charge carriers:

- Drift velocity: $v_D = \mu E$ - μ mobility
- Specific resistance: ρ (Ωm)
- Resistance $R = \rho l / A$, with length l and area A transverse to E

As in gases: random thermal motion + drift in electric field

In intrinsic semiconductors:

- $\mu \approx \text{const.}$ for $E < 10^3$ V/cm
- $\mu \propto 1/\sqrt{E}$ for 10^3 V/cm $< E < 10^4$ V/cm
- $\mu \propto 1/E$ for $E > 10^4$ V/cm $\rightarrow v_D = \mu \cdot E$ is **CONSTANT !!**

Saturates at about 10^7 cm/ μs (similar to gases / trade off between energy acquired and collisions with the lattice here)

\rightarrow **fast collection of charges: 10 ns for 100 μm drift**

$\rightarrow v_h \approx 0.3 - 0.5 v_e$ (very different from gases!)

$I = e \cdot n_i (\mu_e + \mu_h) E = \sigma E \rightarrow$ conductivity: $\sigma = 1/\rho$ ρ : resistivity

Properties of intrinsic Si and Ge

		Si	Ge
Atomic number		14	32
Atomic weight	u	28.09	72.60
Stable isotope mass numbers		28-29-30	70-72-73-74-76
Density (300 K)	g/cm ³	2.33	5.32
Atoms/cm ³	cm ⁻³	$4.96 \cdot 10^{22}$	$4.41 \cdot 10^{22}$
Dielectric constant		12	16
Forbidden energy gap (300 K)	eV	1.115	0.665
Forbidden energy gap (0 K)	eV	1.165	0.746
Intrinsic carrier density (300 K)	cm ⁻³	$1.5 \cdot 10^{10}$	$2.4 \cdot 10^{13}$
Intrinsic resistivity (300 K)	Ωcm	$2.3 \cdot 10^5$	47
Electron mobility (300 K)	cm ² /Vs	1350	3900
Hole mobility (300 K)	cm ² /Vs	480	1900
Electron mobility (77 K)	cm ² /Vs	$2.1 \cdot 10^4$	$3.6 \cdot 10^4$
Hole mobility (77 K)	cm ² /Vs	$1.1 \cdot 10^4$	$4.2 \cdot 10^4$
Energy per electron-hole pair (300 K)	eV	3.62	
Energy per electron-hole pair (77 K)	eV	3.76	2.96

Source: G. Bertolini and A. Coche (eds.), Semiconductor Detectors, Elsevier-North Holland, Amsterdam, 1968

Recombination and trapping

Relatively rare: **direct recombination**: an electron falls from the conduction to the valence band to fill a hole → produces a photon. It is a rare process, with long lifetime (the exact energy is needed)

IMPURITIES in the crystal lattice can produce: (ALWAYS present!!)

RECOMBINATION CENTERS: additional levels in the forbidden gap can capture electrons from the conduction band, or holes from the valence band → reduction of the mean time a charge carrier remains free

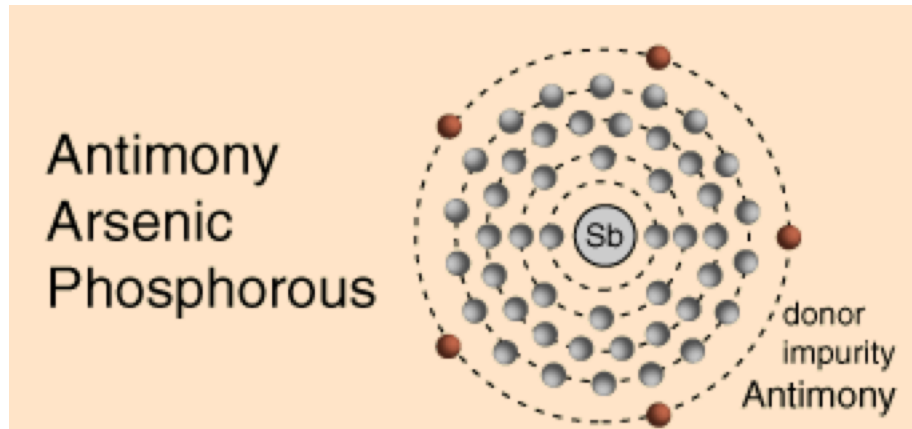
TRAPPING: of only electrons or holes, for some time

→ If the release time of the charge carriers is longer than the collection time in the detector, these processes produce a **LOSS OF CHARGE**

STRUCTURAL DEFECTS include point defects (vacancies, positions in between lattice) and dislocations (displacement of a full line of atoms). Produced during growth of crystal or by thermal shock, plastic deformation, stress and radiation damage.

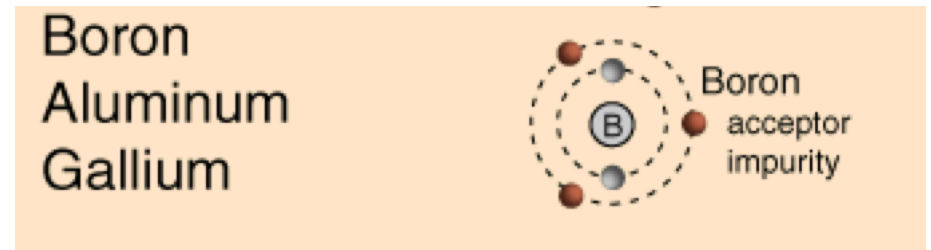
Doping of semiconductors

n-type
pentavalent impurities



Sb
As
P

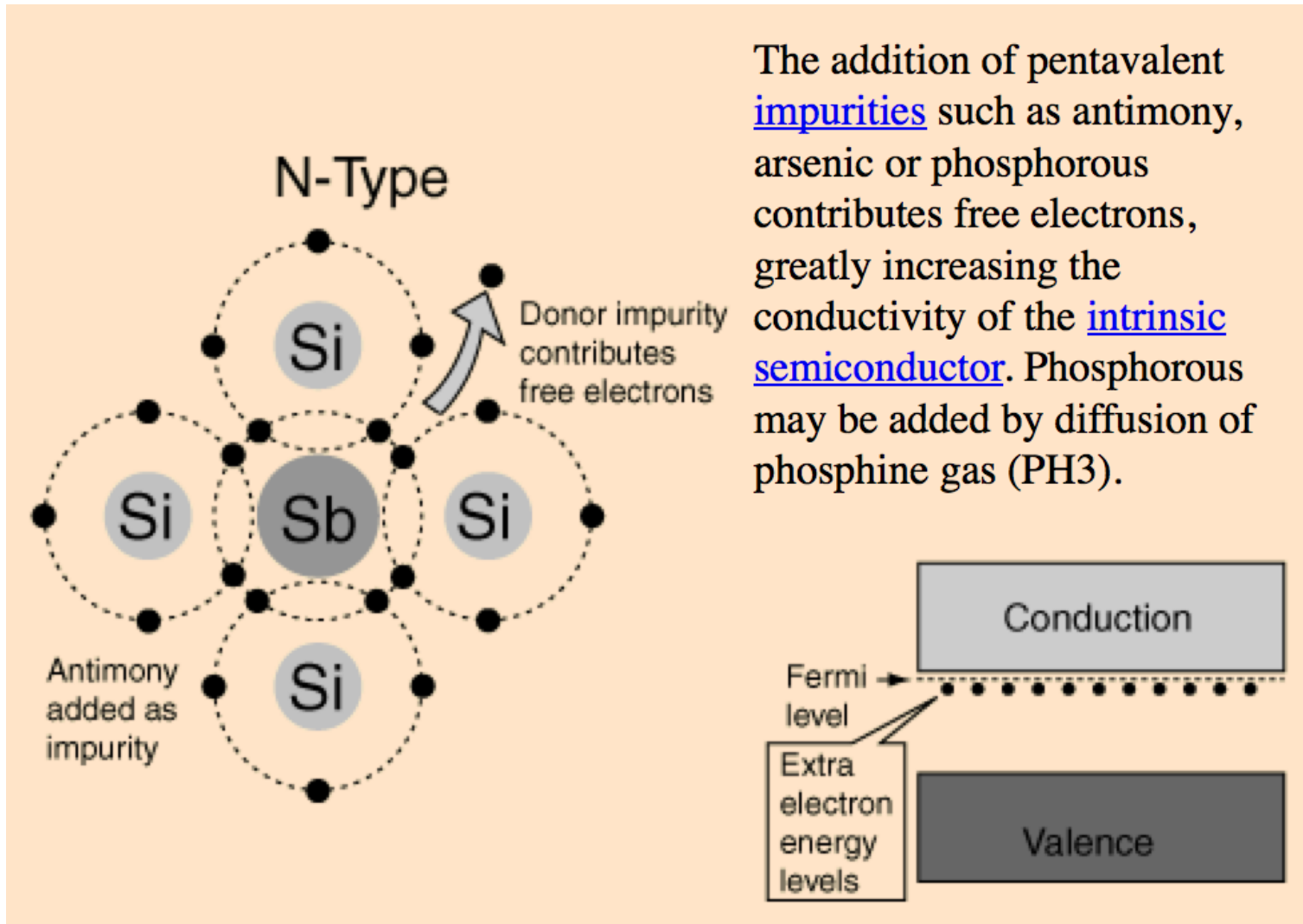
p-type
trivalent impurities



B
Al
Ga
In

Extra electrons (n) and holes (p) respectively enhance the conductivity of the material!

n-type

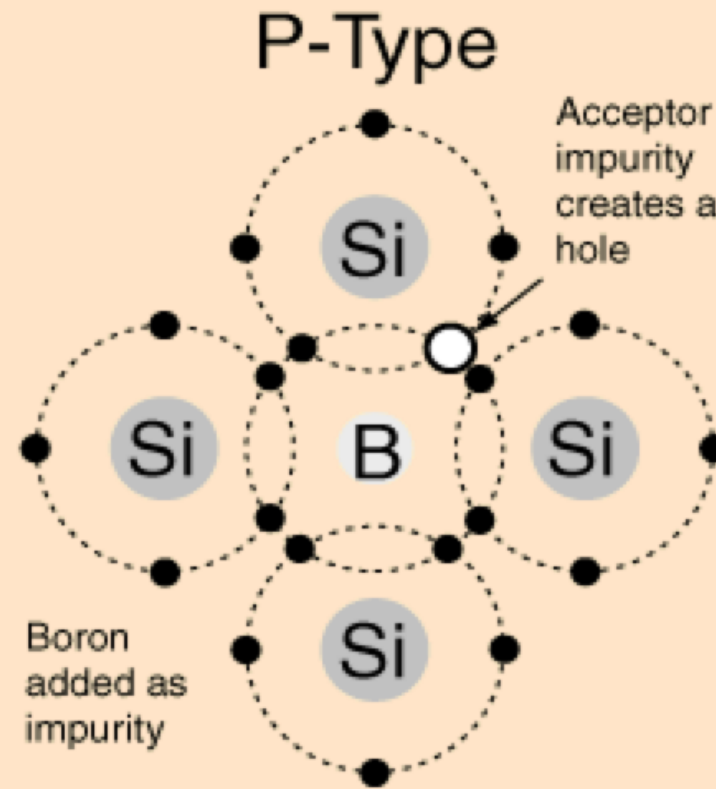
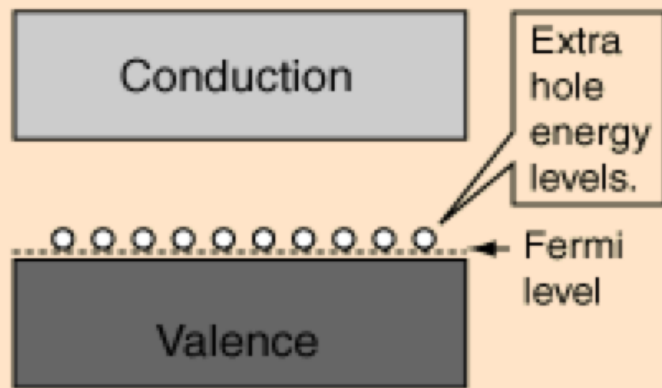


The addition of pentavalent impurities such as antimony, arsenic or phosphorous contributes free electrons, greatly increasing the conductivity of the intrinsic semiconductor. Phosphorous may be added by diffusion of phosphine gas (PH_3).

Majority charge carriers: electrons
Minority charge carriers: holes

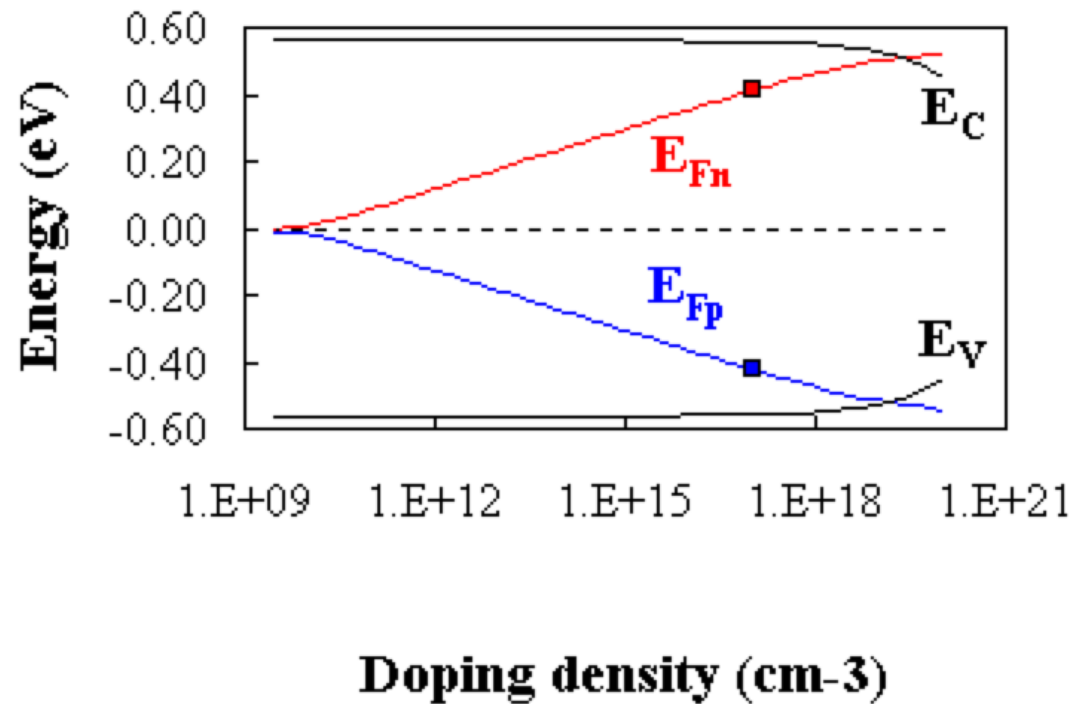
p-type

The addition of trivalent impurities such as boron, aluminum or gallium to an intrinsic semiconductor creates deficiencies of valence electrons, called "holes". It is typical to use B_2H_6 diborane gas to diffuse boron into the silicon material.



Majority charge carriers: holes
Minority charge carriers: electrons

Fermi level in doped semiconductors



fermiden.xls - fermiden.gif

Fig.2.7.1 Fermi energy of n-type and p-type silicon as a function of doping density at 300 K. Shown are the conduction and valence band edges, E_C and E_V , the intrinsic energy E_i , the Fermi energy for n-type material, E_{Fn} , and for p-type material, E_{Fp} .

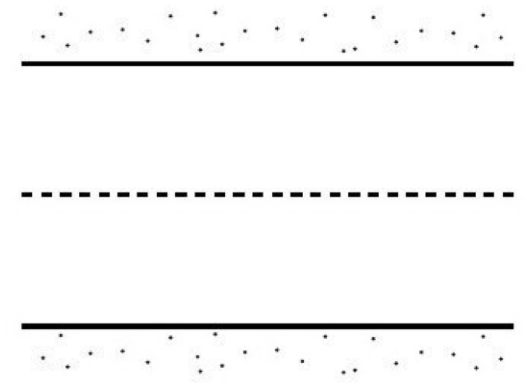
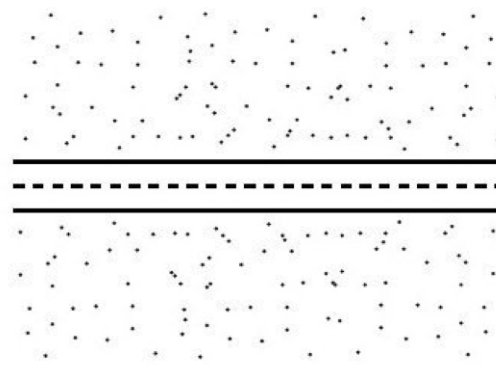
Intrinsic and extrinsic (or doped) semiconductors

Intrinsic: the smaller the band gap, the larger the number of charge carriers

$$n = \int n_- dE$$

$$p = \int n_+ dE$$

$$n = p$$



Doped semiconductors:

At $T=0 \rightarrow$ not conducting



n- doped

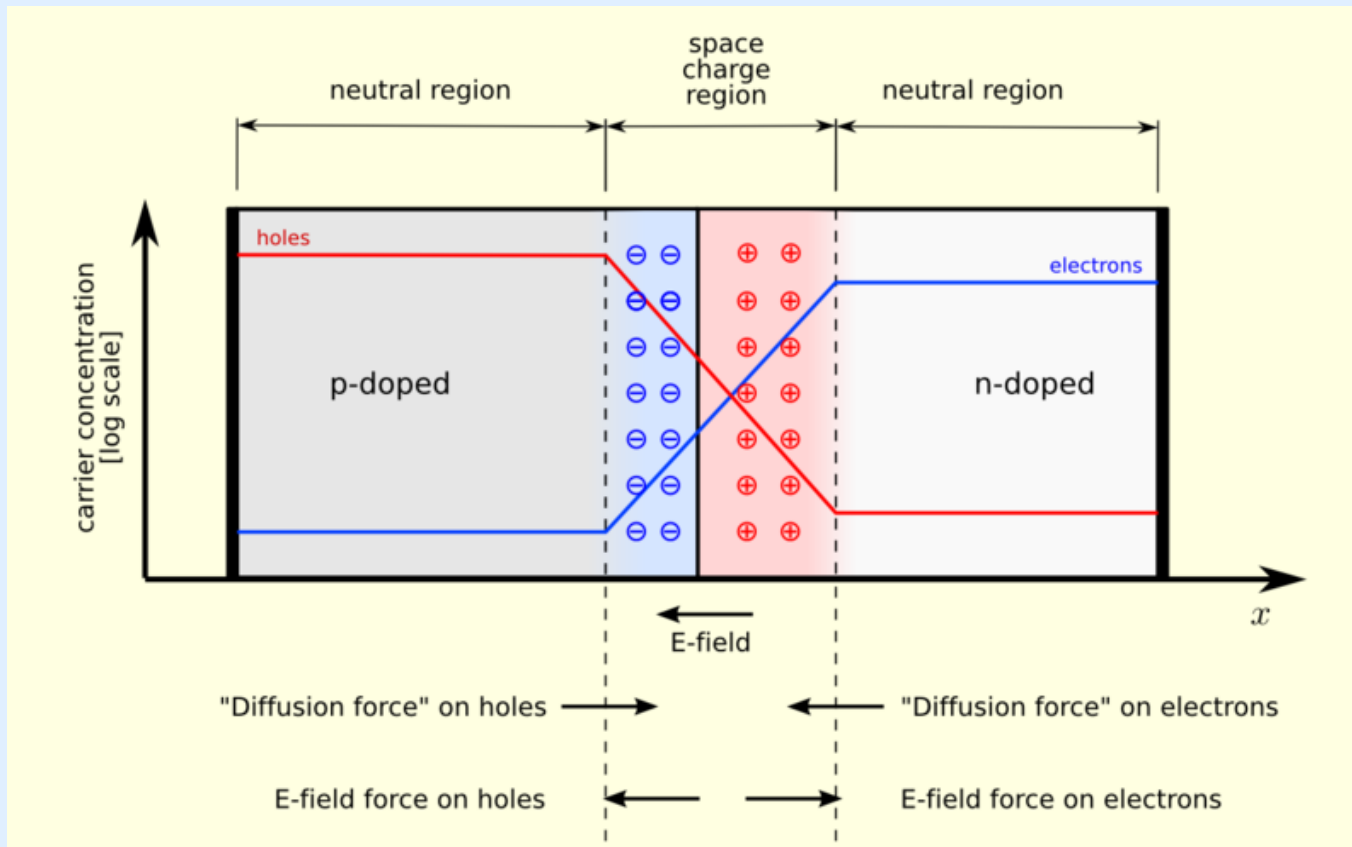
p- doped

At $T>0 \rightarrow$

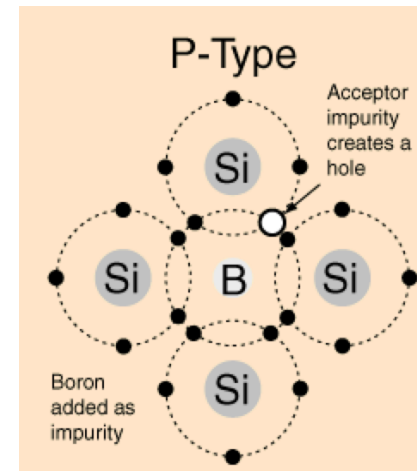
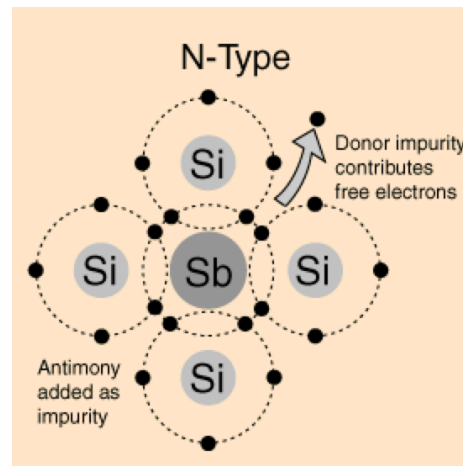
Electrons
conducting

Holes
conducting

p-n junction



- Doping is the replacement of a small number of atoms in the lattice by atoms of neighboring columns from the atomic table (with one valence electron more or less compared to the basic material – usually tetravalent, Si, Ge)
- The doping atoms create energy levels within the band gap and therefore **alter the conductivity**
- An undoped semiconductor is called an intrinsic semiconductor
- A doped semiconductor is called an extrinsic semiconductor
- In an intrinsic semiconductor, for each electron in the conduction band there is a hole in the valence band. In extrinsic semiconductors there is a surplus of electrons (n-type) or holes (p-type)



p-n junction

- Bring p and n materials “into contact” (in reality, done otherwise) → thermodynamic equilibrium
- Electrons diffuse from n to p semiconductor, and holes from p to n
- At the boundary there will be a zone with few free charge carriers (electrons and holes) → depletion layer
- Fixed charges are left behind (ionized donors and acceptors) → space charge

E-field builds up and counteracts the diffusion, which stops eventually with $n \approx N_D$ and $p \approx N_A$

- Difference between Fermi energies on both sides gives:

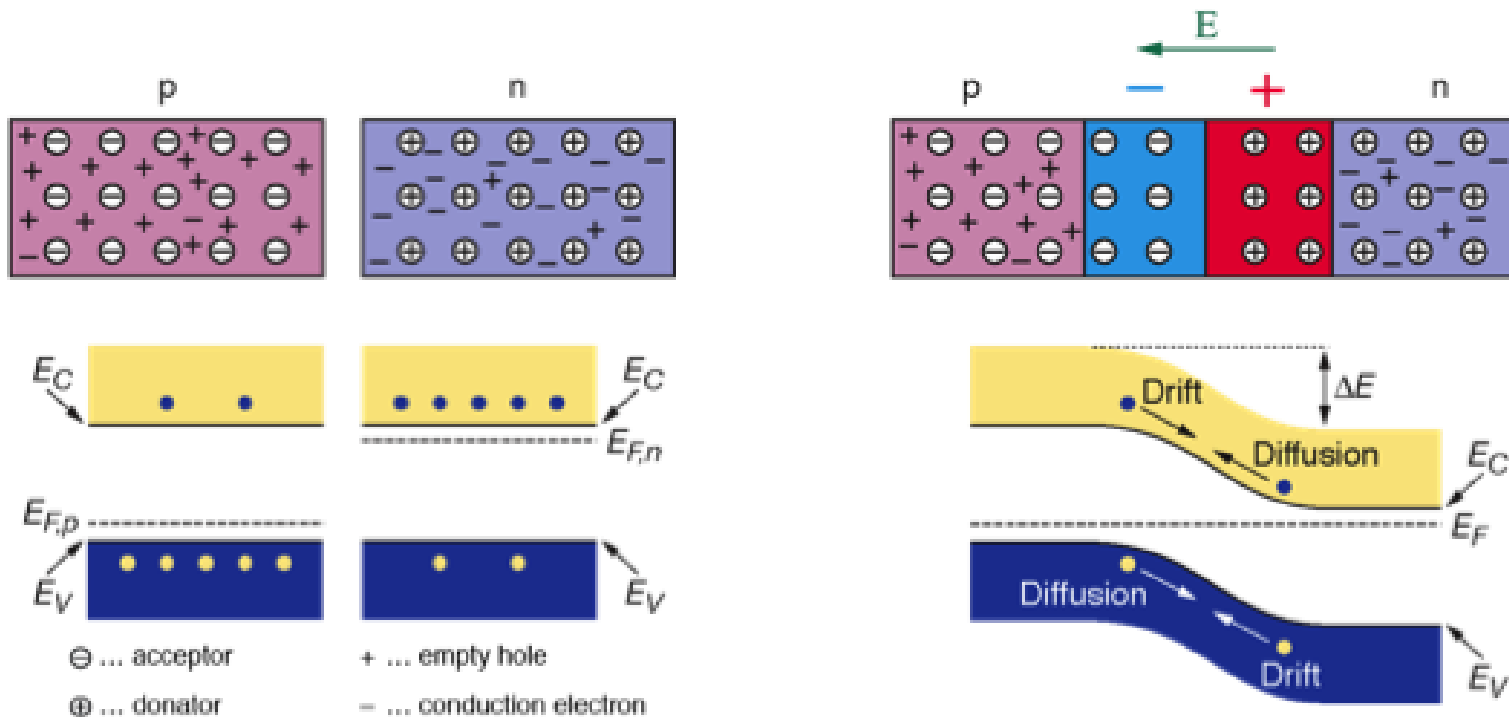
$$\begin{aligned} eV_D &= E_c - kT \ln \frac{N_c}{N_D} - E_v - kT \ln \frac{N_v}{N_A} \\ &= E_{\text{gap}} - kT \ln \frac{N_c N_v}{N_D N_A} \end{aligned}$$

V_D = diffusion or contact potential

p-n junction

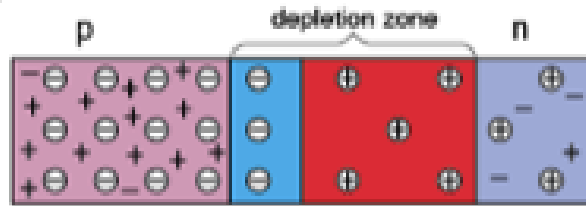
At the interface of an n-type and p-type semiconductor the difference in the fermi levels cause diffusion of surplus carries to the other material until thermal equilibrium is reached. At this point the fermi level is equal. The remaining ions create a space charge and an electric field stopping further diffusion (contact potential).

The stable space charge region is free of charge carriers and is called the **depletion zone**.

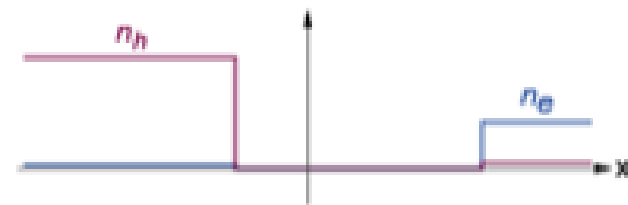


p-n junction

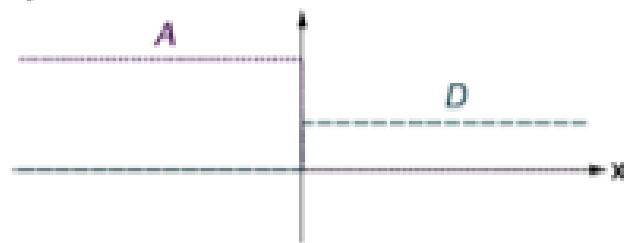
pn junction scheme



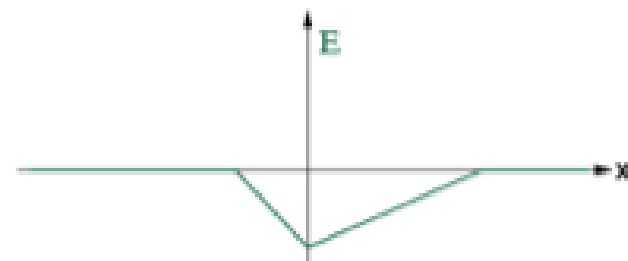
concentration of free charge carriers



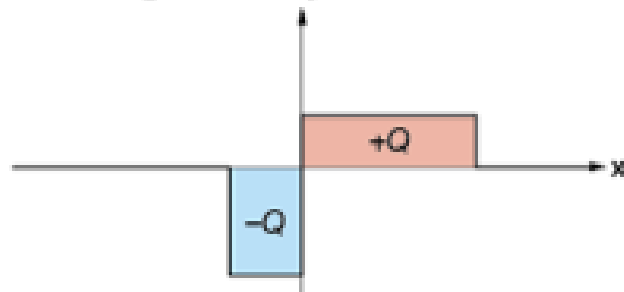
acceptor and donator concentration



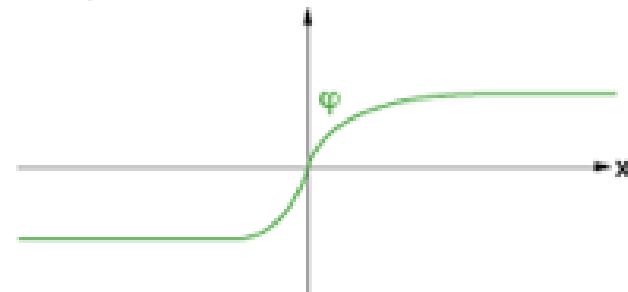
electric field



space charge density



electric potential

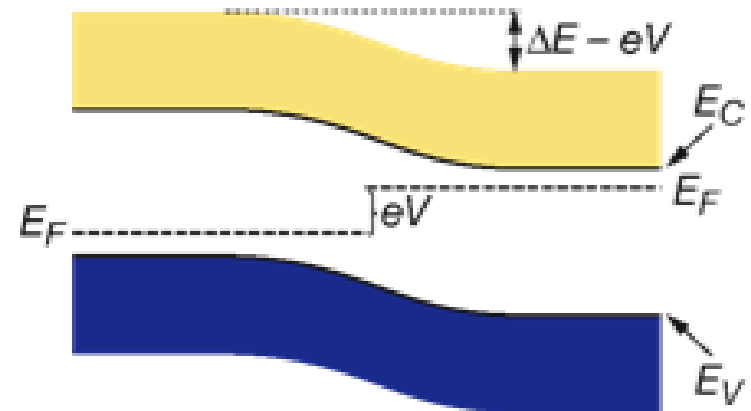
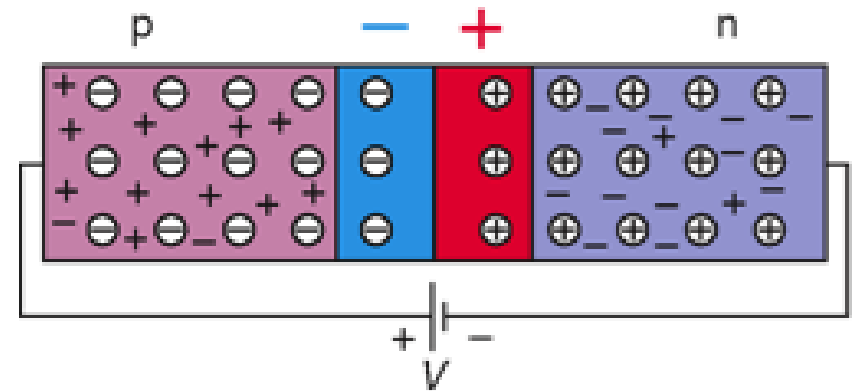


- ⊖ ... acceptor
- ⊕ ... donator
- + ... empty hole
- ... conduction electron

p-n junction: forward bias

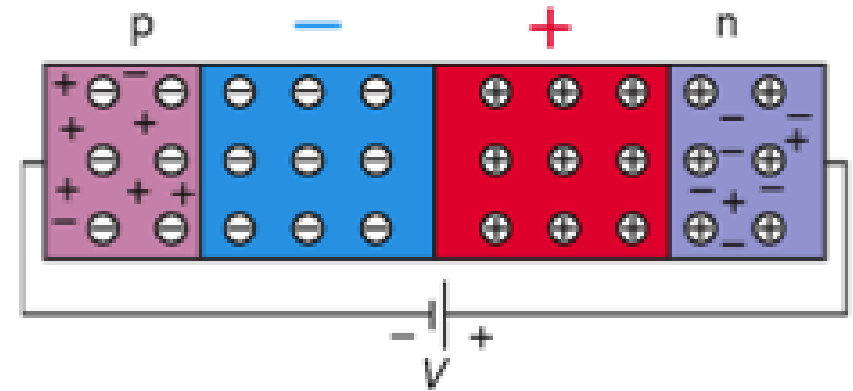
Applying an external voltage V with the anode to p and the cathode to n e- and holes are refilled to the depletion zone. The depletion zone becomes narrower.

The potential barrier becomes smaller by eV and diffusion across the junction becomes easier. The current across the junction increases significantly.

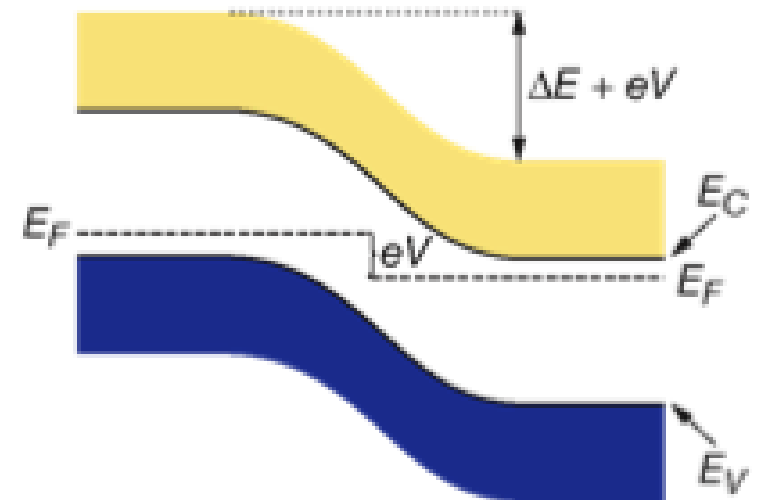


p-n junction: reverse bias

Applying an external voltage V with the cathode to p and the anode to n e- and holes are pulled out of the depletion zone. The depletion zone becomes larger.



The potential barrier becomes higher by eV and diffusion across the junction is suppressed. The current across the junction is very small “leakage current”.



p-n junction

Example of a typical p⁺-n junction in a silicon detector:

Effective doping concentration $N_a = 10^{15} \text{ cm}^{-3}$ in p⁺ region and $N_d = 10^{12} \text{ cm}^{-3}$ in n bulk.

Without external voltage:

$$W_p = 0.02 \text{ } \mu\text{m}$$

$$W_n = 23 \text{ } \mu\text{m}$$

Applying a reverse bias voltage of 100 V:

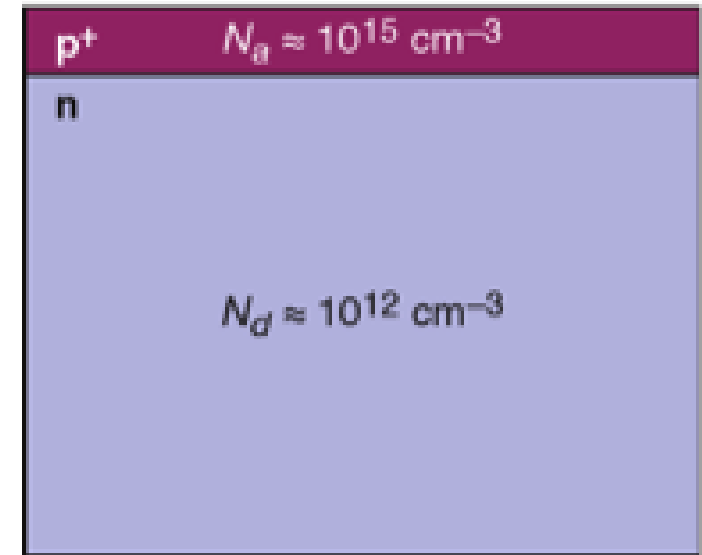
$$W_p = 0.4 \text{ } \mu\text{m}$$

$$W_n = 363 \text{ } \mu\text{m}$$

Width of depletion zone in n bulk:

$$W = \sqrt{2\varepsilon_0\varepsilon_r\mu\rho|V|}$$

$$\rho = \frac{1}{e\mu N_{\text{eff}}}$$

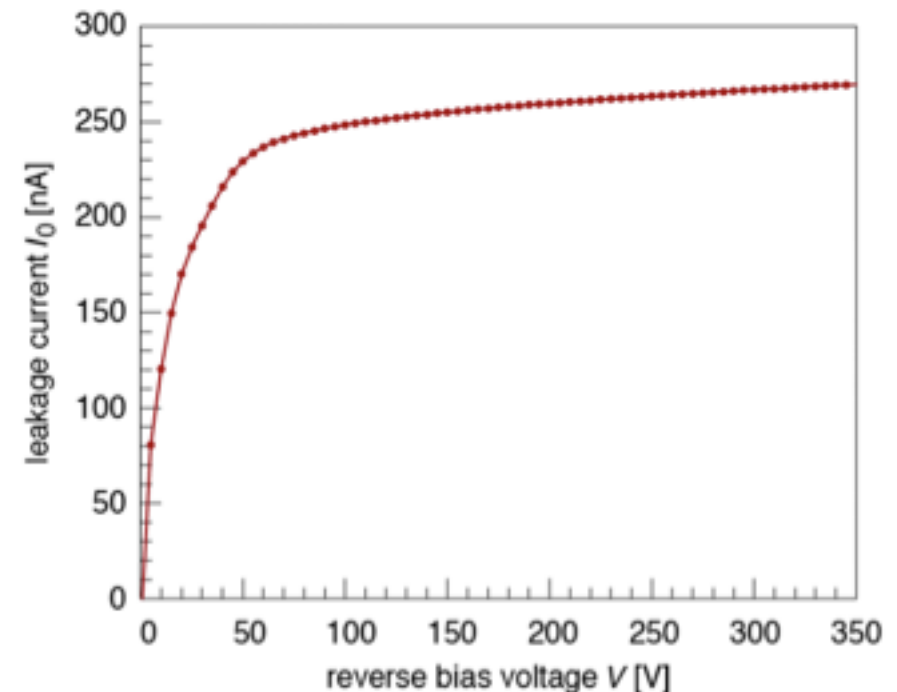


- V ... External voltage
- ρ ... specific resistivity
- μ ... mobility of majority charge carriers
- N_{eff} ... effective doping concentration

p-n junction: leakage current

- Movement of minority carriers (small)
- Thermally generated electron-hole pairs originating from recombination and trapping centers in the depletion region
- Surface channels (surface chemistry, contaminants, type of mounting, etc.)

It is essential to keep the leakage current low! That is the reference noise level with respect to which the desired SIGNALs have to be measured!!! (S/N)



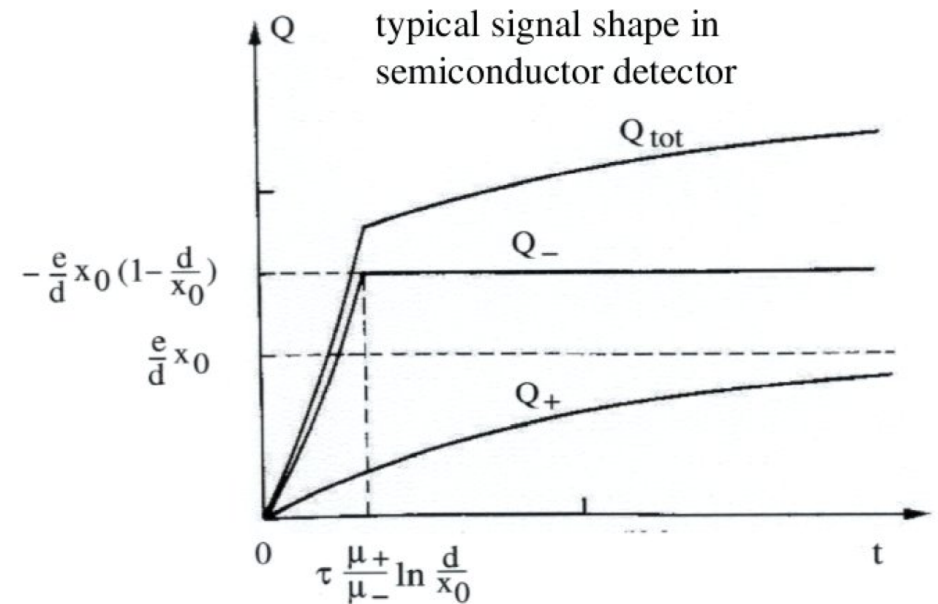
Signal generation in semiconductor detectors

Total charge signal:

$$Q_-(t_d) + Q_+(+\infty) = -e$$

Signal rise time essentially determined by:

$$\tau = \rho \cdot \epsilon \cdot \epsilon_0$$



In reality a bit more complicated:

- Track not exactly a line charge (distributed over typically 50 μm width)
- $\mu_{\pm} \neq \text{constant}$
- Some loss of charges due to recombination at impurities

For silicon: $\tau = \rho \cdot 10^{-12} \text{ s}$ (ρ in Ωcm), $\rho = 1000 \Omega\text{cm} \rightarrow \tau = 1 \text{ ns}$

Ionization yield and Fano factor

Ionization yield and resolution

Mean energy per electron-hole pair:

~1/3 in ionization, ~2/3 in excitation of crystal lattice

	$E_0^{300\text{ K}}$	$E_0^{77\text{ K}}$	E_{gap}
Si	3.6 eV	3.8 eV	1.1 eV
Ge	-	2.9 eV	0.7 eV

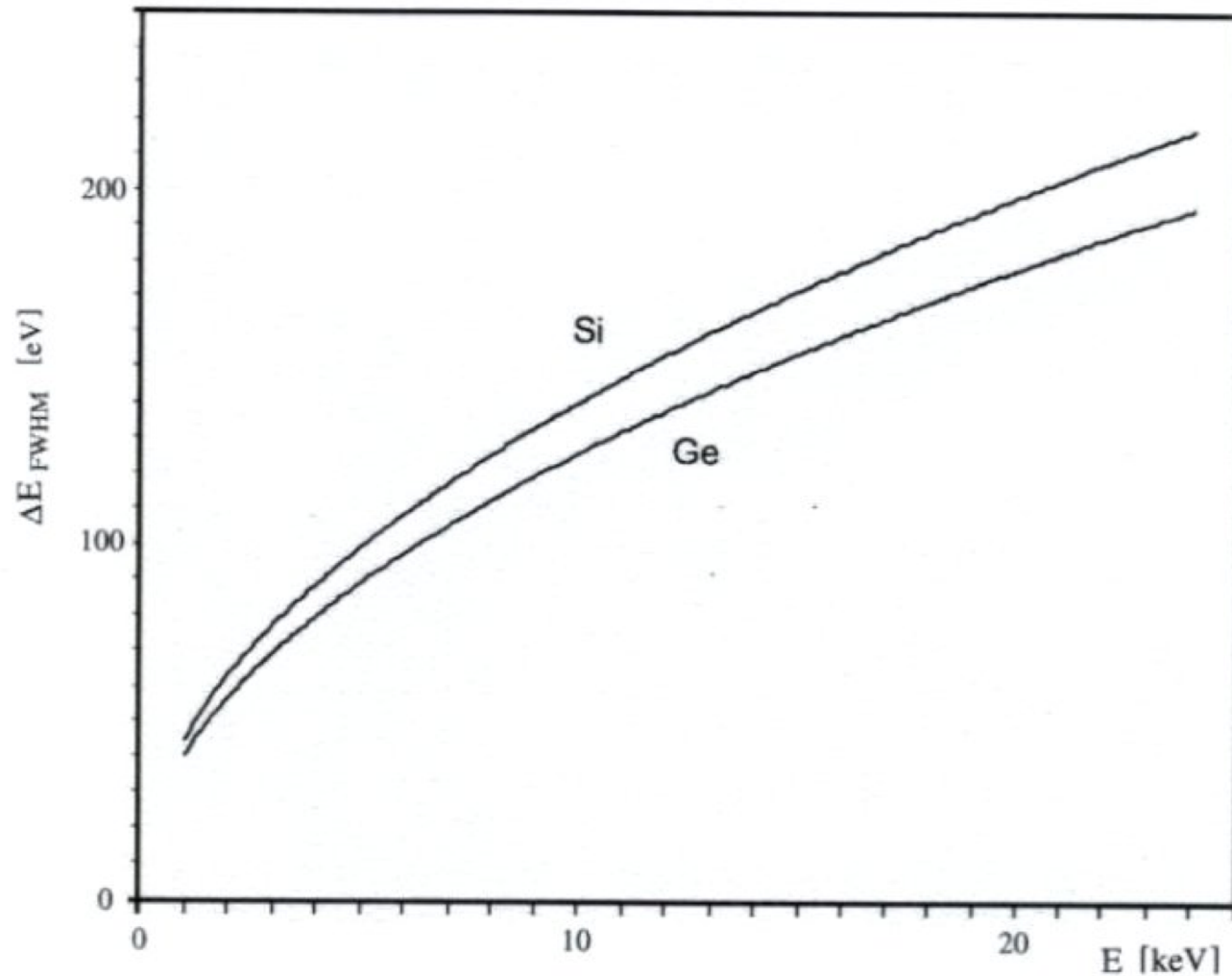
For both processes, we assume a Poisson distribution: $\sigma_i = \sqrt{N_i}$, $\sigma_x = \sqrt{N_x}$

However!! the effective variance is much smaller!! When F is the **Fano factor**:

$$\sigma_i = \sqrt{N_i} \sqrt{F} \quad \text{smaller than the naïve expectation!}$$

the Fano factor results from the energy loss in a collision not being purely statistical. The process giving rise to each individual charge carrier is not independent as the number of ways an atom may be ionized is limited by the discrete electron shells. The net result is a better energy resolution than predicted by purely statistical considerations.

Energy resolution



Statistics of charge carriers generated + noise + non-uniformities in charge-collection efficiency

Energy measurements

- Particularly suited for low energies: e.g. α -particles, low energy electrons, X- and γ - rays
- Via dE/dx in thin detectors
or full stopping in thick detectors

Detector types used for energy measurements:

- Ion implanted or diffusion barrier detectors
- Surface barrier detectors
- p-i-n detectors: Ge(Li), Si(Li)
- High purity of intrinsic Ge detectors

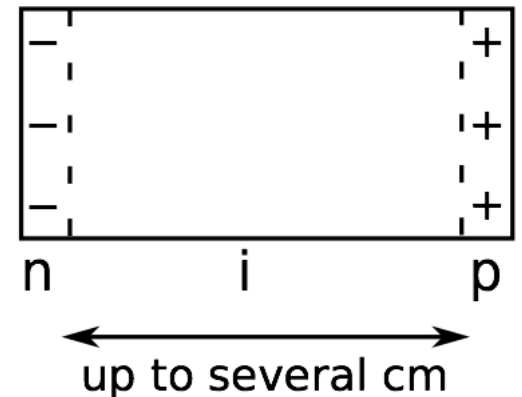
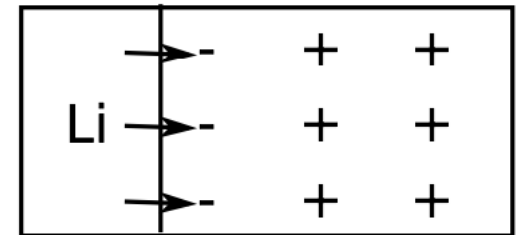
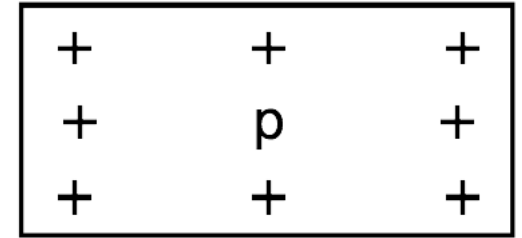
p-i-n detectors: Ge(Li), Si(Li)

Way to get beyond a few mm thickness:

From the 1960ies: create a thick (1-2 cm) depletion layer with **COMPENSATED** material (very high resistivity)

E. M. Pell

- Start with high-purity p-type Ge or Si (acceptor is typically Boron)
- Bring in contact with liquid Li bath (350-400 °C) the lithium diffuses into Ge/Si
- Apply external field → positive Li-ions drift far into the crystal and compensate Boron ions locally



Typically $10^9 / \text{cm}^3$ Li atoms

p-Si + Li⁺ ≈ neutral

$\rho = 2 \cdot 10^5 \Omega\text{cm}$ possible

i.e. like true intrinsic material

Achieve high resistivity!

p-i-n detectors: Ge(Li), Si(Li)

Needs to be **cooled PERMANENTLY!** (liquid N₂) to avoid separation of Li impurities by diffusion!

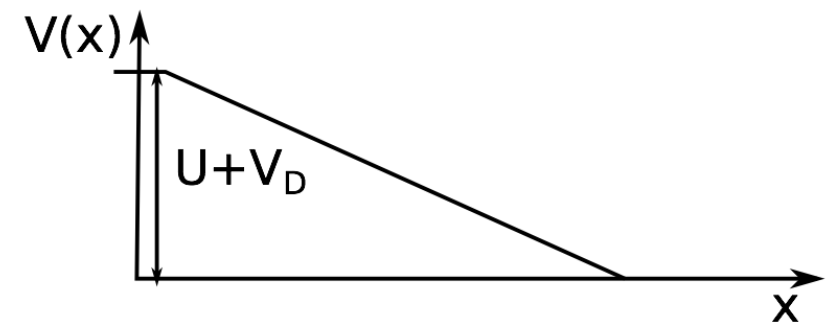
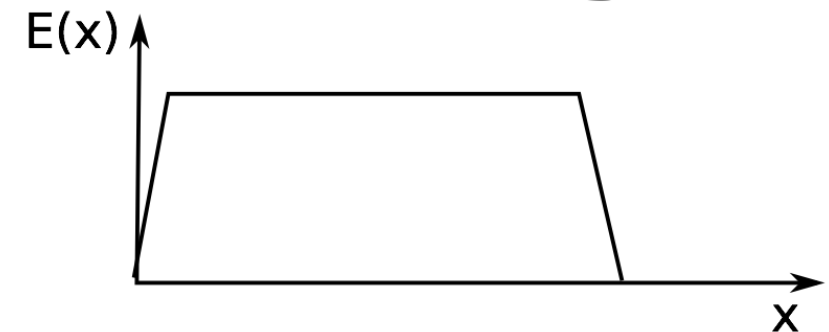
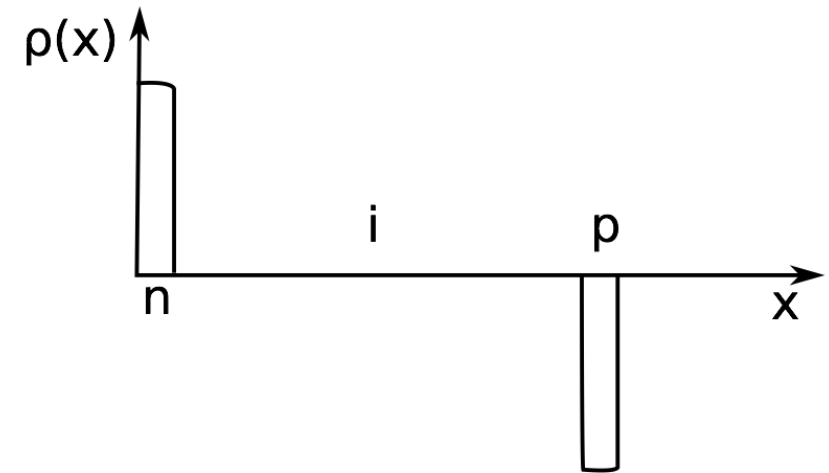
Application: **γ spectroscopy**

Larger cross section for photoelectric effect in Ge wrt Si:

→ Ge(Li) preferred!

However: full energy peak contains only order of 10% of the signal in a 50 cm³ crystal (30% in a 170 cm³ crystal)

- Resolution much better than NaI (sodium iodide - scintillator)
- Efficiency significantly lower



external voltage U and diffusion voltage V_D

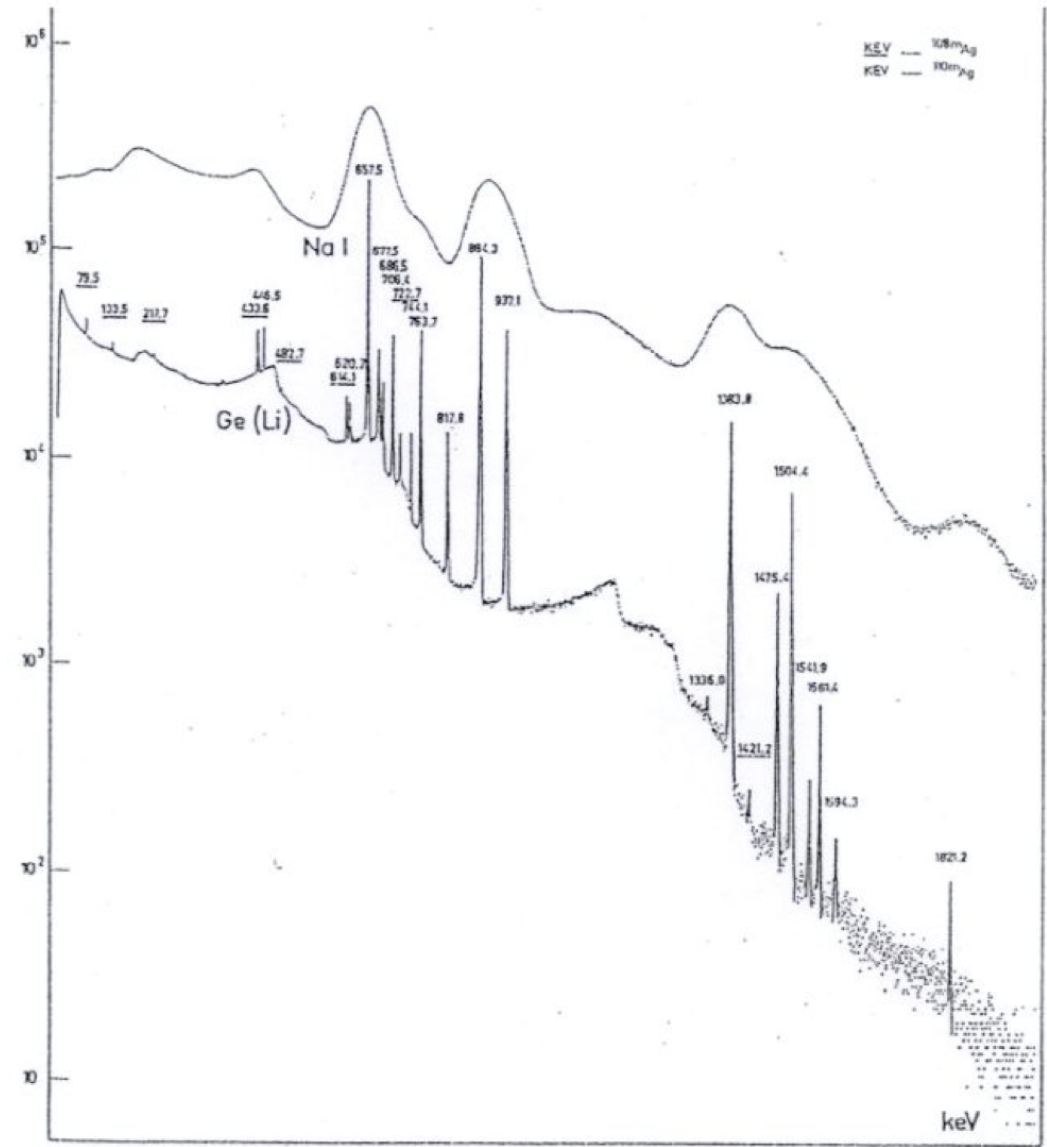
p-i-n detectors: Ge(Li), Si(Li)

Ge(Li) detectors: a revolution in γ spectroscopy in the mid 1960ies

Comparison of spectra obtained with NaI (state of the art technique until then) and Ge(Li)

Decays of ^{108m}Ag and ^{110m}Ag

Energies of peaks are labeled in keV



High purity or intrinsic Germanium detectors

From the late 1970ies: improvements in material quality

Keep dark current low not by compensating impurities but by making the material **VERY CLEAN** itself

Extremely pure Ge obtained by repeating the purification process (zone melting) → $\leq 10^9$ impurities per cm^3

Intrinsic later like compensated zone in Ge(Li), similar sizes possible

Advantage: cooling only needed during use, to reduce the noise

Other applications:

- Low energy electrons
- Strongly ionizing particles
- dE/dx for particle identification

High purity or intrinsic Germanium detectors

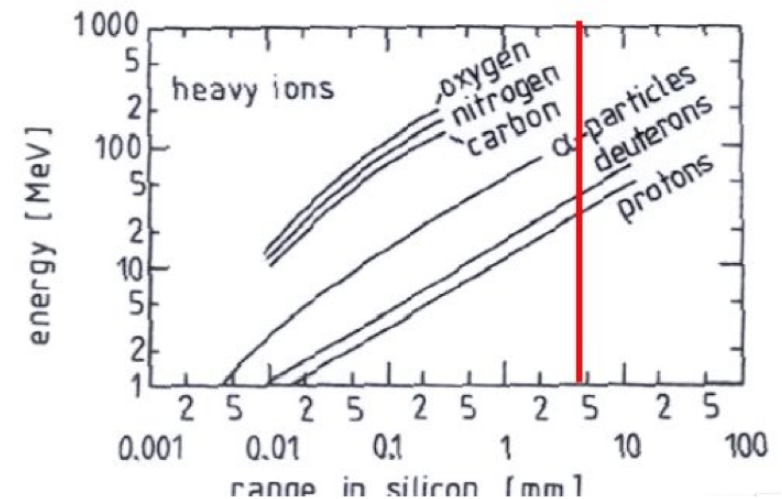
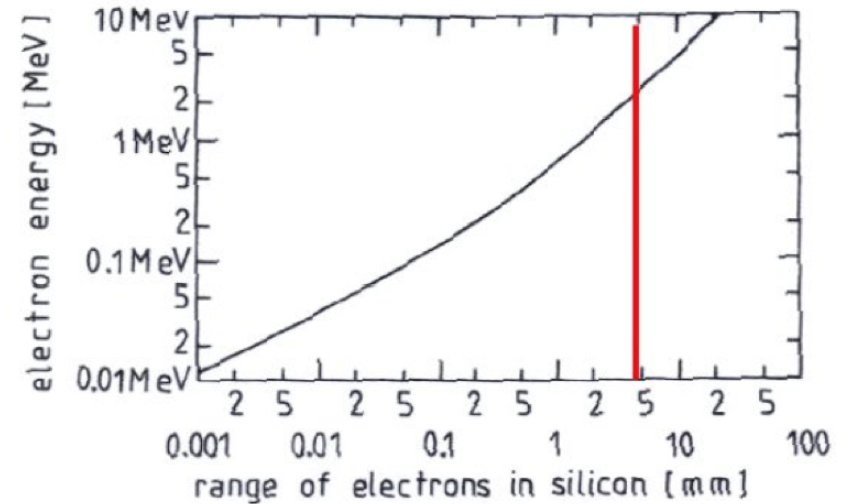
The energy range addressed by a device is determined by the range of particles compared to the size of the detector



Range of electrons, p, d, α , etc. in Si

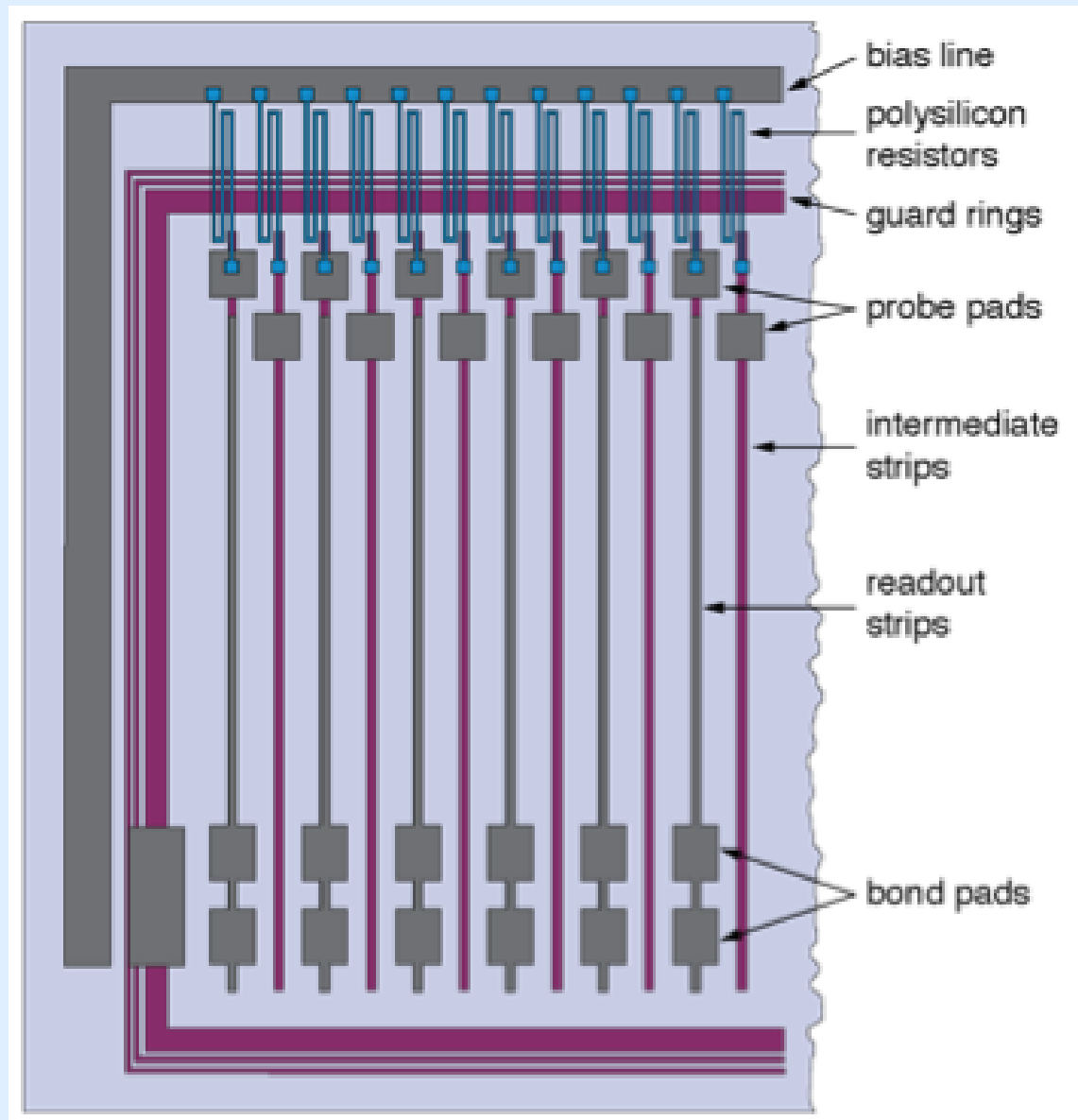
Particles stopped in 5mm Si(Li) detectors:

- α up to 120 MeV kinetic energy
- p up to 30 MeV
- e up to 3 MeV



energy-range relation for electrons (top) and more massive particles (bottom)

Position sensitive detectors

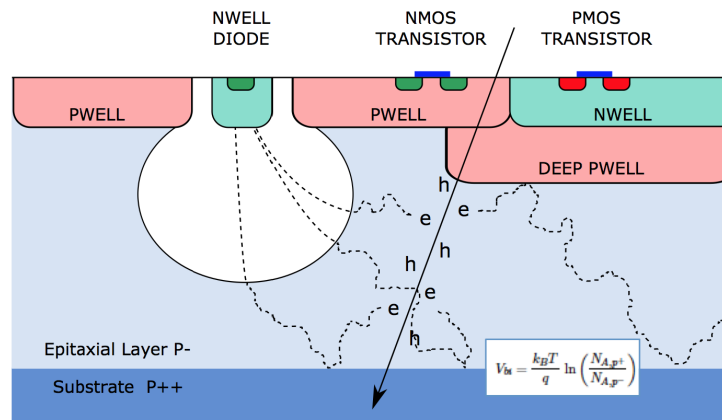
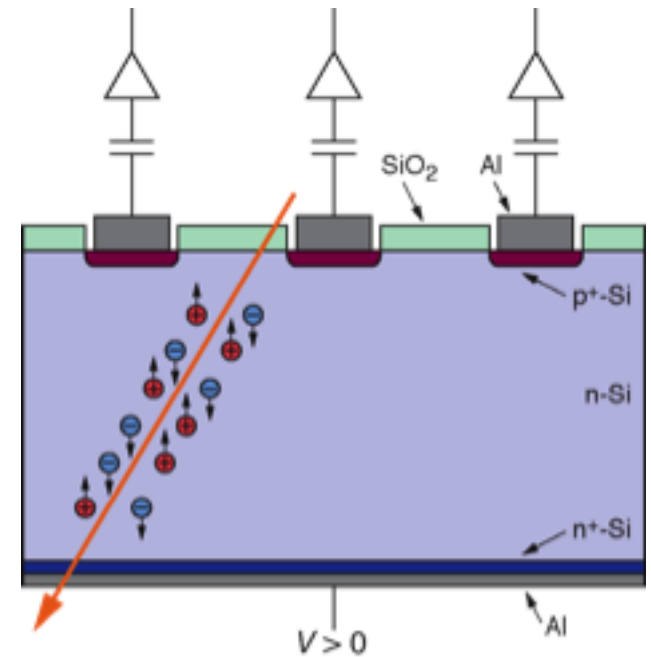
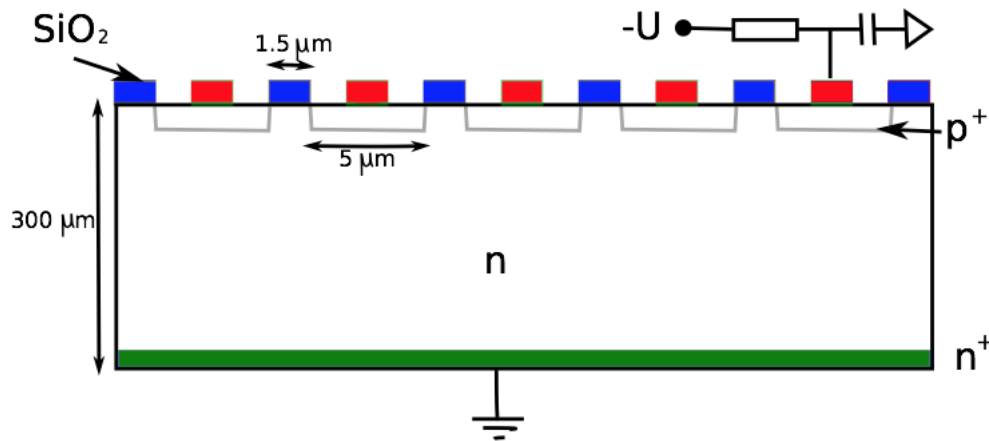


Detectors for position measurements

Segment the readout electrodes into strips, pads, pixels

First use in 1980ies

By now standard part of high energy experiments since LEP (CERN) and Tevatron (Fermilab) era

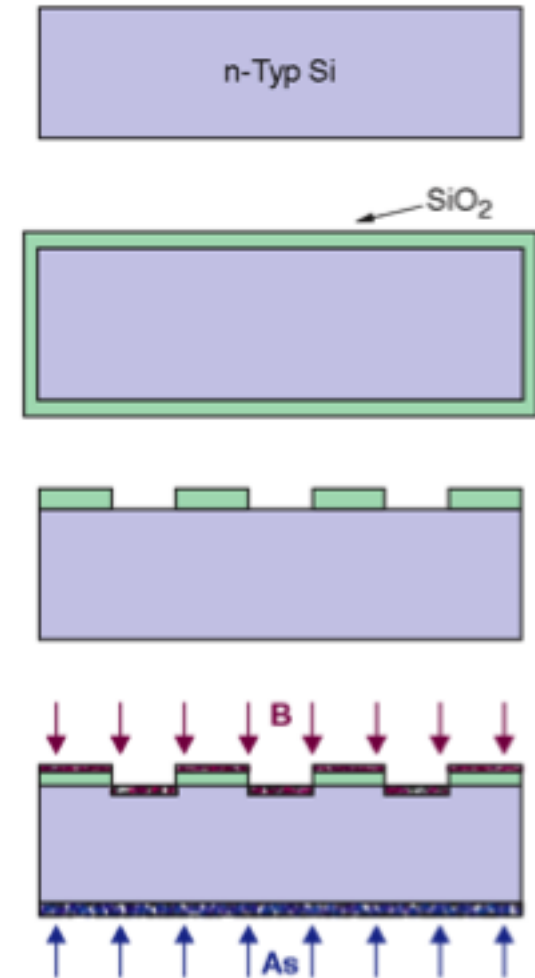


History of semiconductor detectors

- 1951: First detector was a germanium-pn-diode (McKay).
- 1960: p-i-n semiconductor detectors for α - and β -spectroscopy (E.M. Pell)
- 1960ies: Semiconductor detectors from germanium but also silicon are more and more important for the energy measurement in nuclear physics.
- 1980: First silicon surface barrier micro strip detector (E. Heijne)
- 1983: First use of a planar silicon strip detector in a fix target experiment - NA11 at CERN. (J. Kemmer)
- 1980ies and after: micro structured silicon detectors gain rapid importance for tracking detectors in high energy physics experiments!

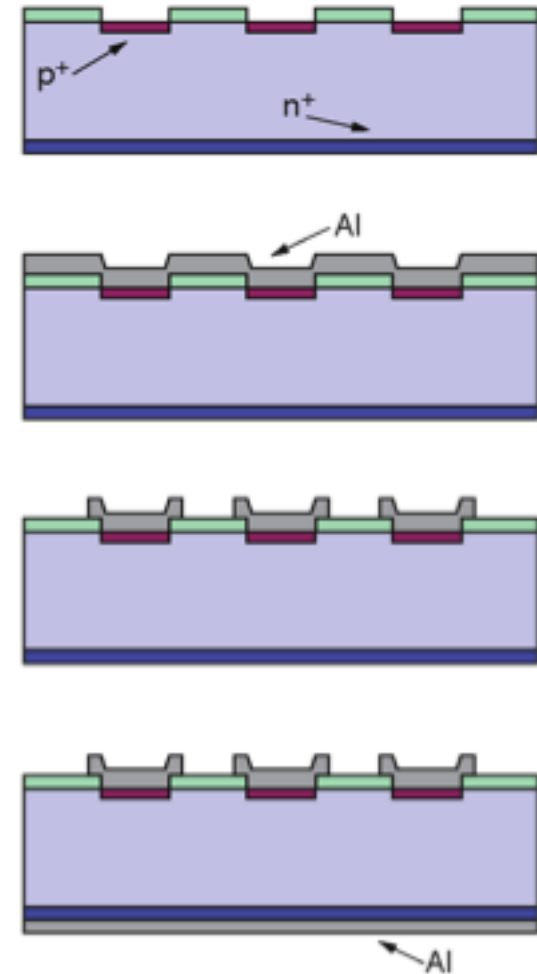
Manufacturing by planar process - 1

1. Starting Point: single-crystal n-doped wafer ($N_D \approx 1-5 \cdot 10^{12} \text{ cm}^{-3}$)
2. Surface passivation by SiO_2 -layer (approx. 200 nm thick). E.g. growing by (dry) thermal oxidation at 1030 °C.
3. Window opening using **photolithography technique** with etching, e.g. for strips
4. Doping using either
 - Thermal diffusion (furnace)
 - Ion implantation
 - p⁺-strip: Boron, 15 keV, $N_A \approx 5 \cdot 10^{16} \text{ cm}^{-2}$
 - Ohmic backplane: Arsenic, 30 keV, $N_D \approx 5 \cdot 10^{15} \text{ cm}^{-2}$



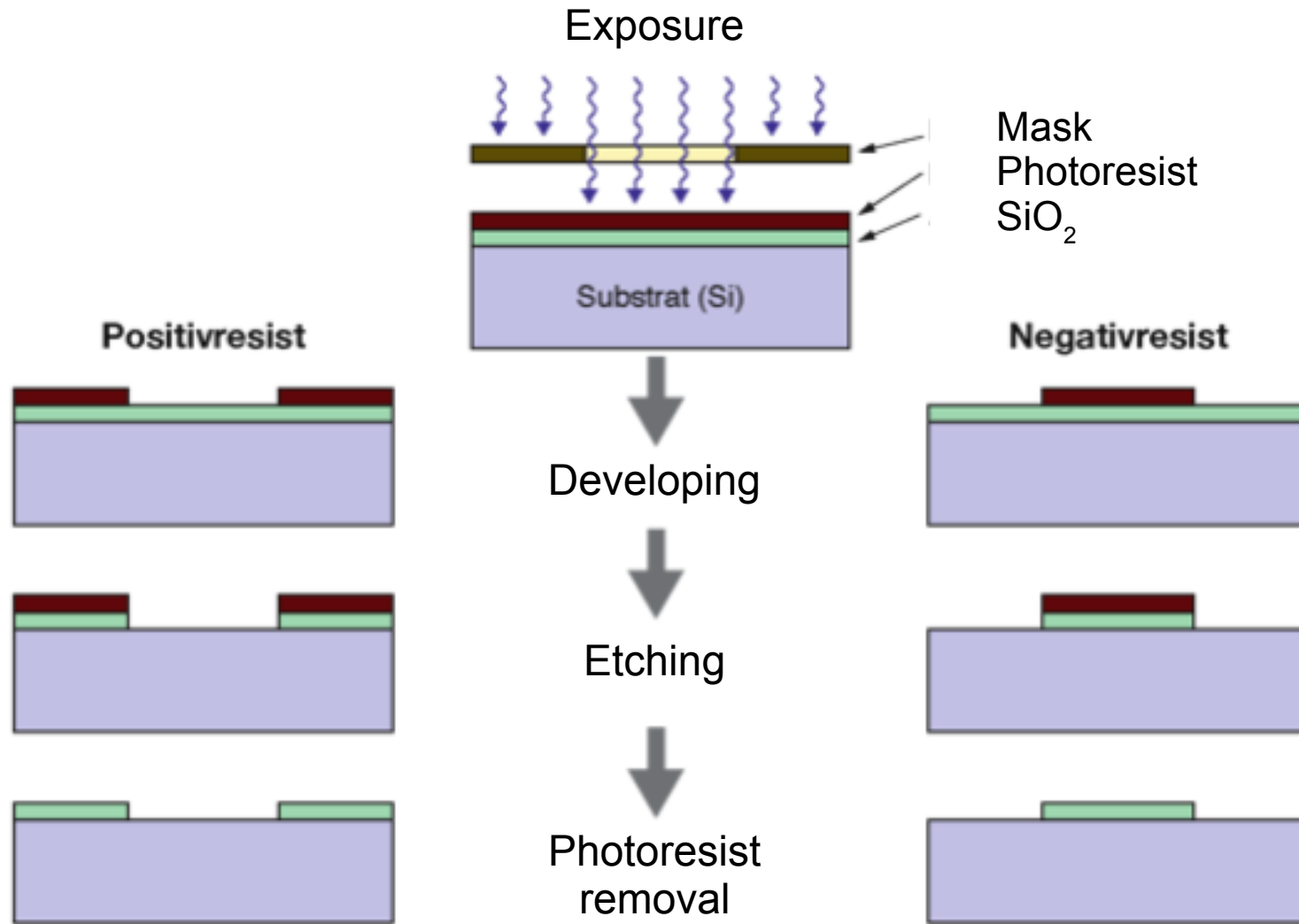
Manufacturing by planar process - 2

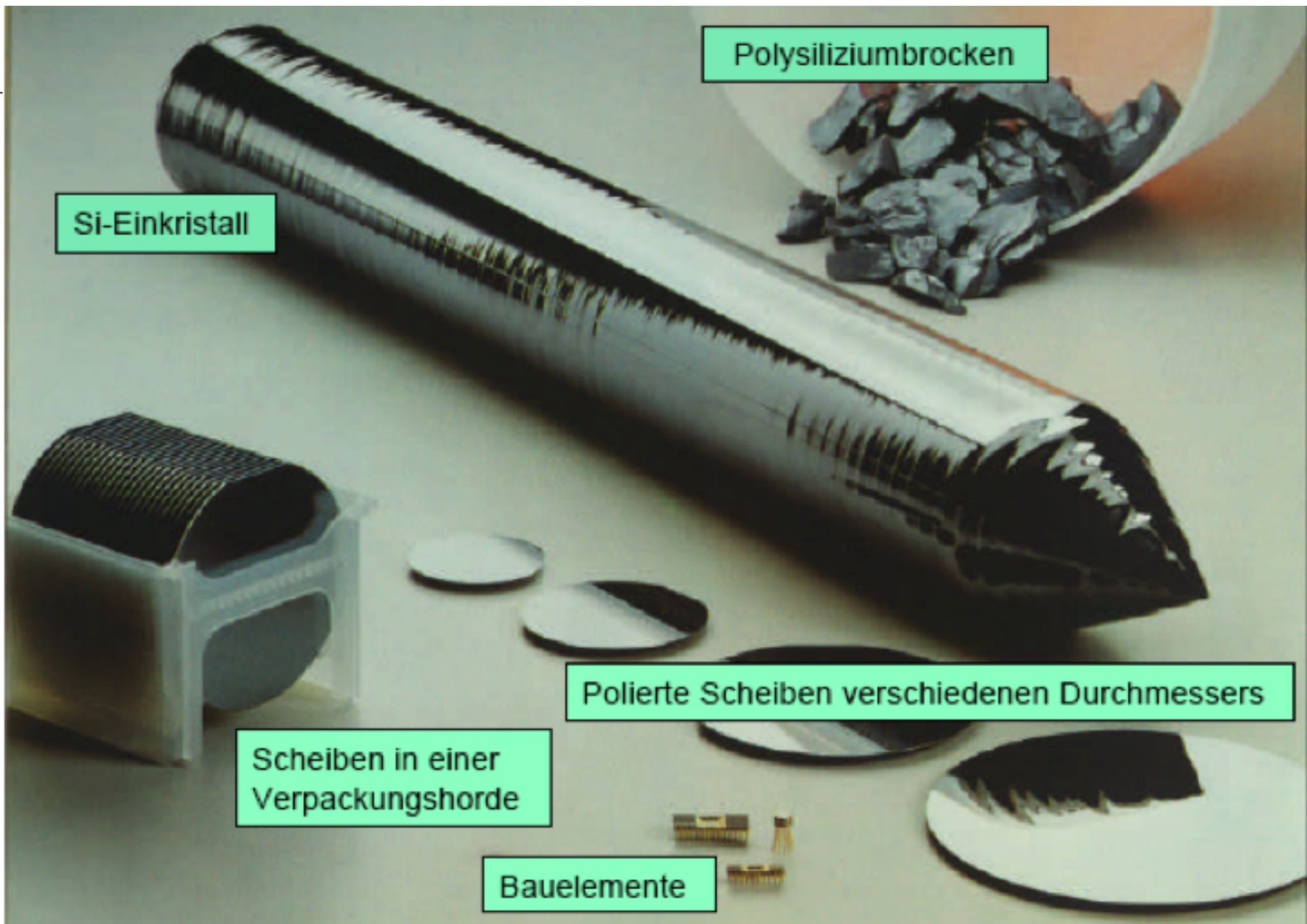
5. After ion implantation: Curing of damage via thermal annealing at approx. 600°C, (activation of dopant atoms by incorporation into silicon lattice)
6. Metallization of front side: sputtering or CVD
7. Removing of excess metal by photolithography: etching of non-covered areas
8. Full-area metallization of backplane with annealing at approx. 450°C for better adherence between metal and silicon
9. Last step: wafer dicing (cutting)



CVD = chemical vapor deposition

Lithography





Polysiliziumbrocken

Si-Einkristall

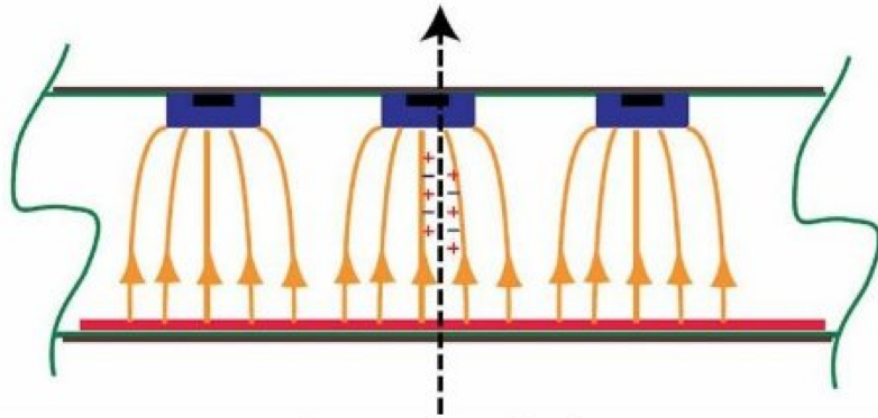
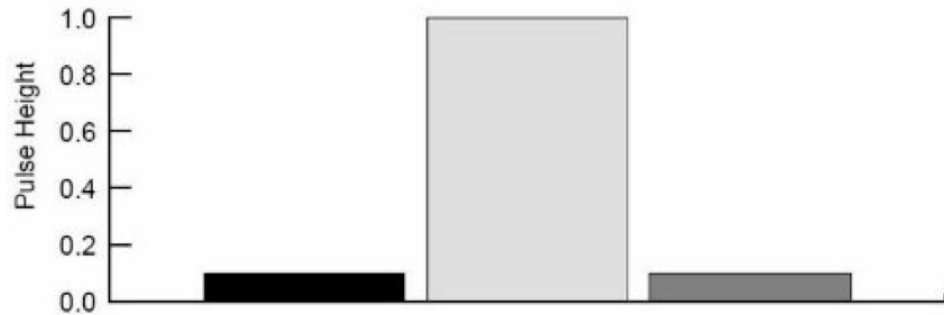
Polierte Scheiben verschiedenen Durchmessers

Scheiben in einer Verpackungshorde

Bauelemente

Position measurement

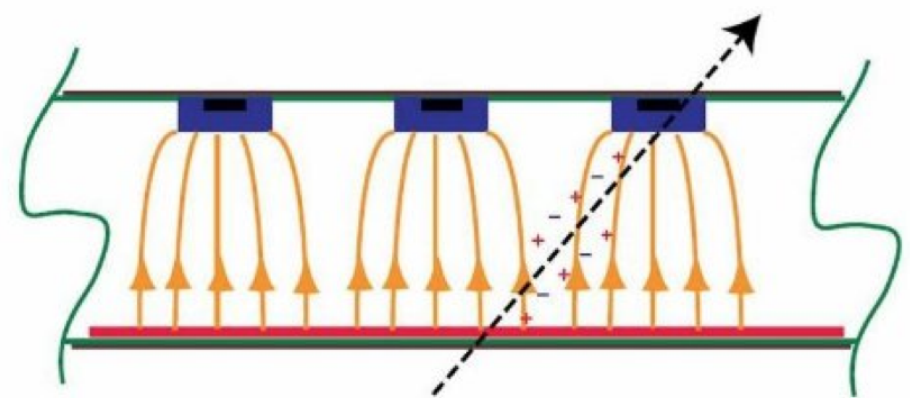
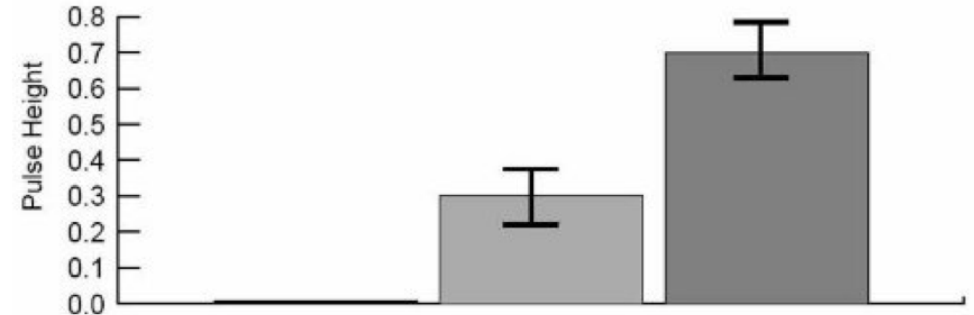
One Strip Clusters



Δs : strip pitch

$$\sigma_x = \Delta s / \sqrt{12}$$

Two Strip Clusters



centroid resolution

$$\sigma_x \approx (\Delta s / 2) (N / S)$$

Position resolution: limits

1. δ -electrons

can shift the center of gravity of the track

N_p primary ionization - includes δ -electron, which travels over a range r_δ

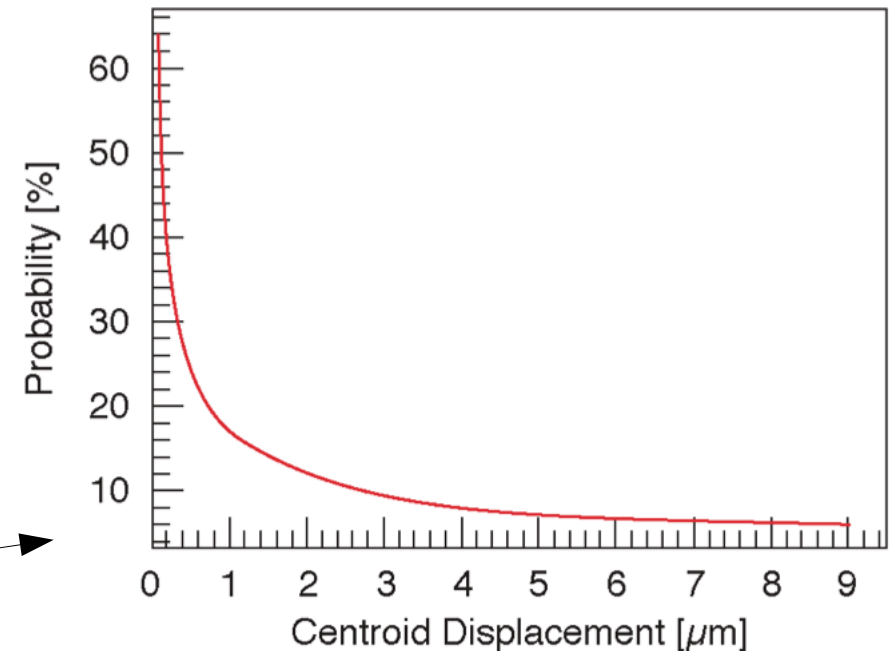
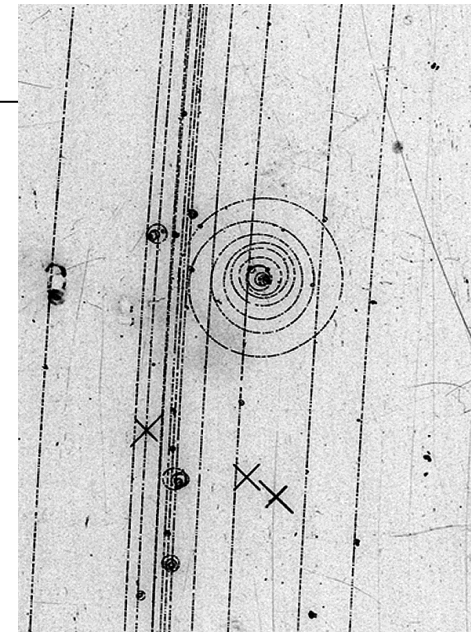
The δ -electron has energy such that it produces further N_δ electron-hole pairs.

Assuming it moves perpendicular to the track:

Example: 100 μm Si, 5 GeV pion \rightarrow 240 eV/ μm \rightarrow $N_p = 6700$

10% probability for δ with $T_\delta > 20$ keV and $r_\delta = 5 \mu\text{m}$ $\rightarrow \Delta x \approx 1 \mu\text{m}$

Worse for 300 μm Si, see figure



Position resolution: limits

2. Noise

Position measurement requires $S \gg N$

- If signal only on one strip or one pad, resolution is $\sigma_x = \text{pitch} / \sqrt{12}$, independent of S/N
- If signal spreads of more strips \rightarrow more precise position by center-of-gravity method, but influenced by S/N

3. Diffusion

Smearing of charge cloud (transverse diffusion)

Initially helps to distribute signal over more than one strip

But 2-track resolution and S/N deteriorate with diffusion

4. Magnetic field

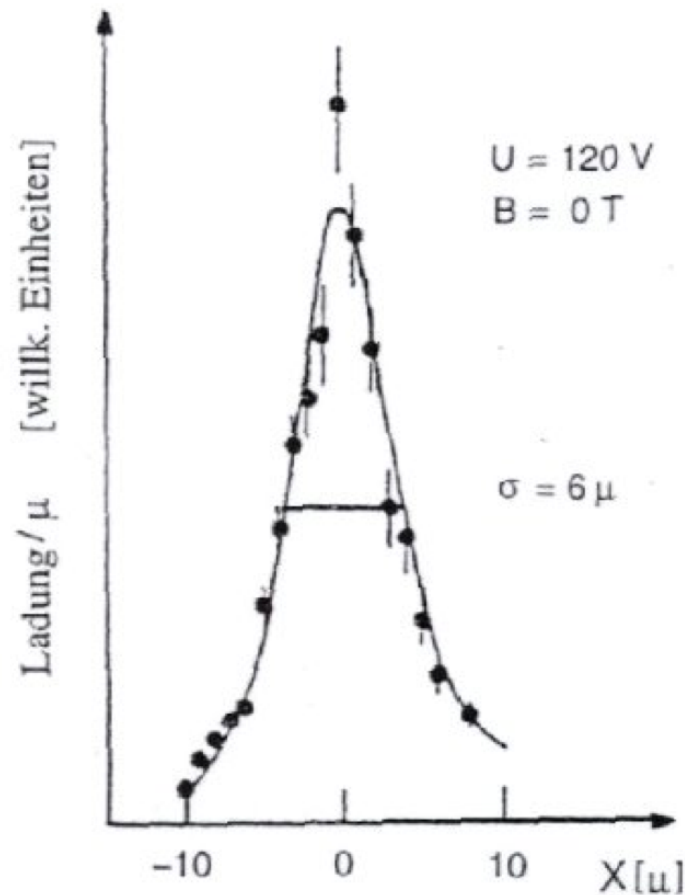
Lorentz force acts on drifting electrons and holes: track signal is displaced if E not parallel to B, increasing displacement with drift length (see next)

Position resolution: limits

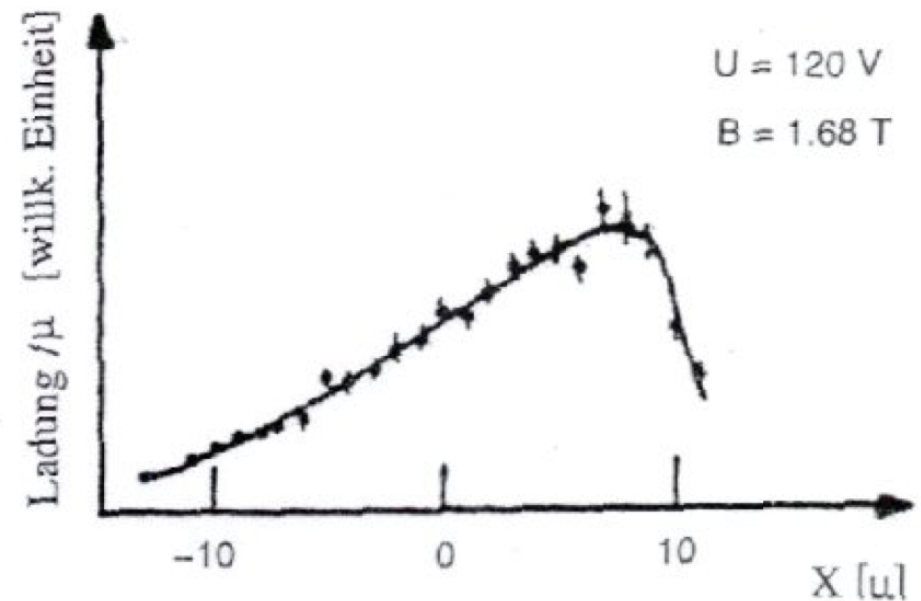
Magnetic field

charge distribution registered for a semiconductor detector with or without magnetic field

no field

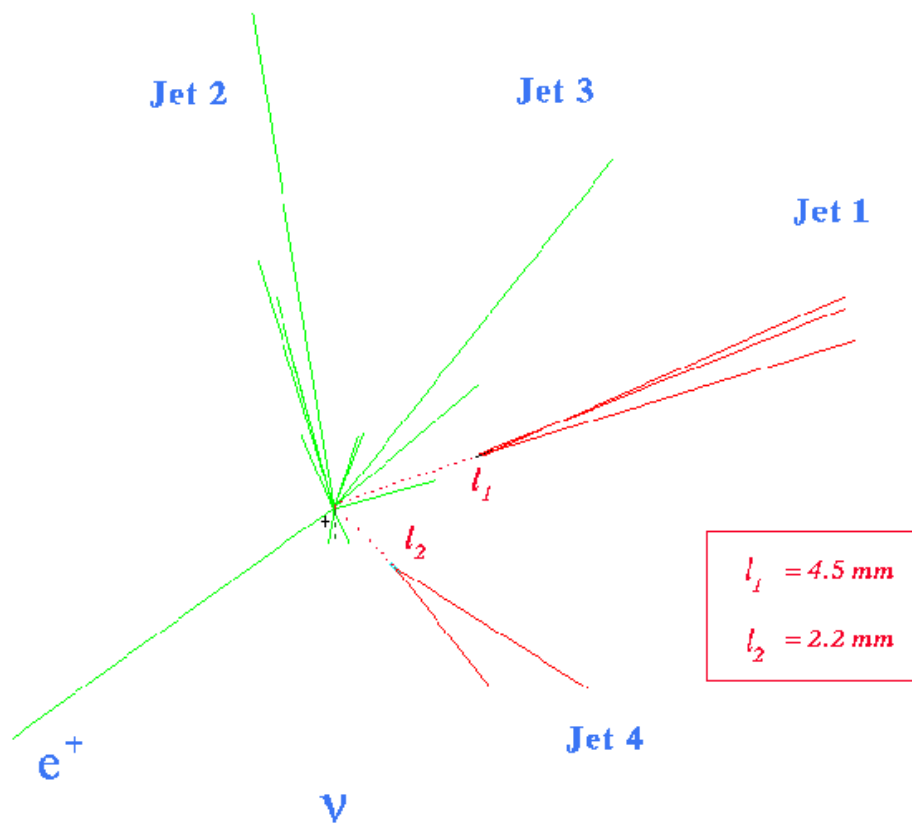


$B = 1.68 T$



Position resolution: vertex reconstruction

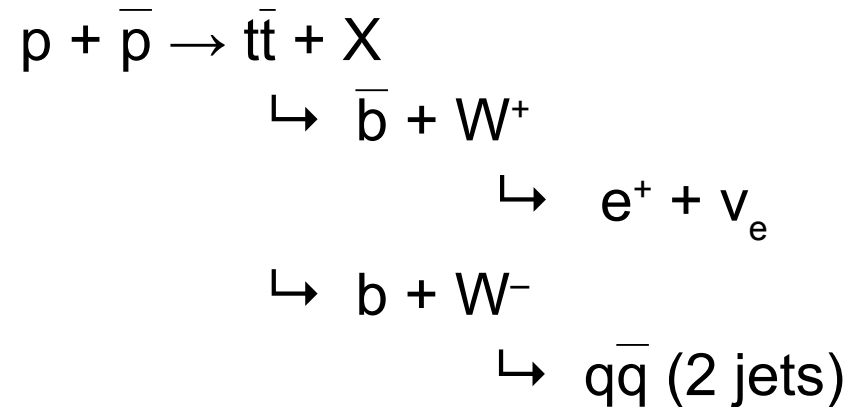
**$t\bar{t}$ Event
SVX Display
CDF**



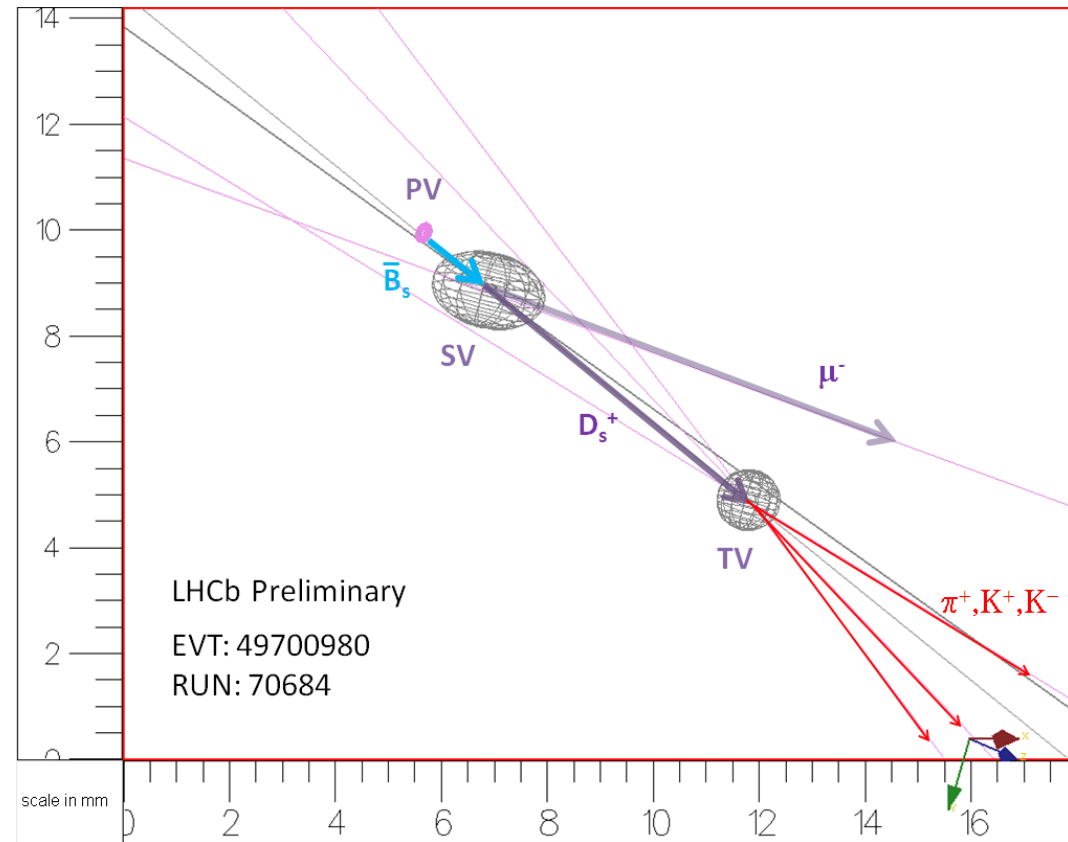
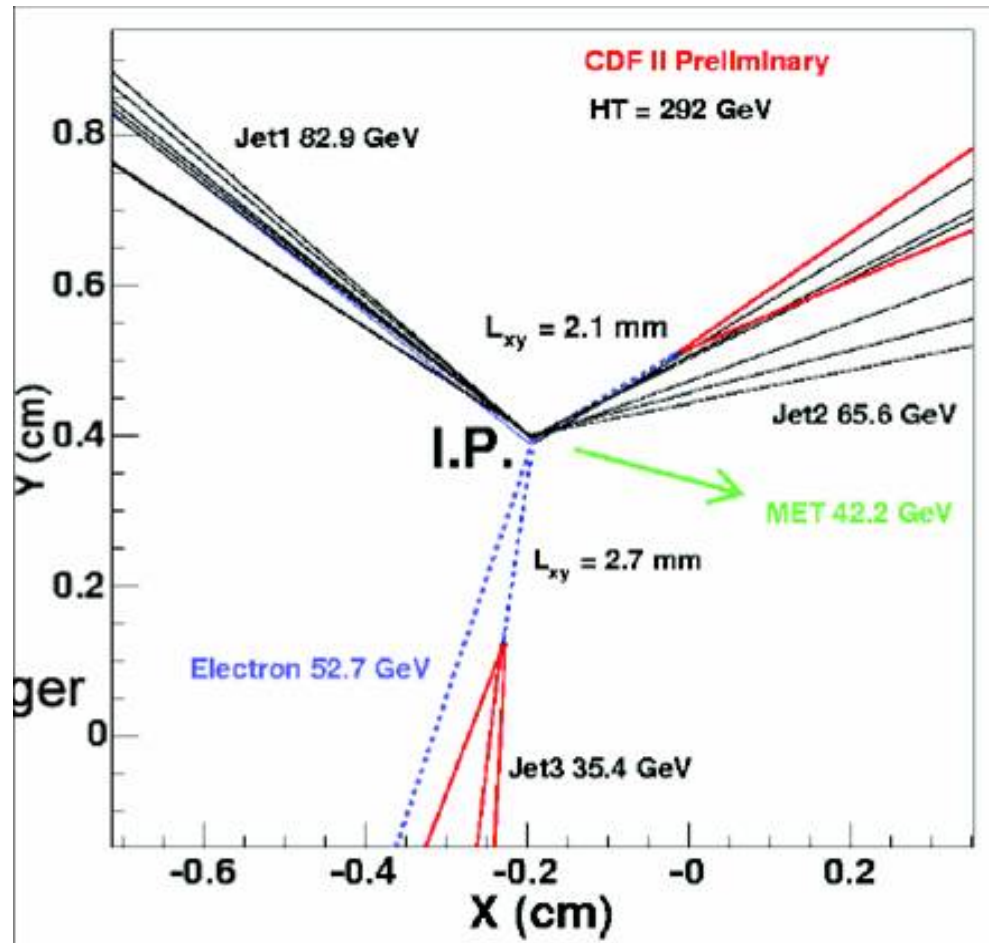
$M_{\text{top}}^{\text{Fit}} = 170 \pm 10 \text{ GeV}/c^2$

24 September, 1992
run #40758, event #44414

CDF (Tevatron, Fermilab)
Two beauty-jets from a $t\bar{t}$ -decay



Position resolution: vertex reconstruction



Position resolution: multiple scattering

Essential for the selection of decay particle trajectories:

Impact parameter: closest distance of primary vertex from the extrapolated track

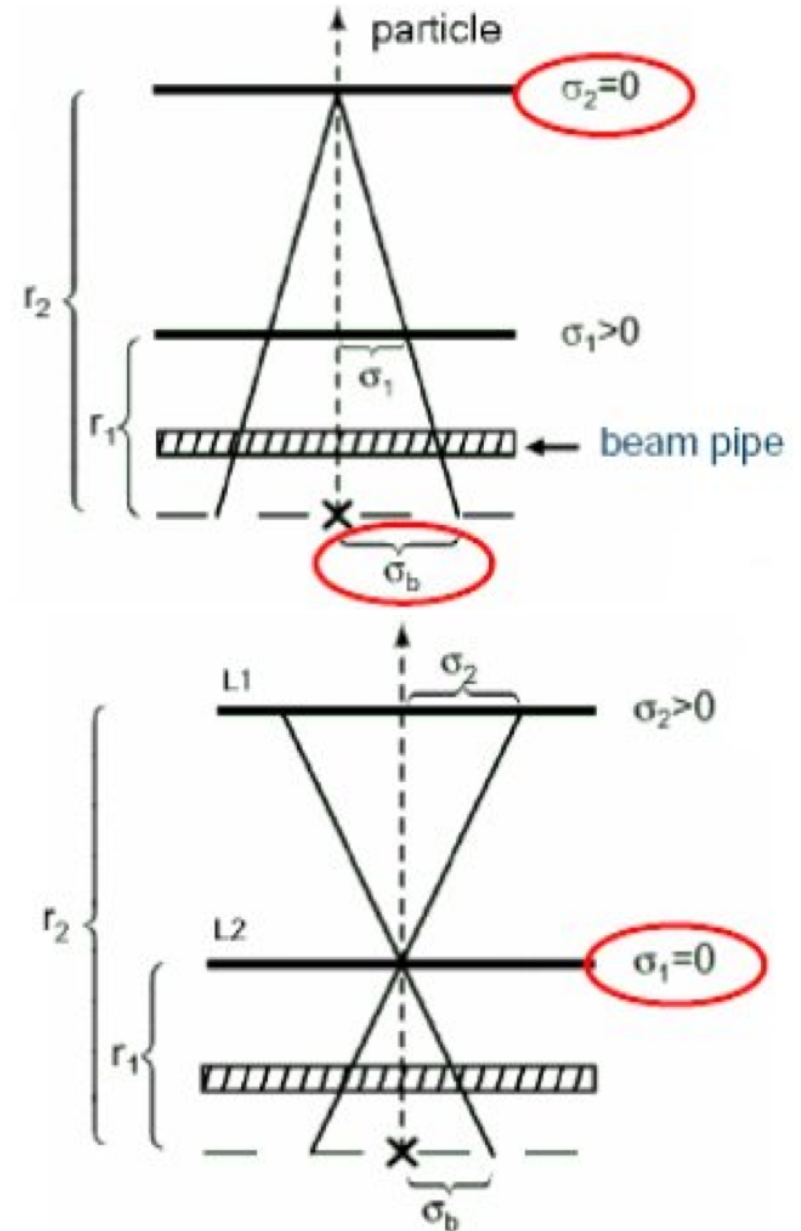
$$\sigma^2 = \left(\frac{r_1}{r_2 - r_1} \sigma_2 \right)^2 + \left(\frac{r_2}{r_2 - r_1} \sigma_1 \right)^2 + \sigma_{MS}^2$$

$$\frac{\sigma_b}{\sigma_1} = \frac{r_2}{r_2 - r_1}$$

$$\frac{\sigma_b}{\sigma_2} = \frac{r_1}{r_2 - r_1}$$

Optimum resolution for:

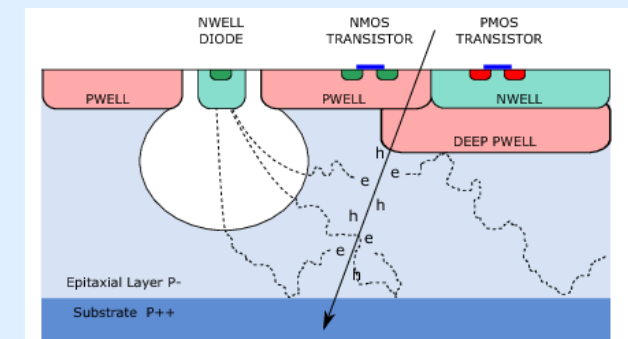
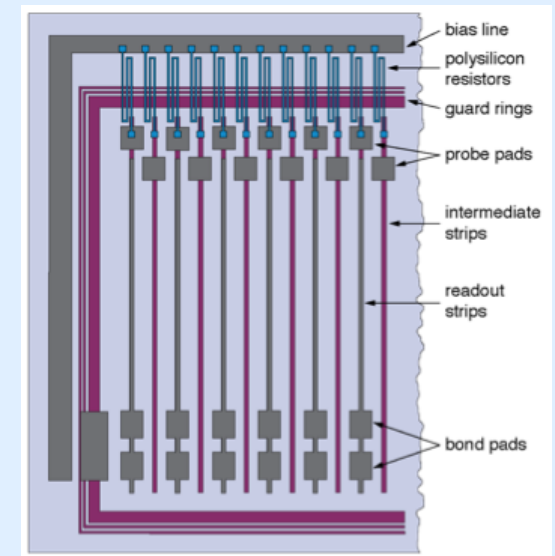
- r_1 small
- r_2 large
- σ_1, σ_2 small
- σ_{MS} as small as possible, by as little material as possible



Position sensitive detectors

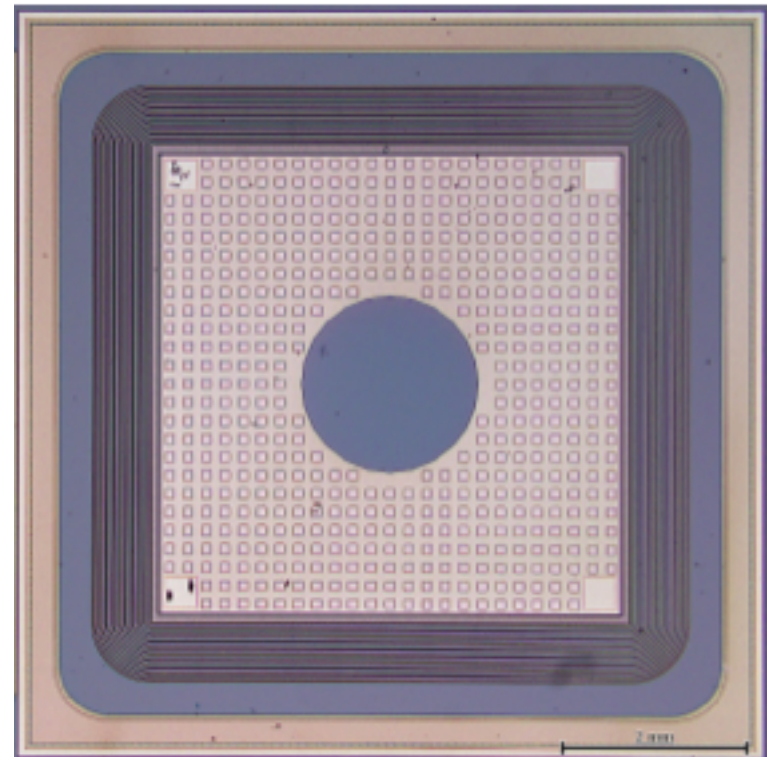
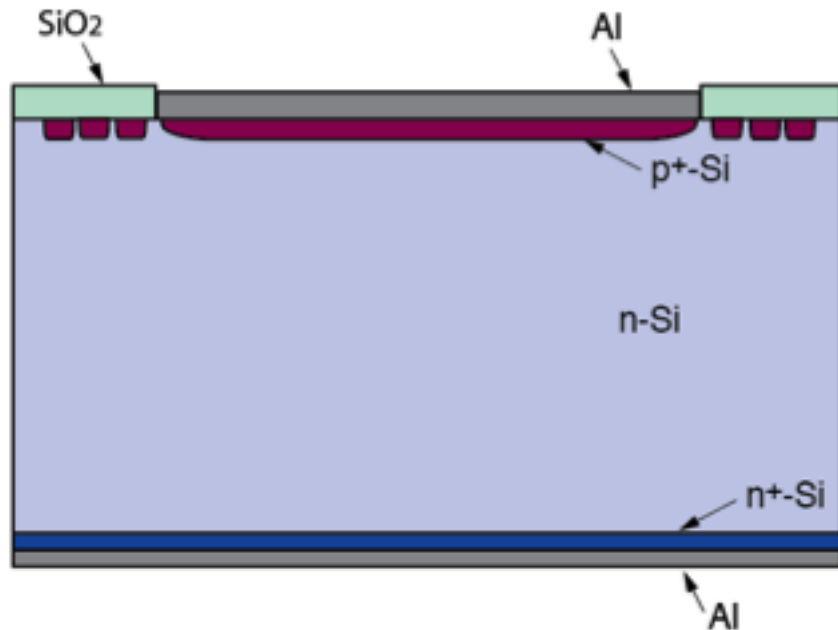
Detector structures:

1. Pad detector
2. Microstrip detectors: single sided
DC coupled, AC coupled, biasing methods
3. Double-sided microstrip detectors
4. Hybrid pixel detectors
5. Silicon drift detectors
6. CCDs
7. Monolithic active pixel detectors
8. 3D detectors



1. Pad detector

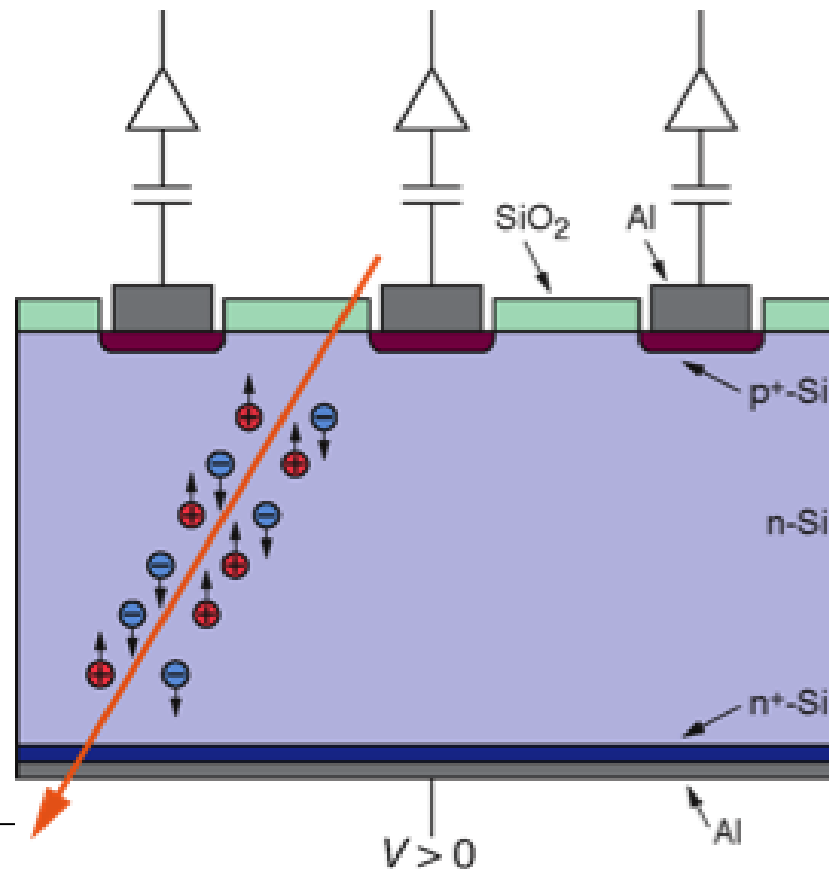
The most simple detector is a large surface **diode** with guard ring(s)



2. Microstrip detectors: DC coupling

Traversing charged particles create e-h⁺ pairs in the depletion zone (about 30,000 pairs in standard detector thickness).

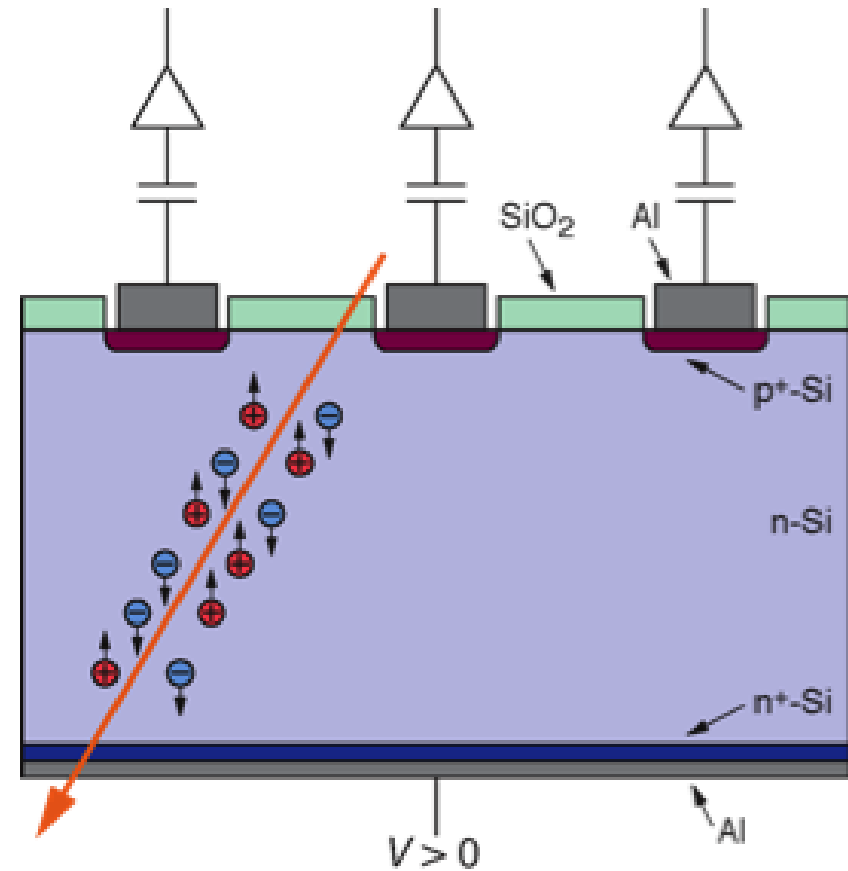
These charges drift to the electrodes. The drift (current) creates the signal which is amplified by an amplifier connected to each strip. From the signals on the individual strips the position of the traversing particle is deduced.



2. Microstrip detectors: DC coupling

A typical n-type Si strip detector:

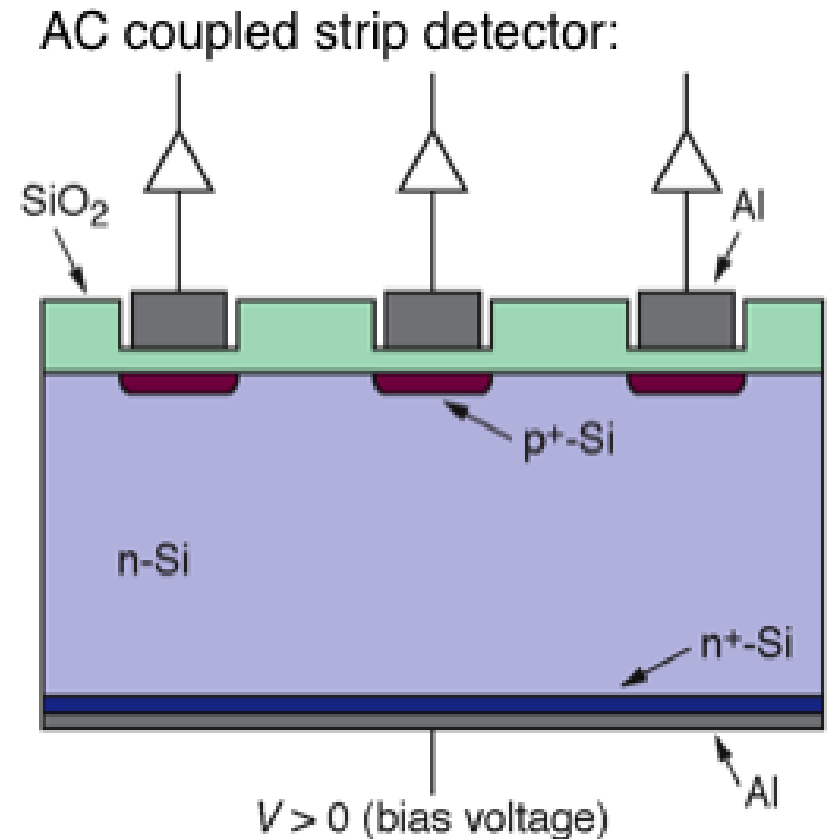
- p+n junction:
 $N_a \approx 10^{15} \text{ cm}^{-3}$, $N_d \approx 1\text{--}5 \cdot 10^{12} \text{ cm}^{-3}$
- n-type bulk: $> 2 \text{ k}\Omega\text{cm}$
- thickness $300 \text{ }\mu\text{m} \rightarrow 22,500 \text{ e-h pairs}$
- Operating voltage $< 200 \text{ V}$
- n+ layer on backplane to improve ohmic contact
- Aluminum metallization
- Strip pitch $25 - 100 \text{ }\mu\text{m}$
- Width of charge distribution $\sim 10 \text{ }\mu\text{m}$
- Possible charge sharing by capacitive coupling ($\sim 1 \text{ pF/cm}$)



2. Microstrip detectors: AC coupling

AC coupling blocks leakage current from the amplifier:

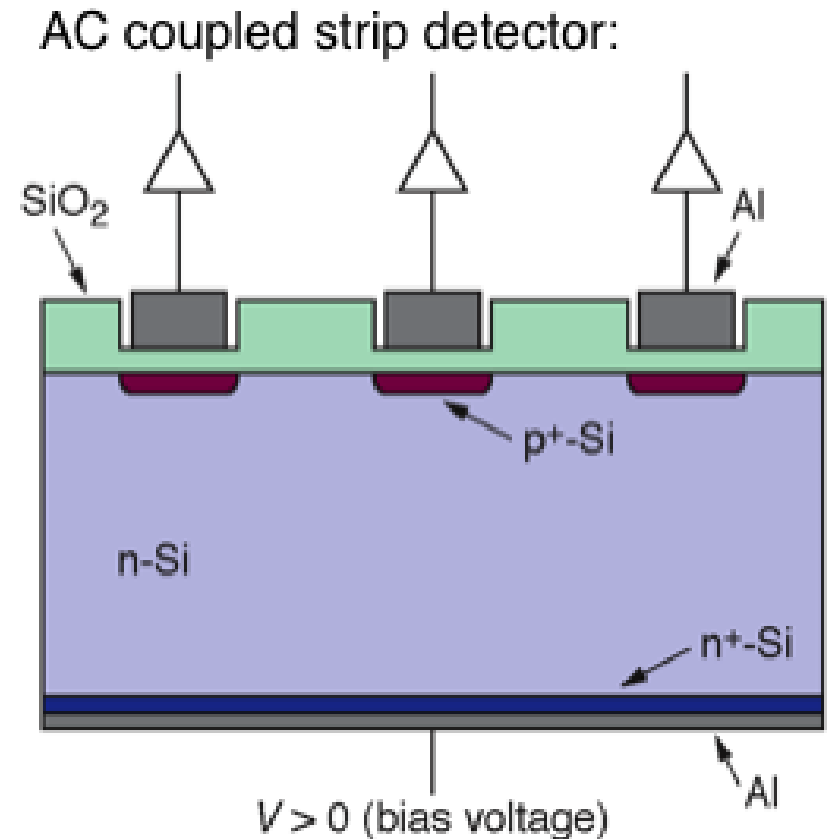
- Integration of coupling capacitances in standard planar process
- Deposition of SiO_2 with a thickness of **100–200 nm** between p+ and aluminum strip
- Depending on oxide thickness and strip width the capacitances are in the range of 8–32 pF/cm
- Problems are shorts through the dielectric (pinholes). Usually avoided by a second layer of Si_3N_4 .



2. Microstrip detectors: AC coupling

AC coupling blocks leakage current from the amplifier:

- Integration of coupling capacitances in standard planar process
- Deposition of SiO_2 with a thickness of **100–200 nm** between p+ and aluminum strip
- Depending on oxide thickness and strip width the capacitances are in the range of 8–32 pF/cm
- Problems are shorts through the dielectric (pinholes). Usually avoided by a second layer of Si_3N_4 .



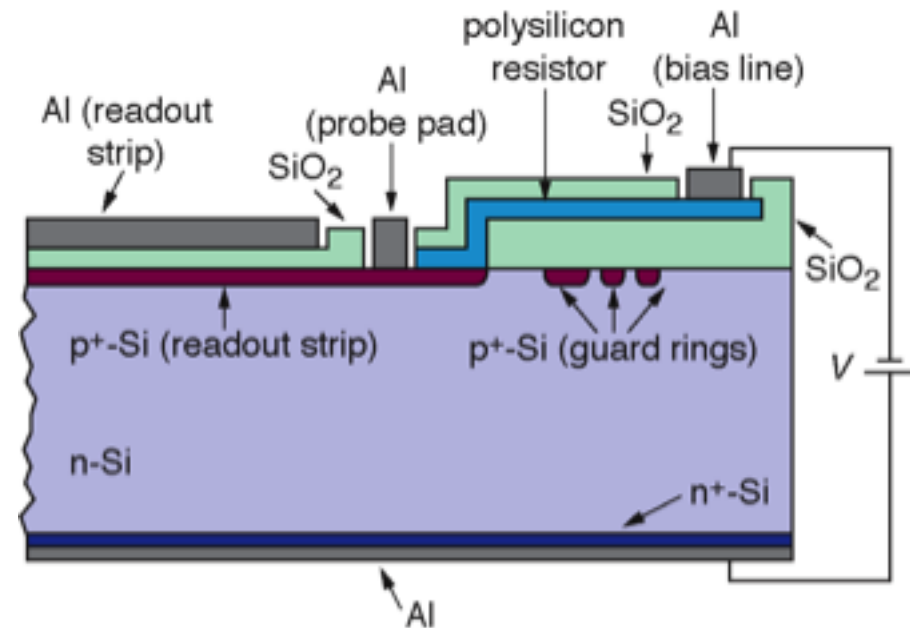
However, the dielectric cuts the bias connection to the strips!

Several methods to connect the bias voltage: polysilicon resistor, punch through bias, FOXFET bias.

2. AC-coupled microstrips: polysilicon resistors

- Deposition of polycrystalline silicon between p⁺ implants and a common bias line
- Sheet resistance of up to $R_s \approx 250 \text{ k}\Omega/\square$
- To achieve high resistor values winding poly structures are deposited. Depending on width and length a resistor of up to $R \approx 20 \text{ M}\Omega$ is achieved ($R = R_s \cdot \text{length}/\text{width}$).
- Drawback: Additional production steps and photo-lithographic masks required.

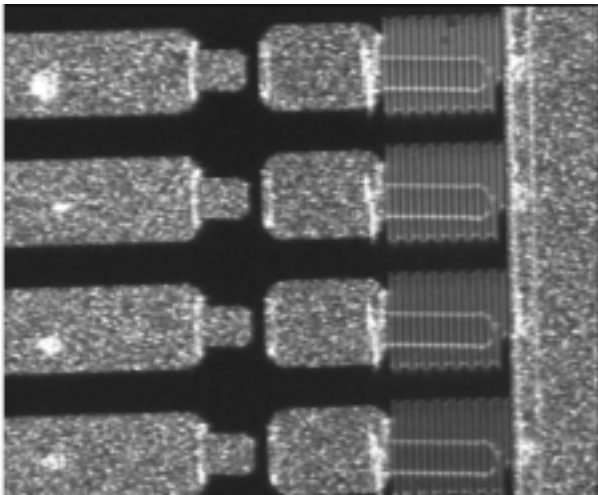
Cut through an AC coupled strip detector with integrated poly resistors



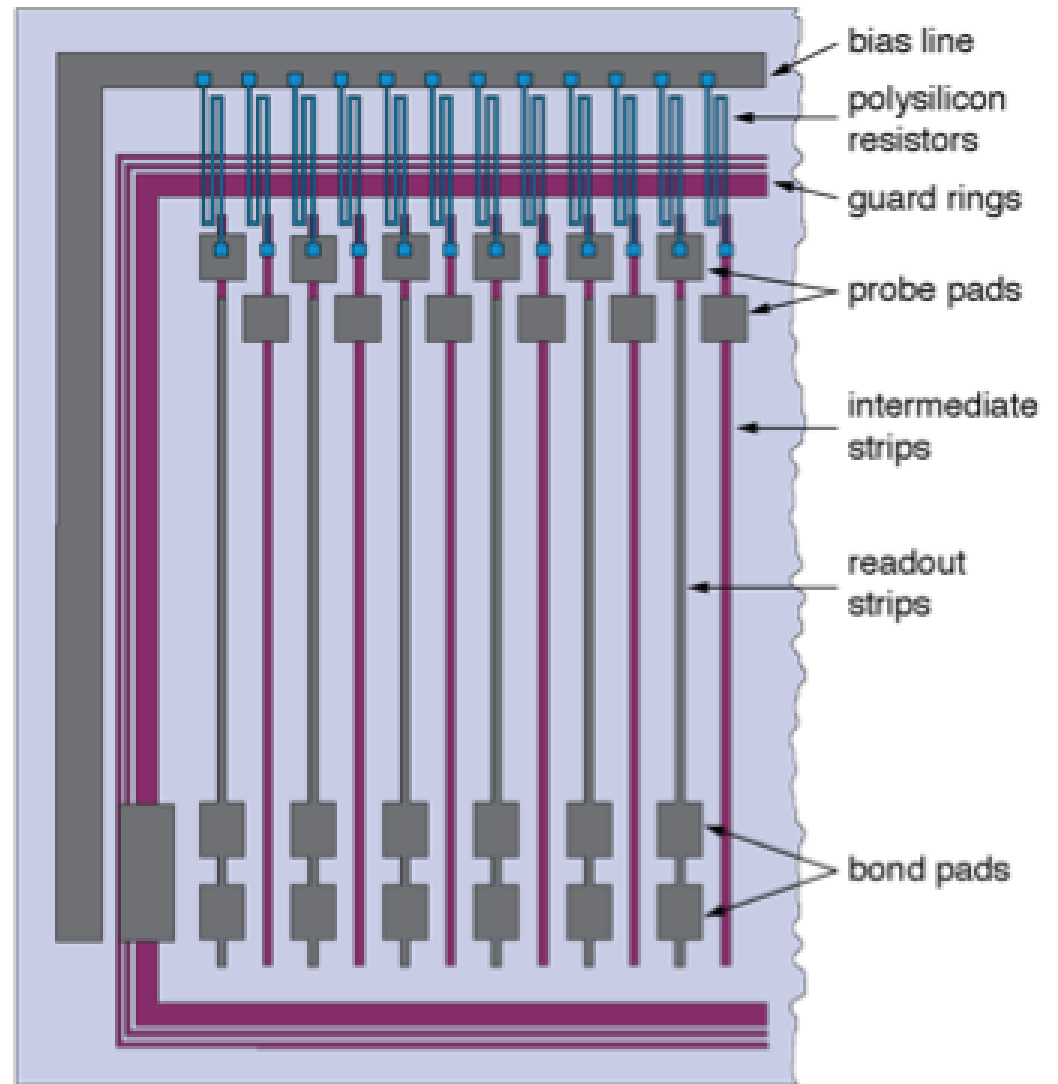
2. AC-coupled microstrips: polysilicon resistors

Top view of a strip detector with polysilicon resistors:

CMS-Microstrip-Detector: close view of area with polysilicon resistors, probe pads, strip ends.



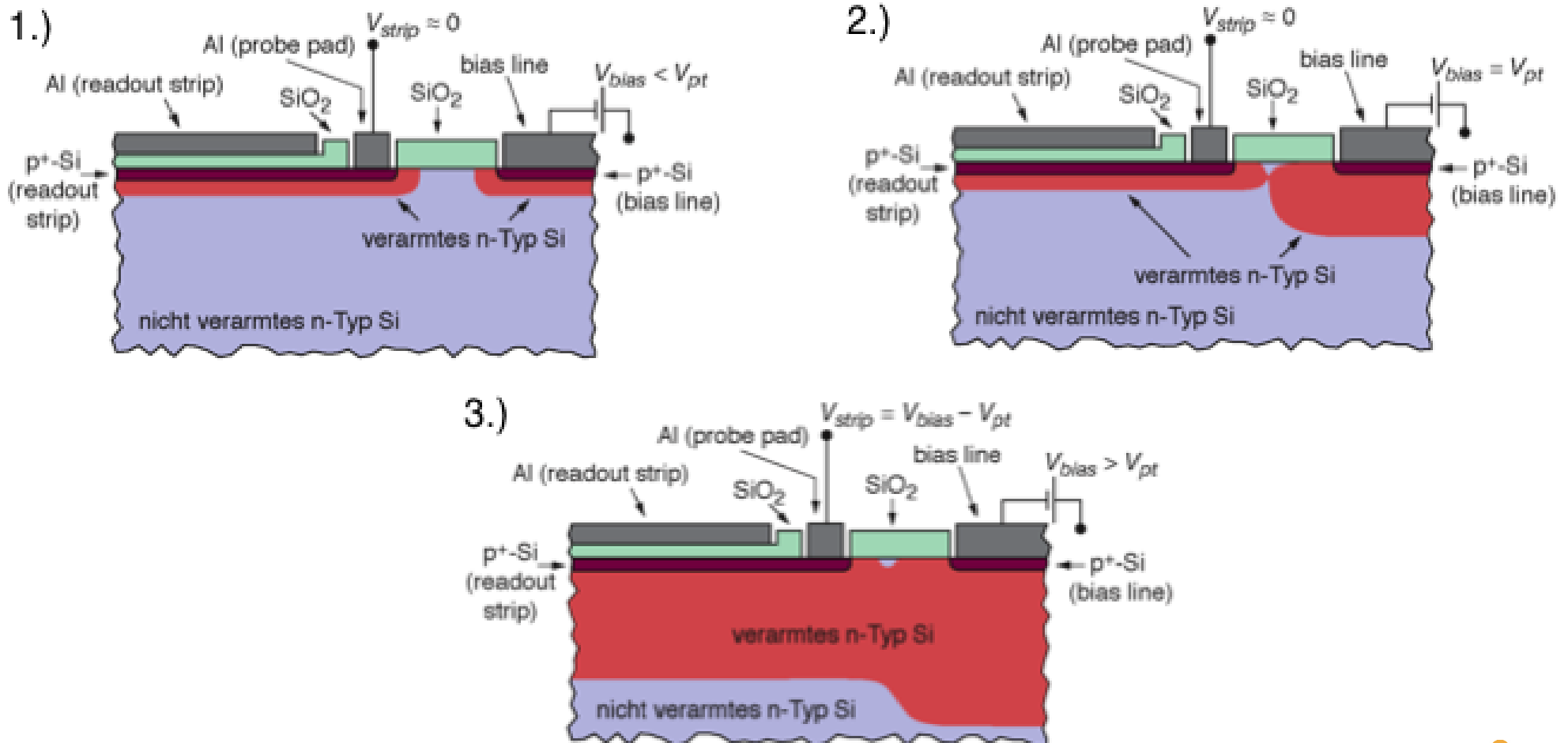
CMS Collaboration, HEPHY Vienna



2. AC-coupled microstrips: punch-through bias

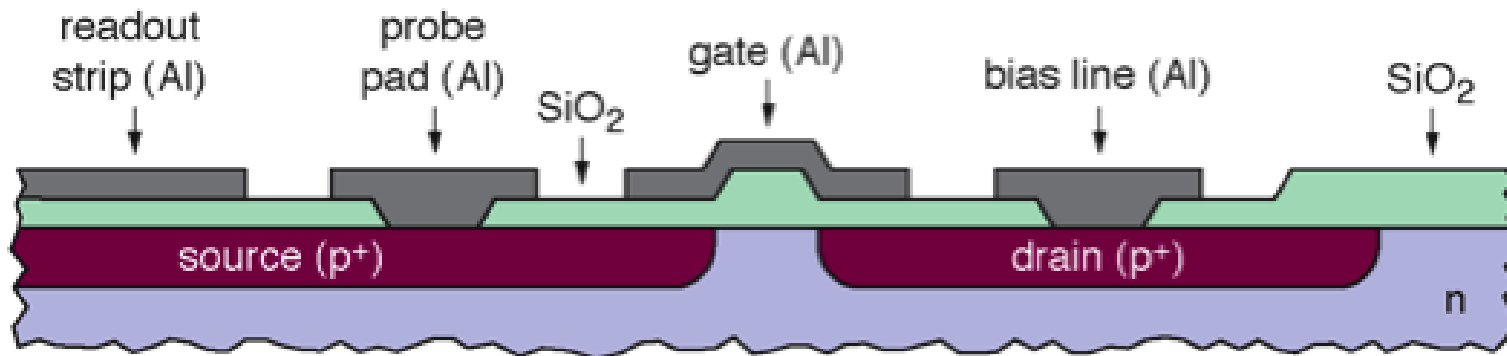
Punch through effect: figures show the increase of the depletion zone with increasing bias voltage (V_{pt} = punch through voltage).

Advantage: No additional production steps required.



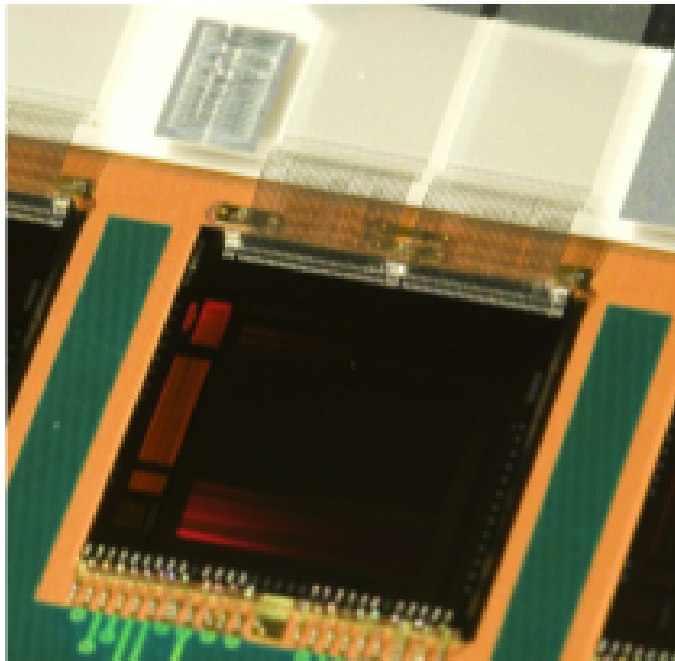
2. AC-coupled microstrips: FOXFET bias

- Strip p⁺ implant and bias line p⁺ implant are source and drain of a field effect transistor - FOXFET (**Field OXide Field Effect Transistor**).
- A gate is implemented on top of a SiO₂ isolation.
- Dynamic resistor between drain and source can be adjusted with gate voltage.



2. Microstrip: wire bond connection

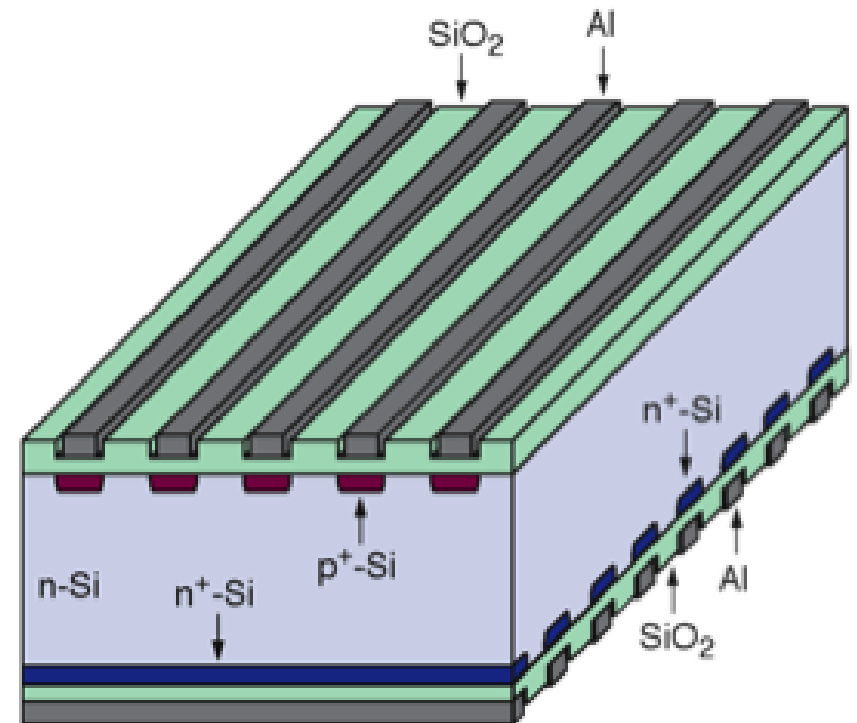
- Ultrasonic welding technique
typically 25 micron bond wire of Al-Si-alloy
- Fully-automatized system with automatic pattern recognition



3. Double-sided microstrip detectors

- Single sided strip detector measures only one coordinate. To measure second coordinate requires second detector layer.
- Double sided strip detector measures two coordinates in one detector layer (minimizes material).
- In n-type detector the n⁺ backside becomes segmented, e.g. strips orthogonal to p⁺ strips.
- Drawback: Production, handling, tests are more complicated and hence double sided detector are expensive.

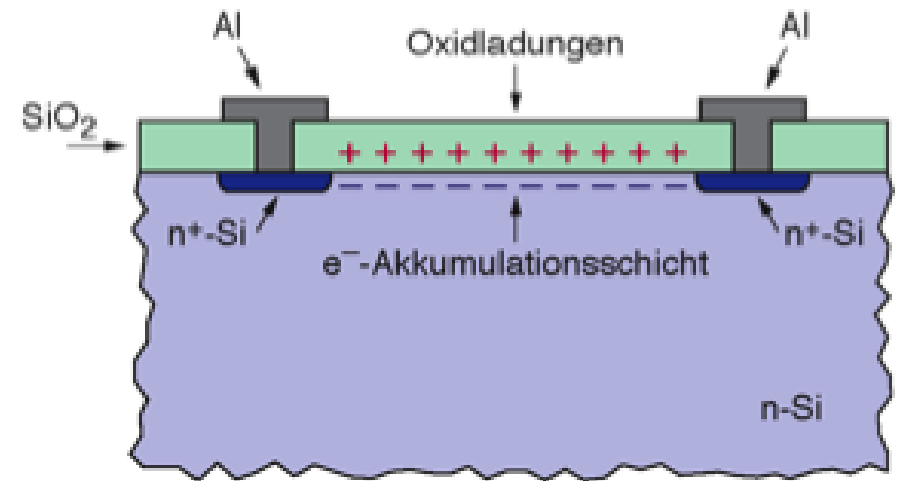
Scheme of a double sided strip detector (biasing structures not shown):



- Holes drift to p⁺ strips
- Electrons drift to n⁺ strips

3. Double-sided microstrip detectors

- Problem with n⁺ segmentation: Static, positive oxide charges in the Si-SiO₂ interface.
 - These positive charges attract electrons. The electrons form an accumulation layer underneath the oxide.
 - n⁺ strips are no longer isolated from each other (resistance ≈ kΩ)
 - Charges generated by through-going particle spread over many strips.
 - **No position measurement possible**
- Solution: Interrupt accumulation layer using p⁺-stops, p⁺-spray or field plates.

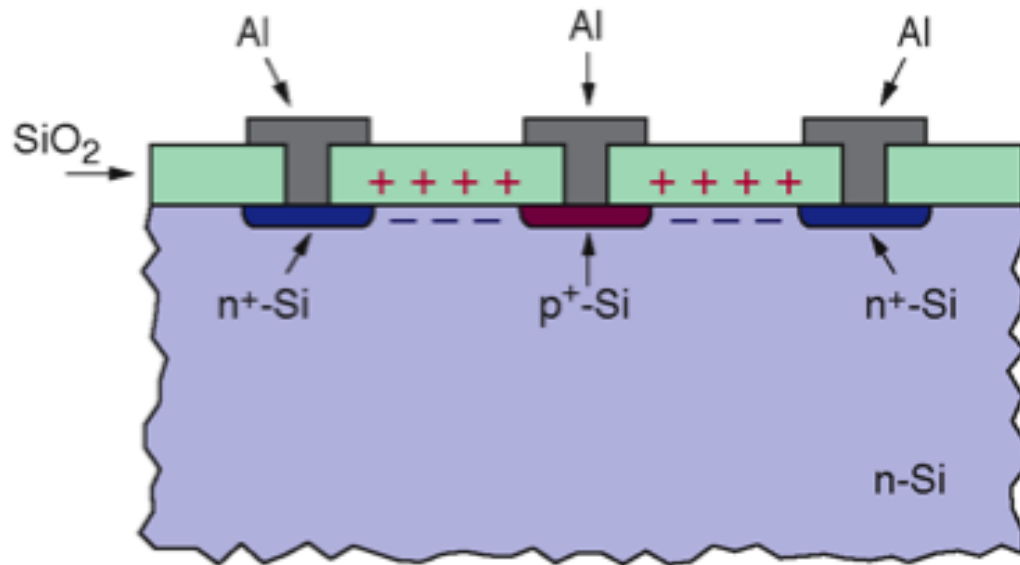


Positive oxide charges cause electron accumulation layer.

3. Double-sided: p⁺-stops

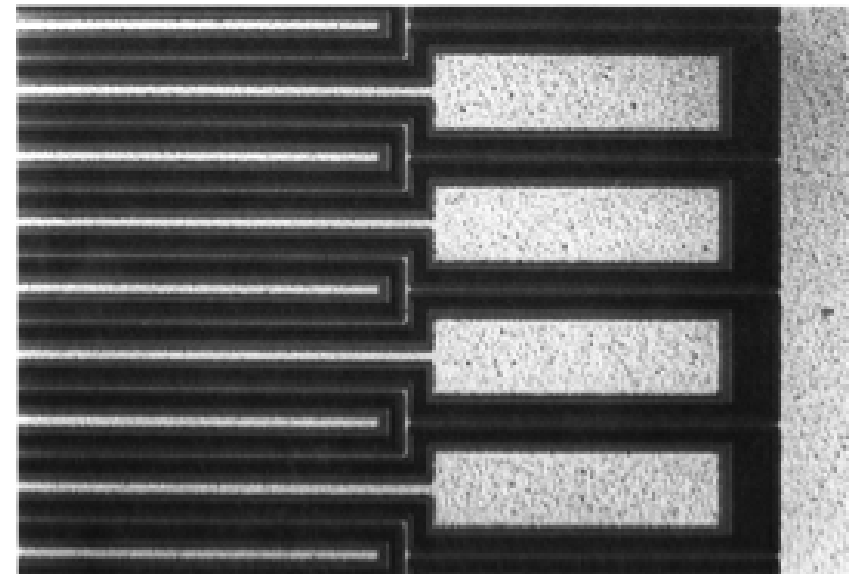
p⁺-implants (p⁺-stops, blocking electrodes) between n⁺-strips interrupt the electron accumulation layer.

→ Interstrip resistance reaches again G



A. Peisert, *Silicon Microstrip Detectors*, DELPHI 92-143 MVX 2, CERN, 1992

Picture showing the n⁺-strips and the p⁺-stop structure:

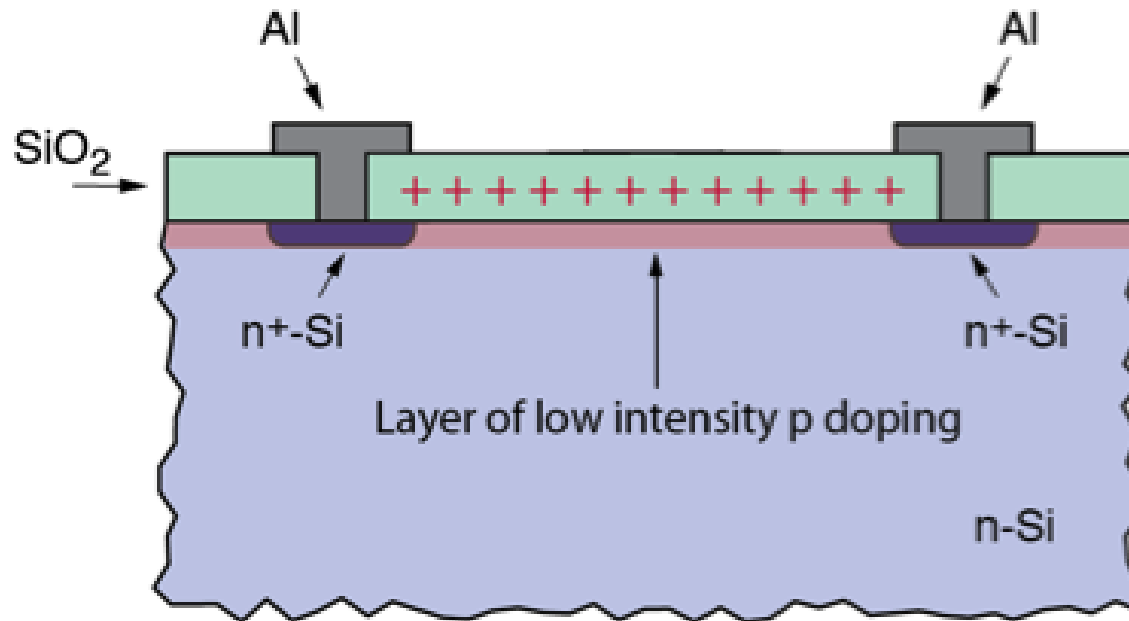


J. Kemmer and G. Lutz, *New Structures for Position Sensitive Semiconductor Detectors*, Nucl. Instr. Meth. A **273**, 588 (1988)

3. Double-sided: p-spray

p doping as a layer over the whole surface.

→ Disrupts the e⁻ accumulation layer.



Some companies use a combination of p⁺ stops and p spray

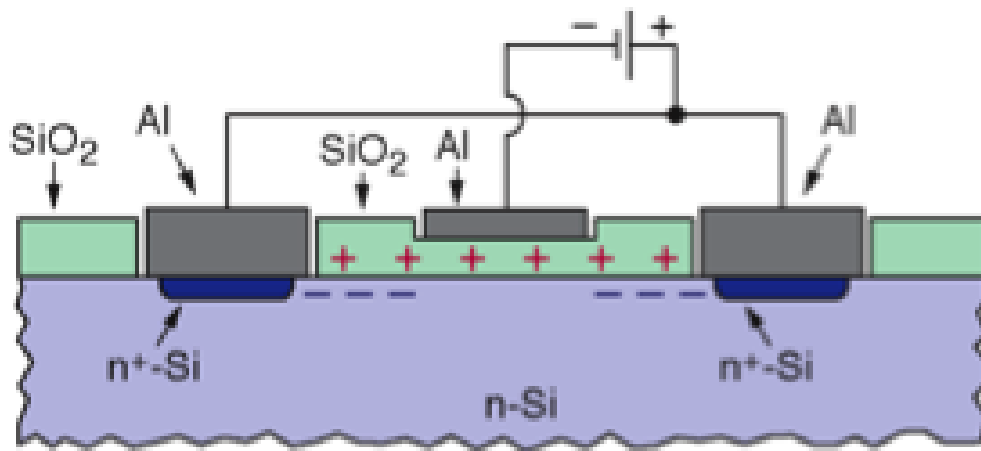
3. Double-sided: field plates

Metal of MOS structure at negative potential compared to the n⁺-strips displace electrons below Si-SiO₂-interface.

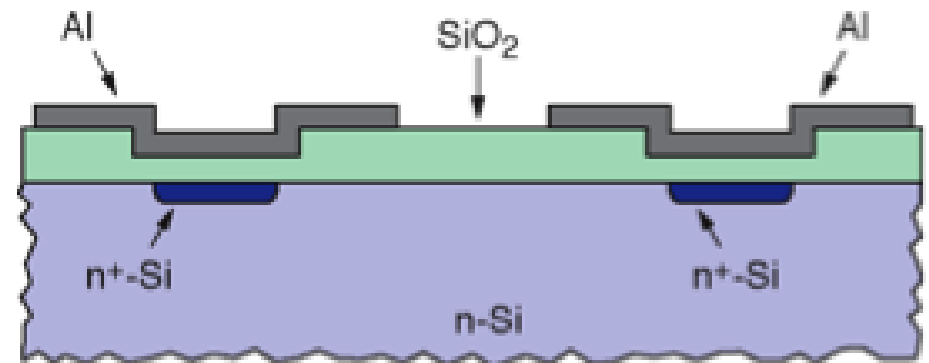
→ Above a threshold voltage n⁺-strips become isolated.

Simple realization of AC coupled sensors: Wide metal lines with overhang in the interstrip region serve as field plates.

A field plate at negative potential interrupts accumulation layer:



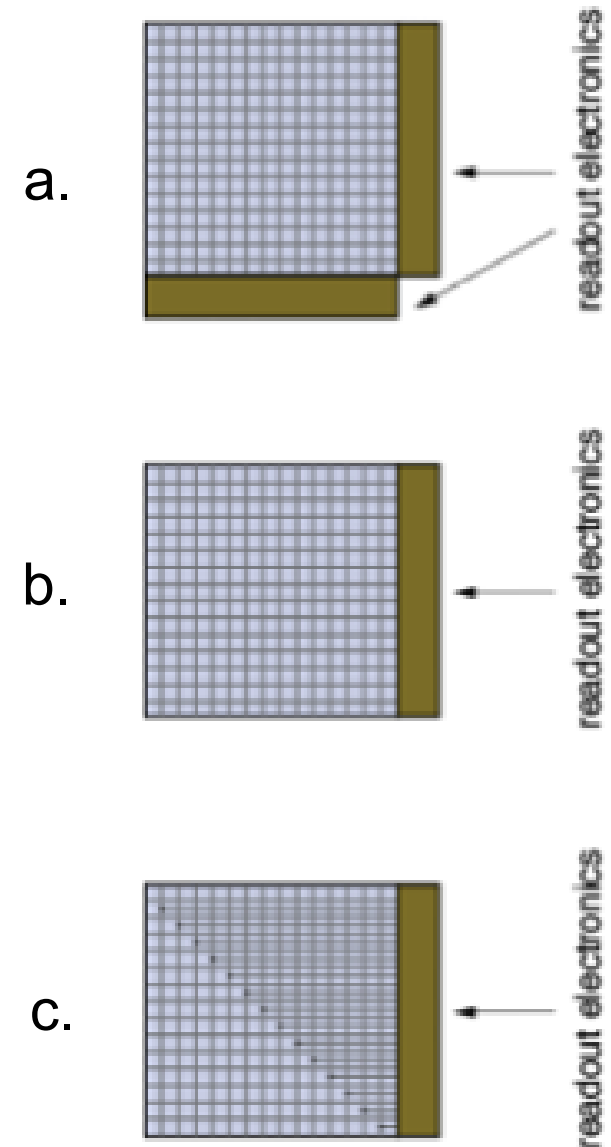
n⁺-strips of an AC coupled detector. The aluminum readout lines act as field plates:



A. Peisert, *Silicon Microstrip Detectors*, DELPHI 92-143 MVX 2, CERN, 1992

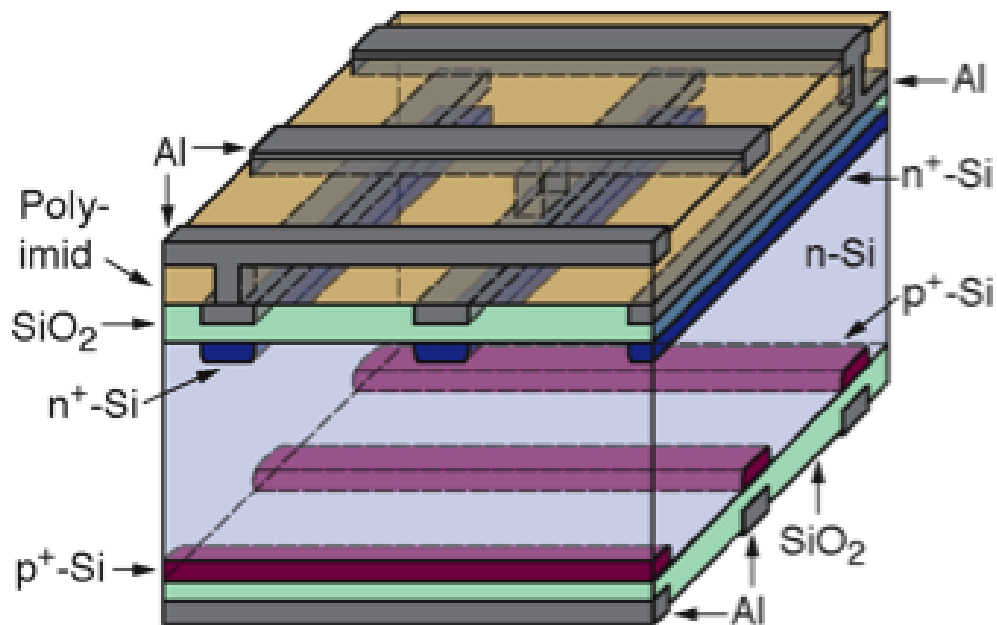
3. Double-sided double metal

- In the case of double sided strip detectors with orthogonal strips the readout electronics is located on two sides (fig. a).
- Many drawbacks for construction and material distribution, especially in collider experiments.
- Electronics only on one side is a preferred configuration (fig. b).
- Possible by introducing a **second metal layer**. Lines in this layer are orthogonal to strips and connect each strips with the electronics (fig. c). The second metal layer can be realized by an external printed circuit board, or better integrated into the detector.

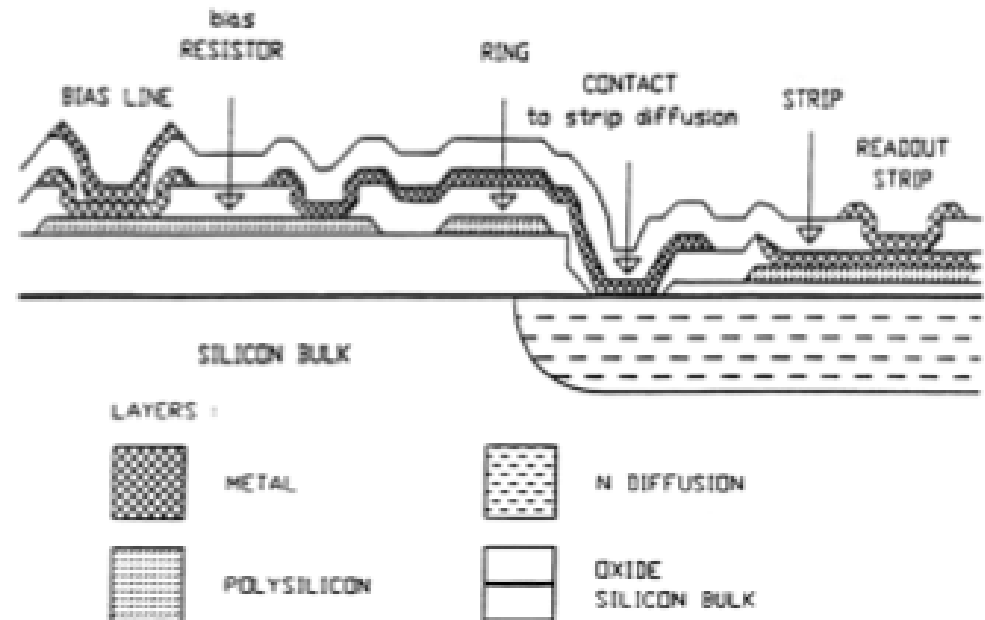


3. Double-sided double metal

3D scheme of an AC coupled double sided strip detector with 2nd metal readout lines (bias structure not shown). The isolation between the two metal layers is either polyimide or SiO₂:



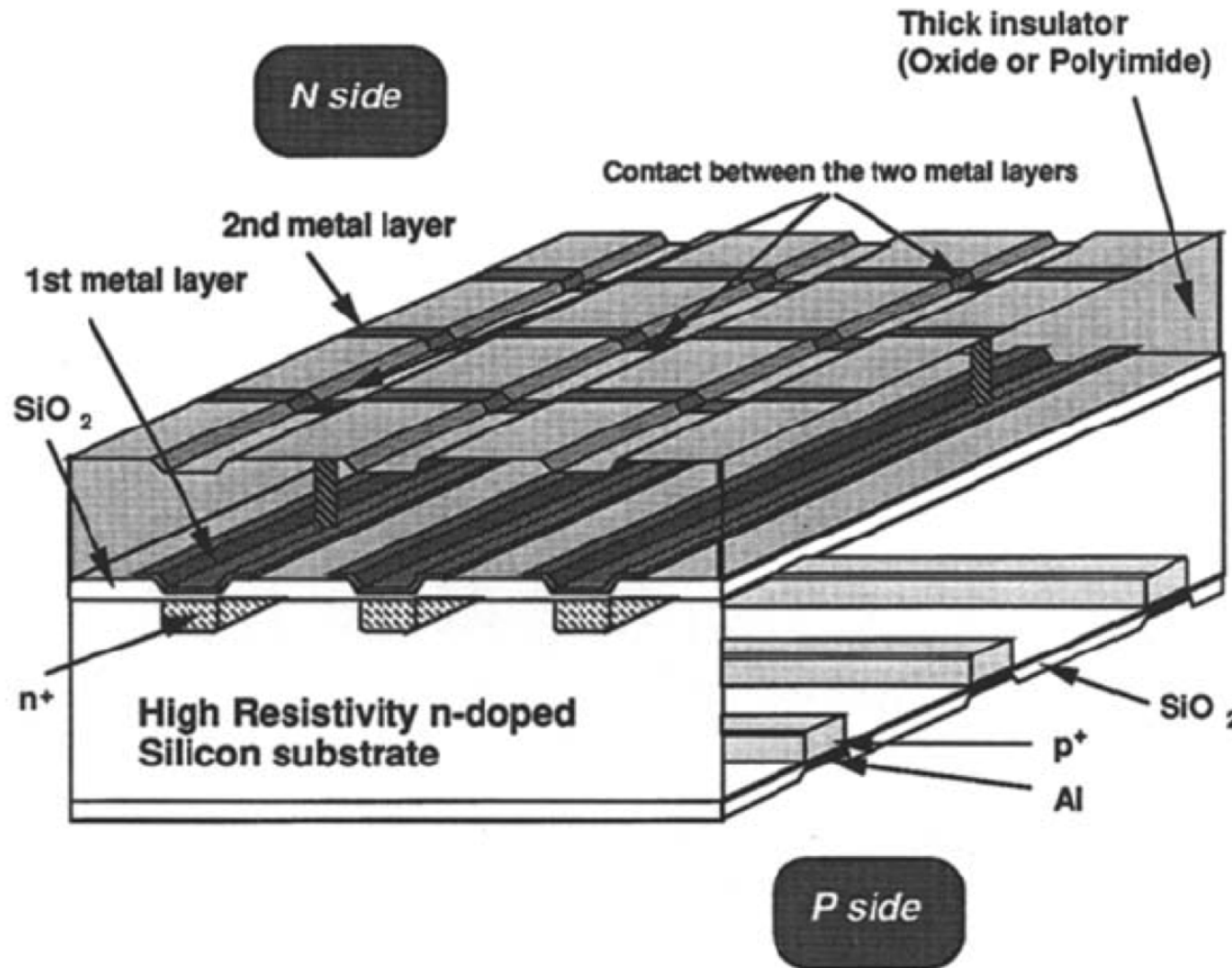
Cross section of the n⁺ side of an AC coupled double sided strip detector with 2nd metal readout lines. Shown is the end of a strip with the bias resistor:



A. Peisert, *Silicon Microstrip Detectors*, DELPHI 92-143 MVX 2, CERN, 1992

3. Double-sided double metal

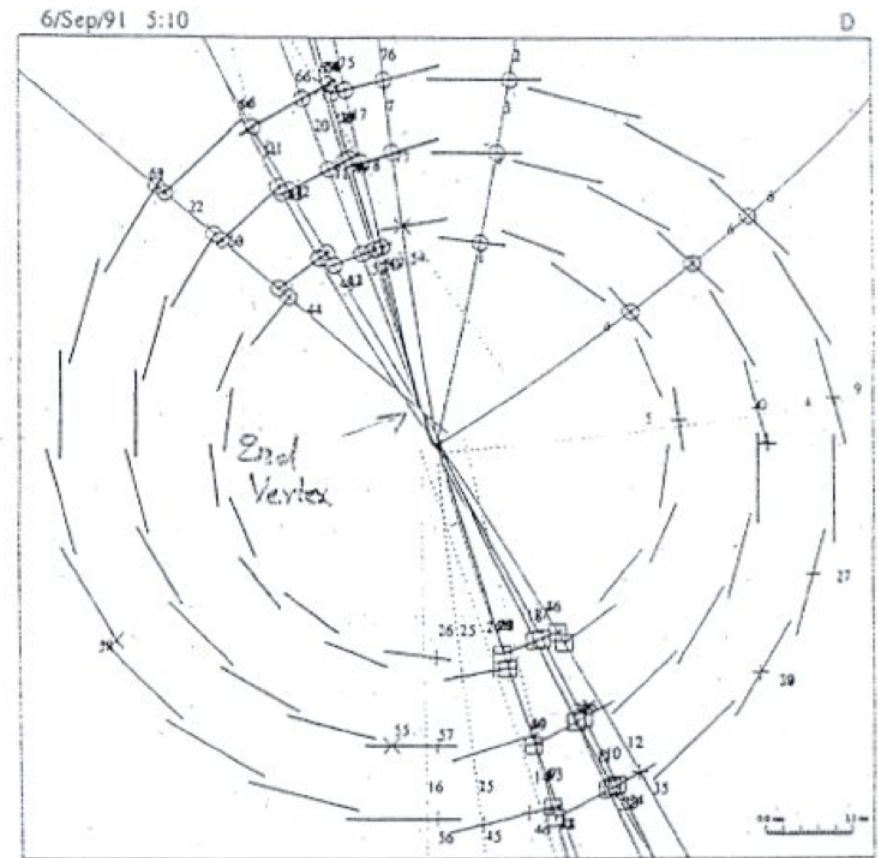
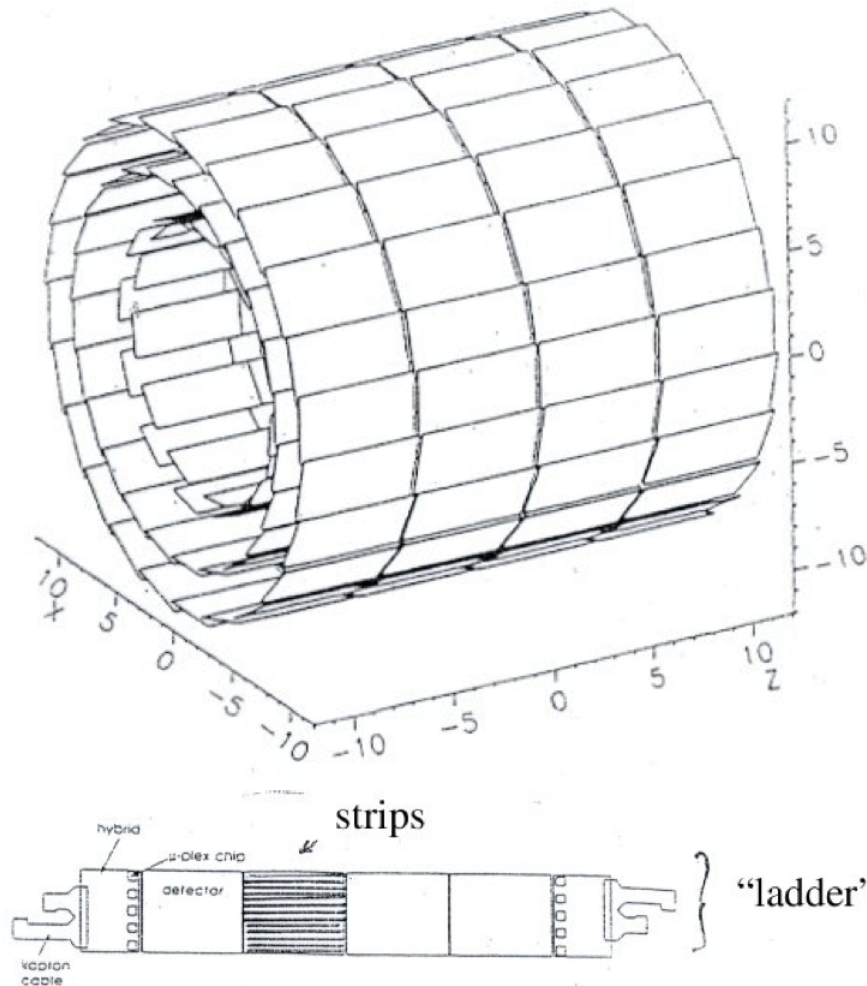
My diploma thesis: double-sided double-metal silicon microstrip detectors for the DELPHI experiment at LEP



3. Double-sided double metal

Initially: only single-sided detectors → only $r\phi$ coordinate measured with high precision

3 coaxial layers of double-sided micro-strips, capacitive coupling, 6.3, 9.0, 10.9 cm from beam axis



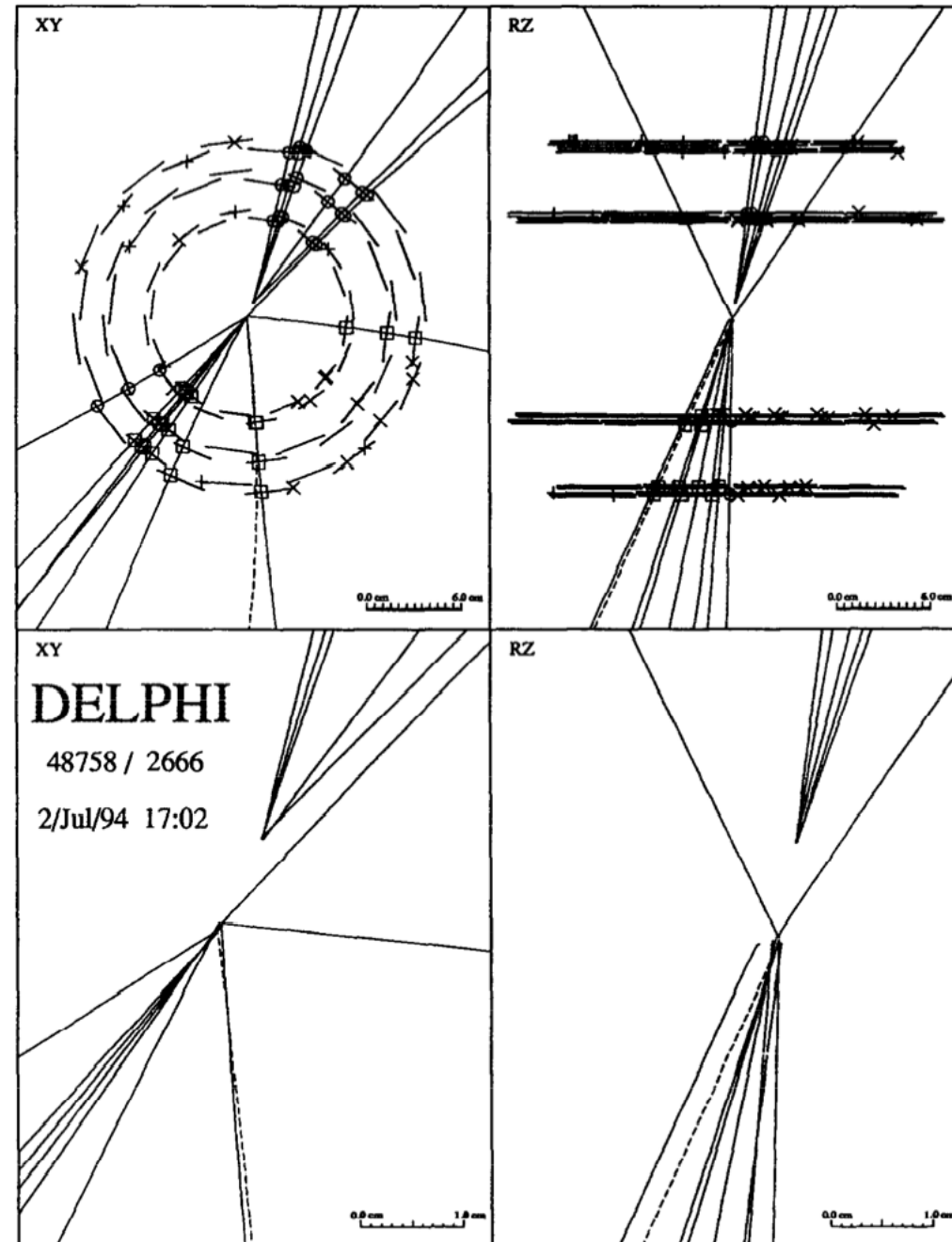
event recorded by the Delphi micro-vertex detector

3. Double-sided double metal

With the double-sided detectors → excellent resolution in rz also!

Very precise tracking in 3D → much more powerful reconstruction of secondary vertices!

V. Chabaud et al., *The DELPHI silicon strip microvertex detector with double sided readout*, NIM A 368 (1996) 314-332



4. Hybrid pixel detectors

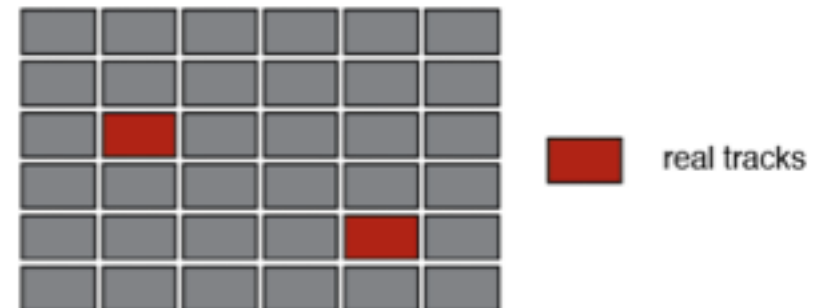
Double sided strip sensors measure the 2 dimensional position of a particle track. However, if more than one particle hits the strip detector the measured position is no longer unambiguous. “Ghost”-hits appear!

True hits and ghost hits in a double sided strip detector in case of two particles traversing the detector:



Pixel detectors produce unambiguous hits!

Measured hits in a pixel detector in case of two particles traversing the detector:



Hybrid = 1 chip with the sensing pixels + 1 chip with the electronics

4. Hybrid pixel detectors

- Typical pixel size is 50 μm x 50 μm .
- If signal pulse height is not recorded, resolution is the digital resolution:

$$\sigma_x = \frac{d}{\sqrt{12}}$$

d = pixel dimension

~14 μm (50 μm pixel pitch)

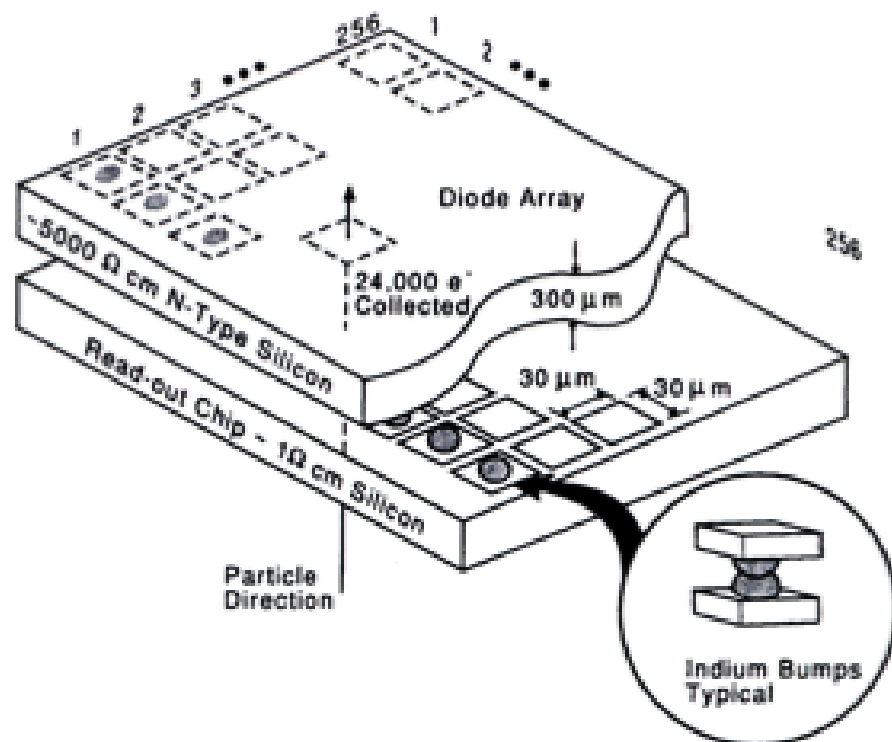
Better resolution achievable with analogue readout

- Small pixel area \rightarrow low detector capacitance (≈ 1 fF/Pixel) \rightarrow large signal to-noise ratio (e.g. 150:1)
- Small pixel volume \rightarrow low leakage current (≈ 1 pA/Pixel)
- Drawback of hybrid pixel detectors: Large number of readout channels
 - Large number of electrical connections in case of hybrid pixel detectors
 - Large power consumption of electronics..

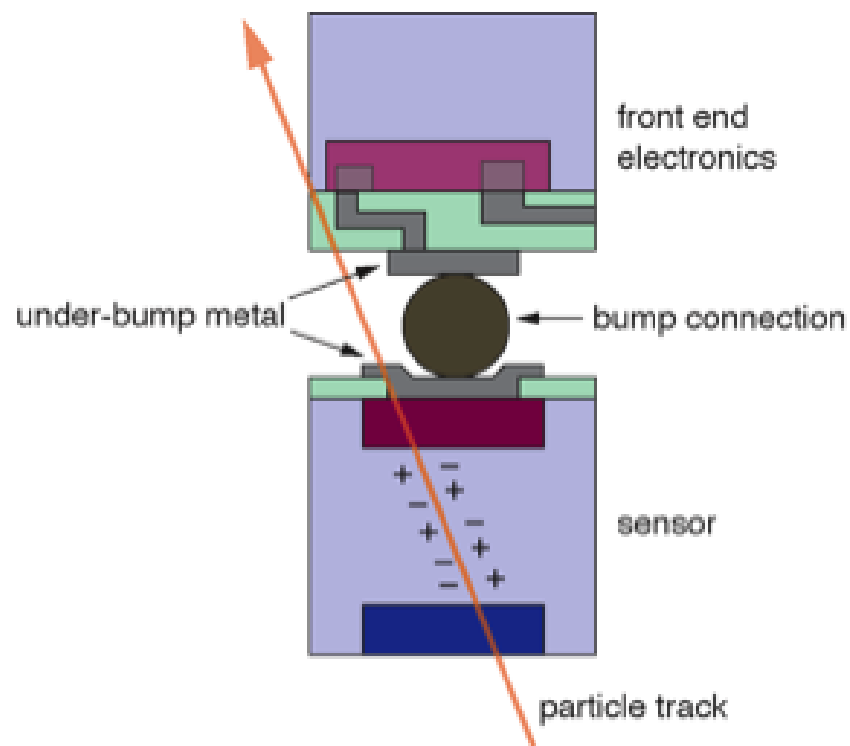
4. Hybrid pixel detectors

“Flip-Chip” pixel detector:

On top the Si detector, below the readout chip, bump bonds make the electrical connection for each pixel.



Detail of bump bond connection. Bottom is the detector, on top the readout chip:



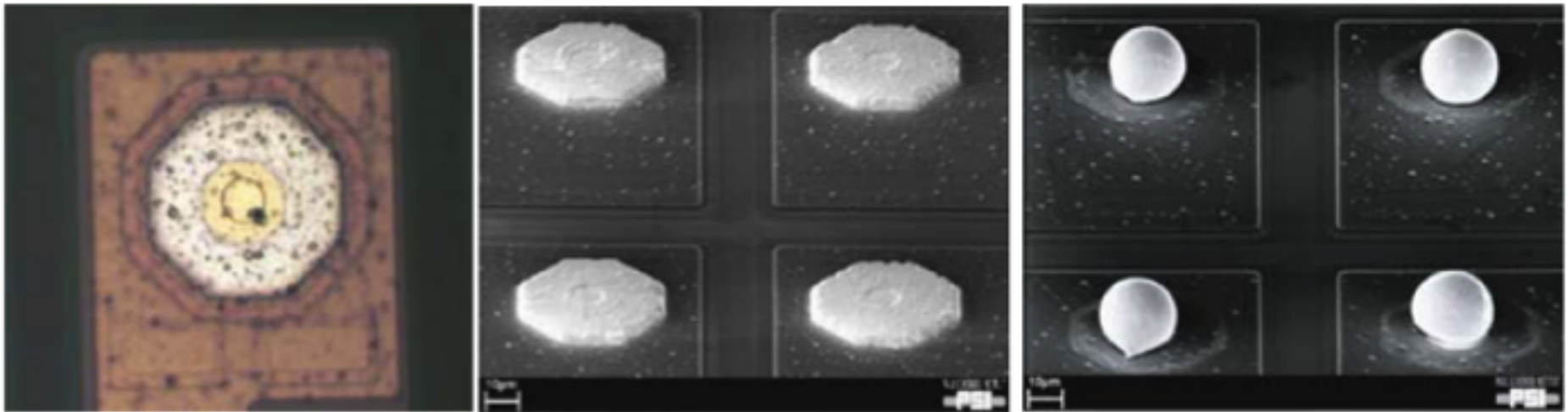
S.L. Shapiro et al., *Si PIN Diode Array Hybrids for Charged Particle Detection*, Nucl. Instr. Meth. A **275**, 580 (1989)

L. Rossi, *Pixel Detectors Hybridisation*, Nucl. Instr. Meth. A **501**, 239 (2003)

4. Hybrid pixel detectors

Electron microscope pictures before and after the reflow production step (where the deposited indium is re-shaped to form spheres).

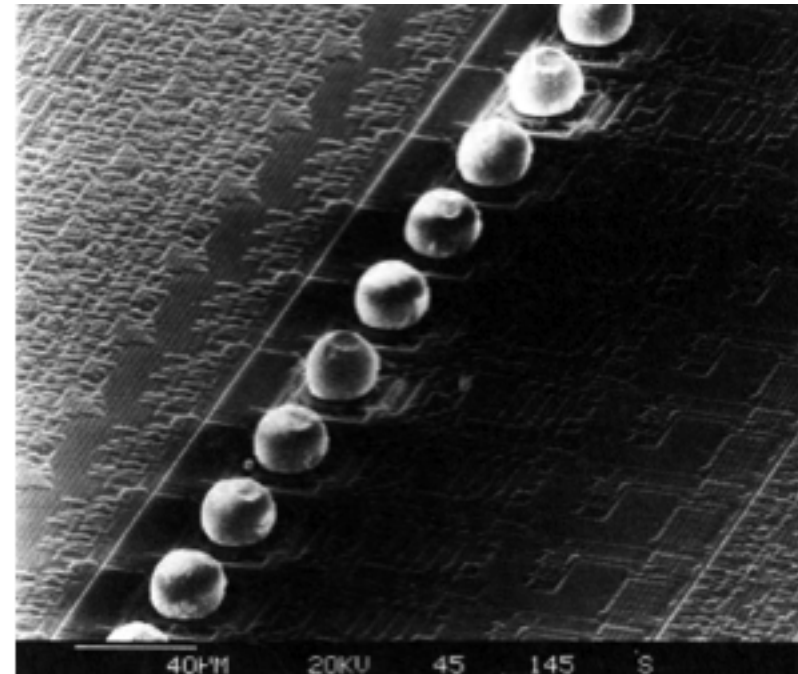
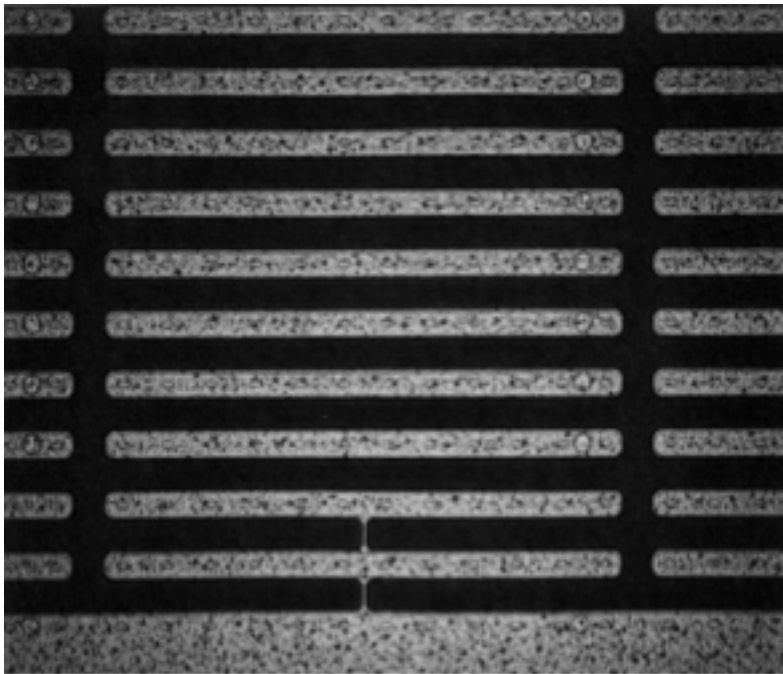
Indium bumps: The distance between bumps is $100\ \mu\text{m}$, the deposited indium is $50\ \mu\text{m}$ wide while the reflowed bump is only $20\ \mu\text{m}$ wide.



C. Broennimann, F. Glaus, J. Gobrecht, S. Heising, M. Horisberger, R. Horisberger, H. Kästli, J. Lehmann, T. Rohe, and S. Streuli, *Development of an Indium bump bond process for silicon pixel detectors at PSI*, *Nucl. Inst. Met. Phys. Res. A565(1)* (2006) 303–308 82

4. Hybrid pixel detectors

Electron microscope picture of pixel detector with long strip.
Left: Detector chip, right: readout chip with bump bonds applied.



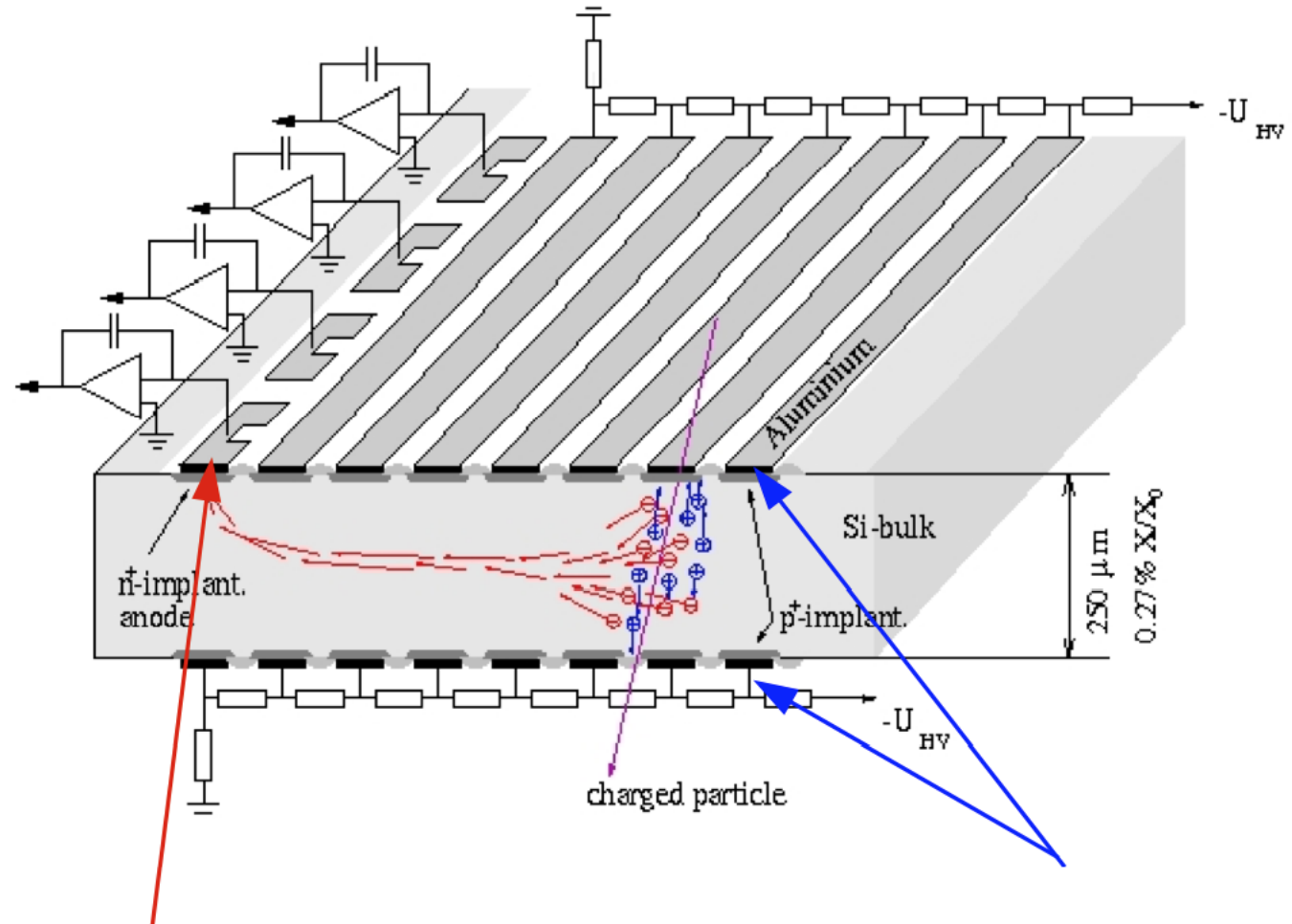
G. Lutz, *Semiconductor Radiation Detectors*, Springer-Verlag, 1999

5. Silicon drift detectors

Proposed by Gatti and Rehak in 1984, first realized in the 1990ies

p⁺ strips and the backplane p⁺ implantation are used to fully deplete the bulk. A drift field transports the generated electrons to the readout electrodes (n⁺).

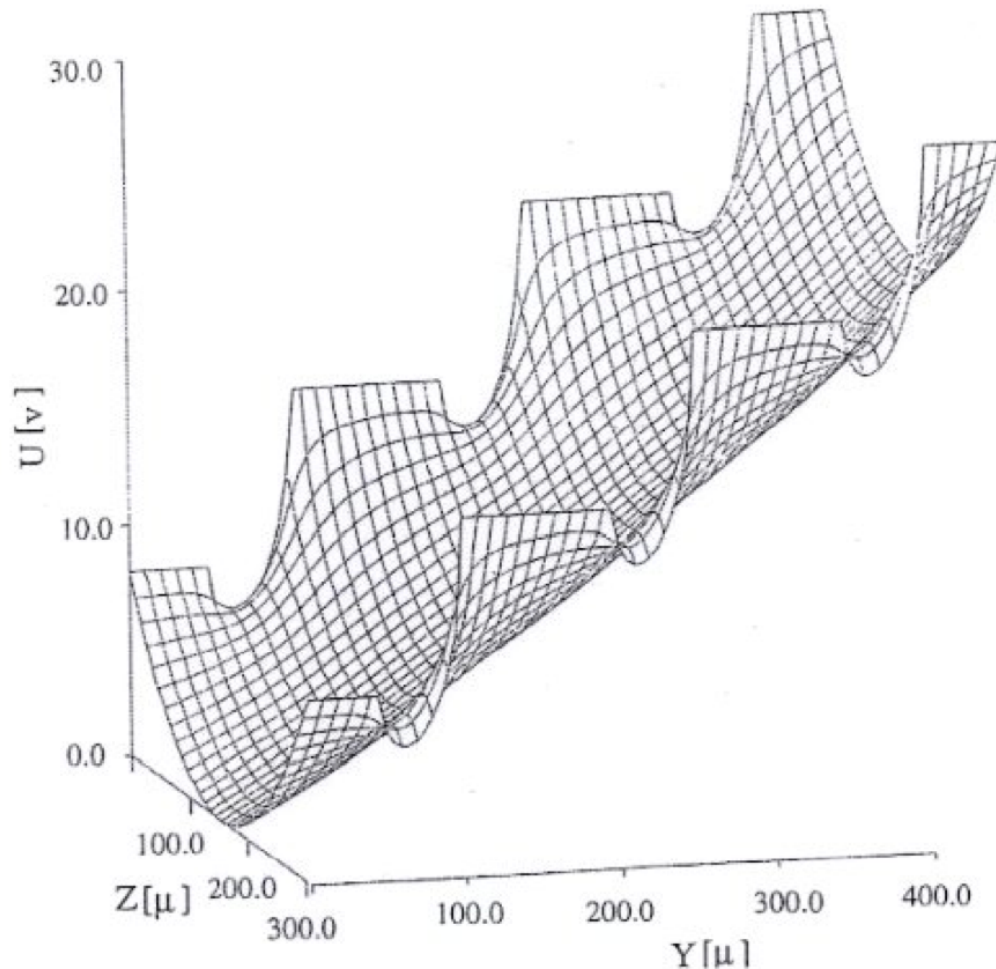
One coordinate is measured by signals on strips, the second by the drift time.



wafer can be fully depleted by reverse bias voltage on a small n⁺ anode implanted on wafer edge

n-type bulk Si with p⁺ electrodes on both flat sides

5. Silicon drift detectors



potential shape in Si drift-chamber:
trough-like shape due to positive space charge in
depletion area, slope from external voltage divider

Charge carriers drift in well
defined E-field

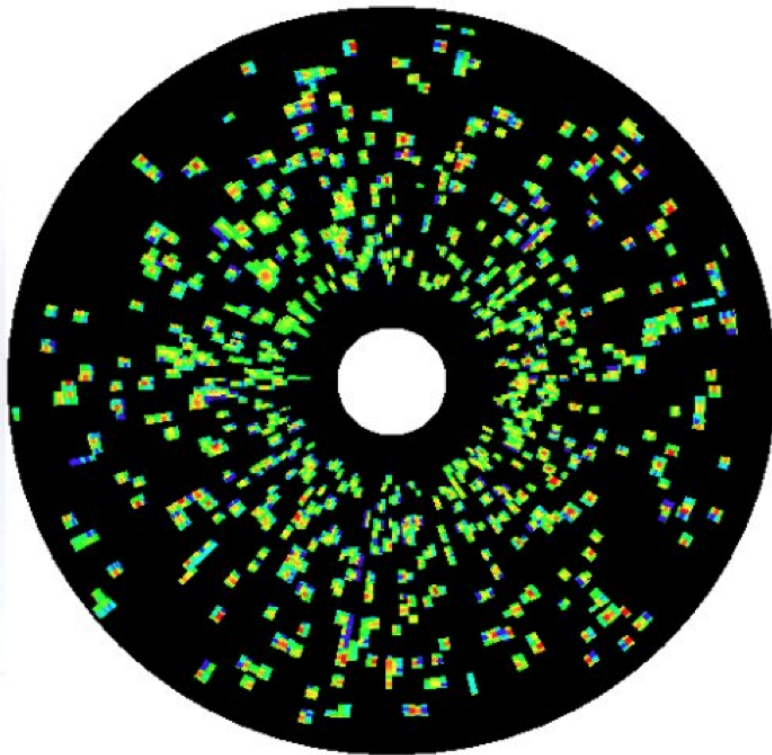
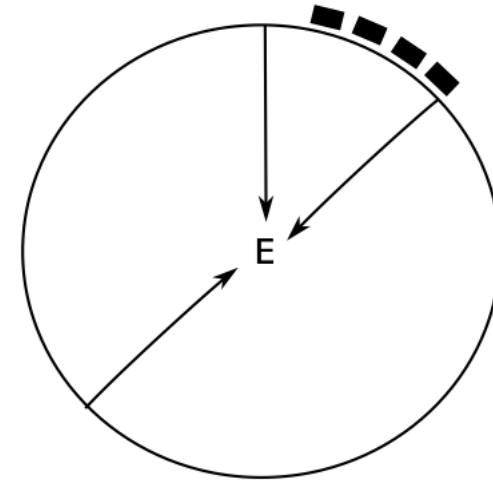
Measurement of drift time →
position of ionizing particle

Typical drift time: a few μs for
5-10 cm
(relatively slow)

5. Silicon drift detectors: CERES

First example: CERES at the SPS:
Radial silicon drift detector (4" wafers)

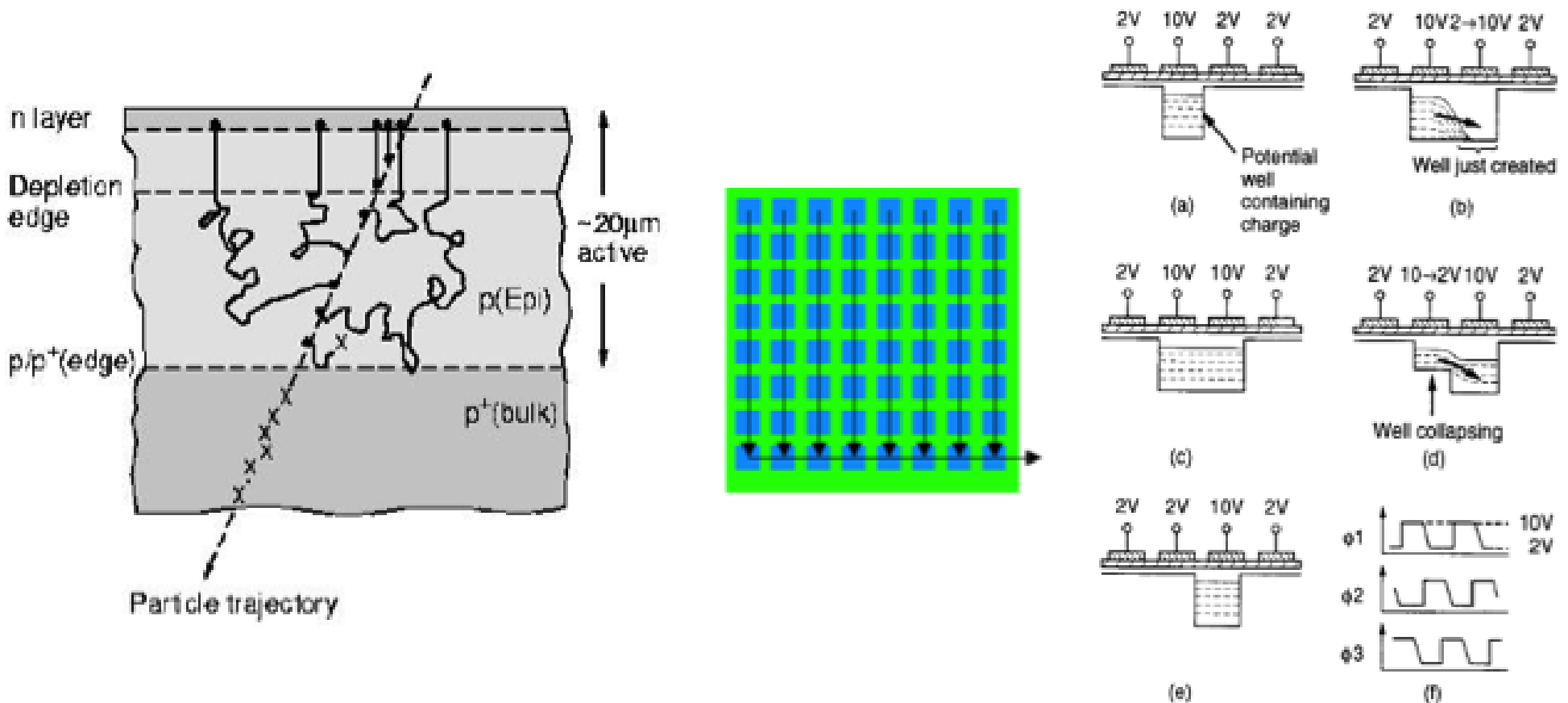
Event display:



active area	52 cm ²
granularity	360 anodes × 256 time bins = 92 160 pixels
max. number of resolved hits	$2 \cdot 10^4$
wafer thickness	250 μm
radiation length	0.27% of X ₀
multiple scattering	≈ 0.54 mrad @ 1 GeV/c

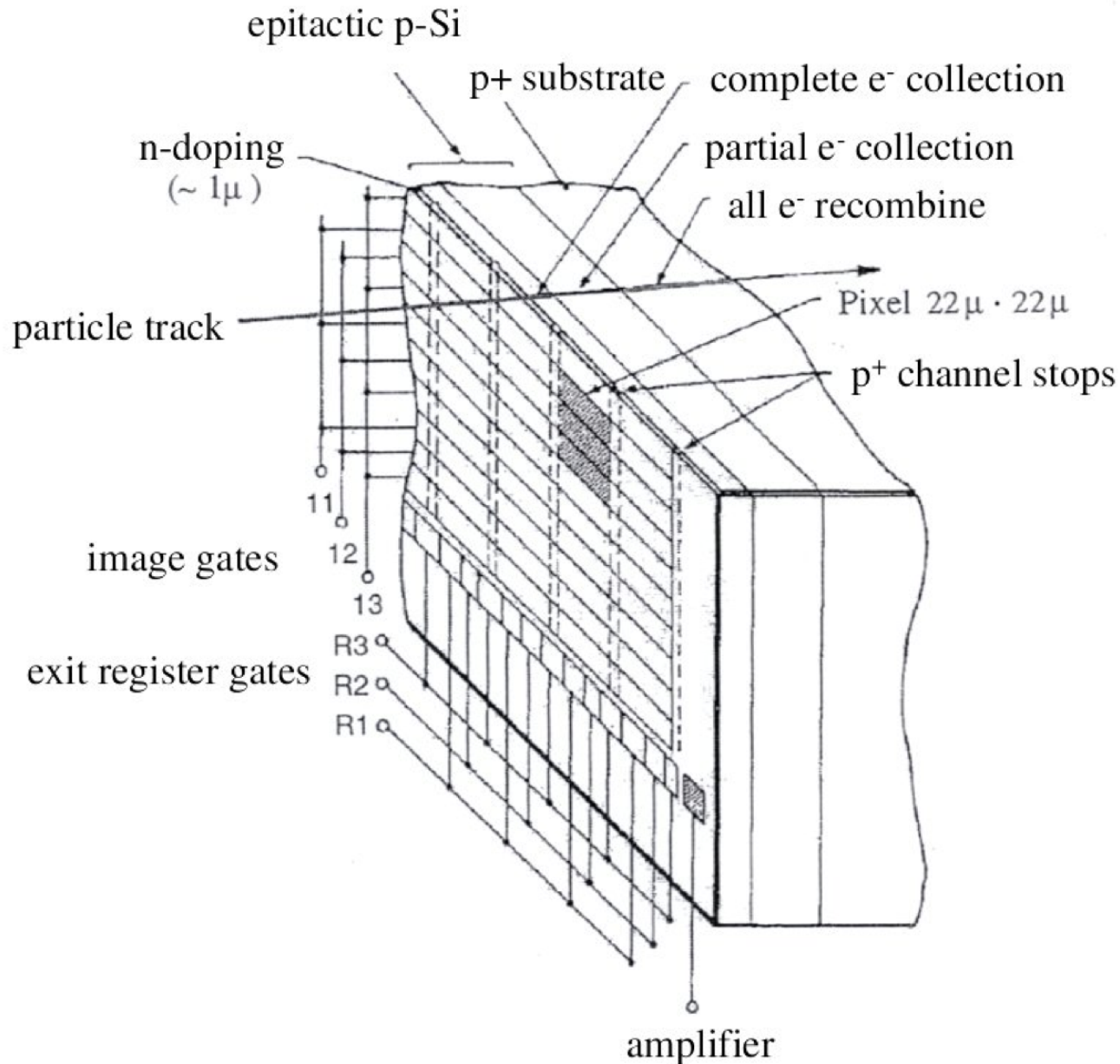
6. Charge-coupled devices (CCD)

Shallow depletion layer (typically 15 μm), relatively small signal, the charge is kept in the pixel and during readout shifted through the columns and through final row to a single signal readout channel:



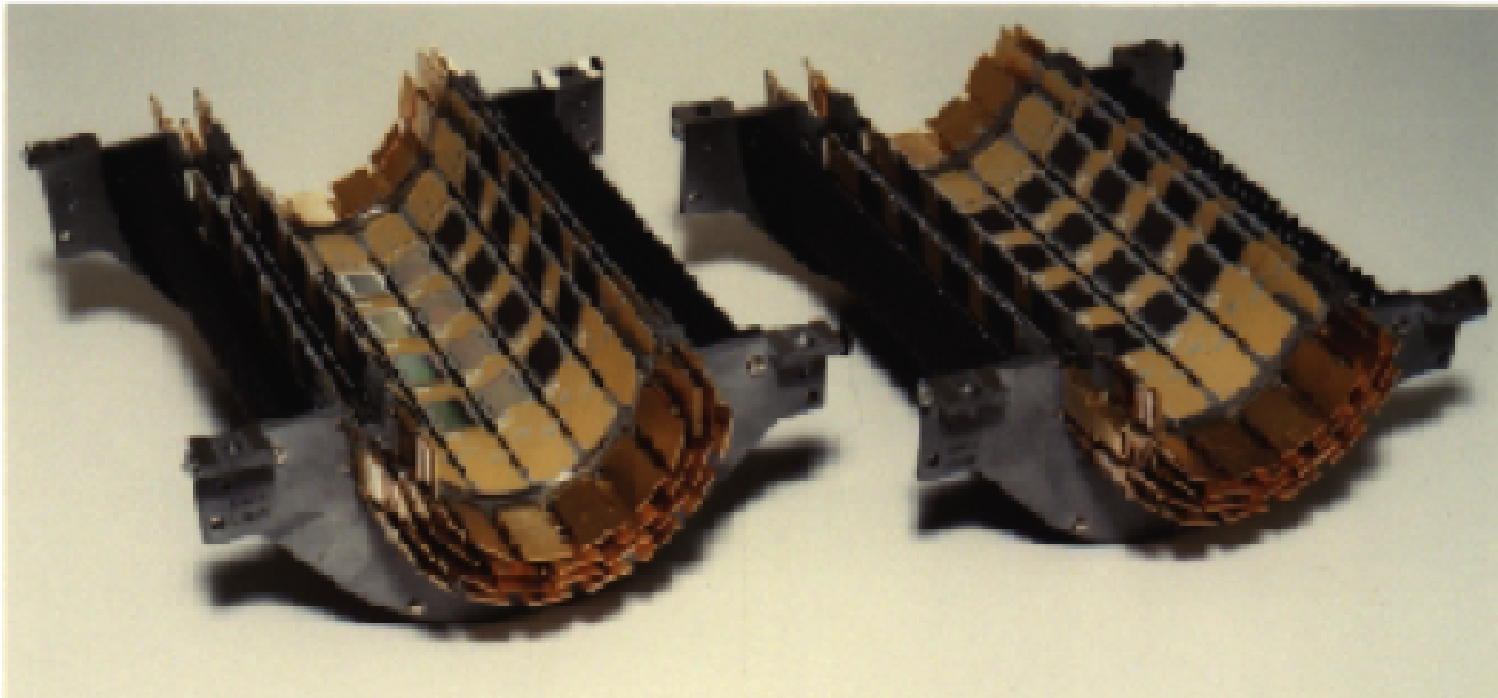
Slow device, hence not suitable for fast detectors.
Improvements are developed, e.g. parallel column readout.

6. Charge-coupled devices (CCD)



6. Charge-coupled devices (CCD): SLD

The SLD (SLAC, USA) silicon vertex detector used large area CCDs. Pixel size $20\ \mu\text{m} \times 20\ \mu\text{m}$, achieved resolution $4\ \mu\text{m}$.



6. Charge-coupled devices (CCD)



The Nobel Prize in Physics 2009

"For groundbreaking achievements concerning the transmission of light in fibers for optical communication"

"For the invention of an imaging semiconductor circuit – the CCD sensor"



Photo: U. Montan

Charles K. Kao

1/2 of the prize



Photo: U. Montan

Willard S. Boyle

1/4 of the prize



Photo: U. Montan

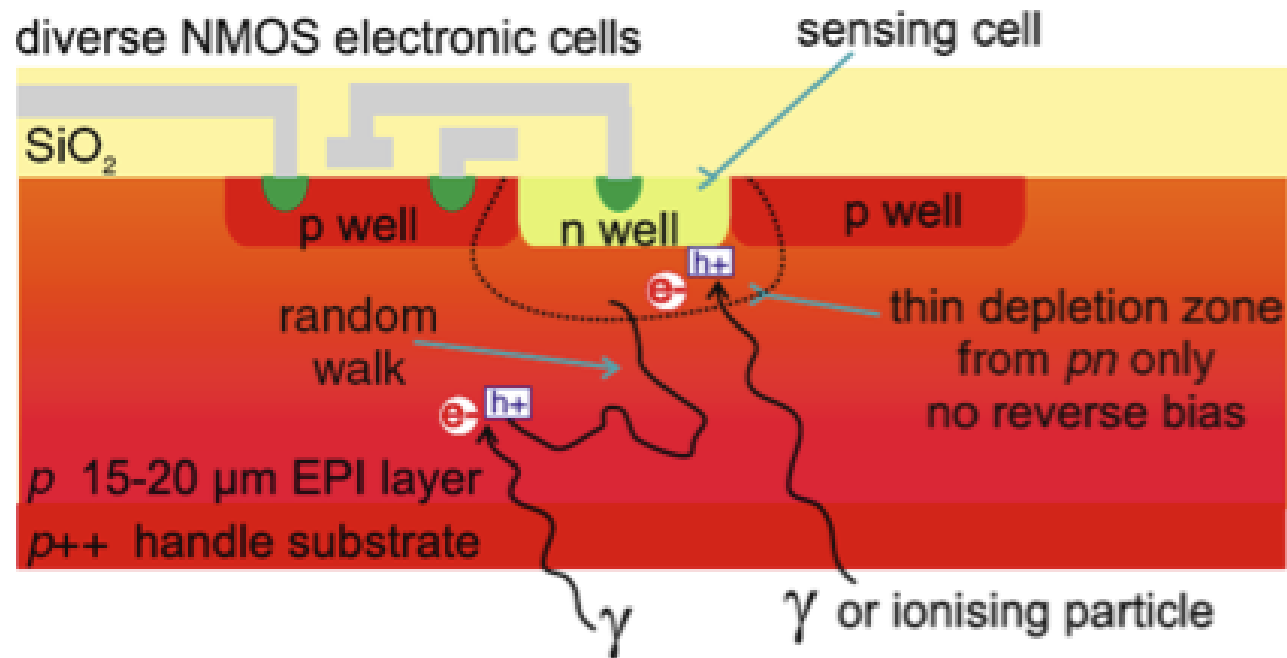
George E. Smith

1/4 of the prize

7. Monolithic active pixel sensors (MAPS)

CMOS

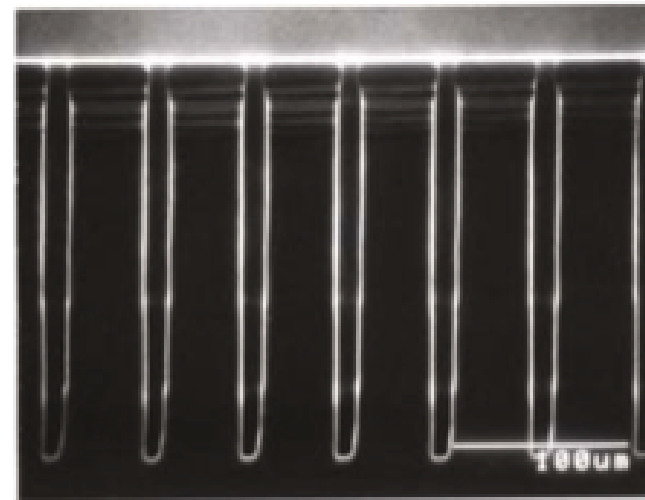
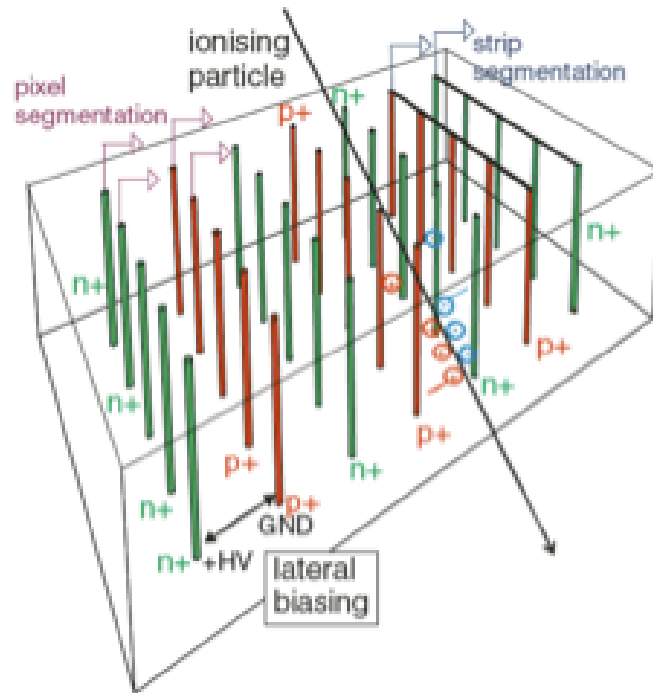
Scheme of a CMOS monolithic active pixel cell with an NMOS transistor. The N-well collects electrons from both ionization and photo-effect.



Evolution of Silicon Sensor Technology in Particle Physics, F. Hartmann, Springer Volume 231, 2009

8. 3D detectors

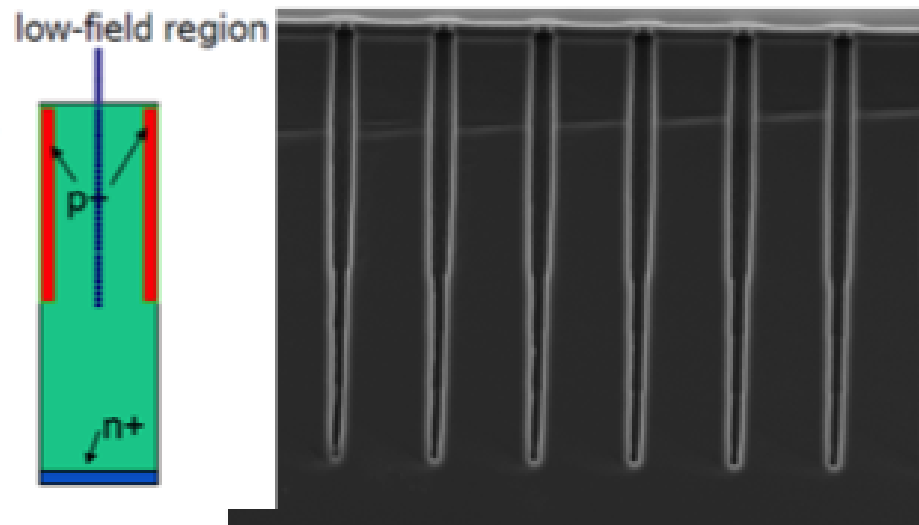
3D detectors are non planar detectors. Deep holes are etched into the silicon and filled with n^+ and p^+ material. Depletion is sideways. The distances between the electrodes are small, hence depletion voltage can be much smaller and charge carriers travel much short distances.



Very radiation tolerant detectors, first use in ATLAS IBL layer.

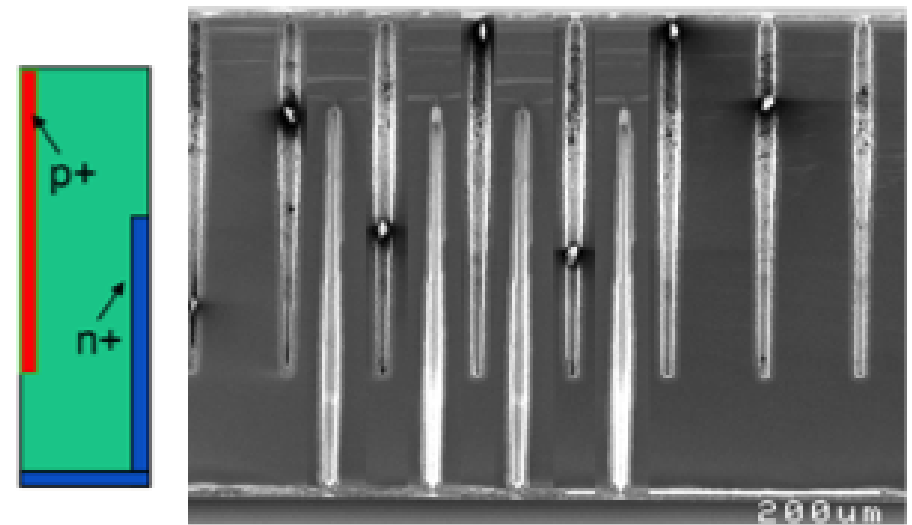
8. 3D detectors: different approaches

Single column:



Low field region between columns

Double-sided double column:



High field, but more complicated

RADIATION DAMAGE

Radiation damage: motivation

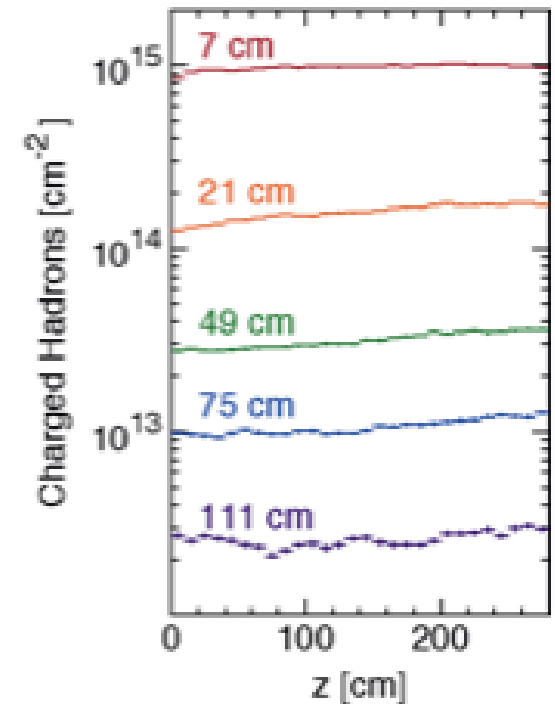
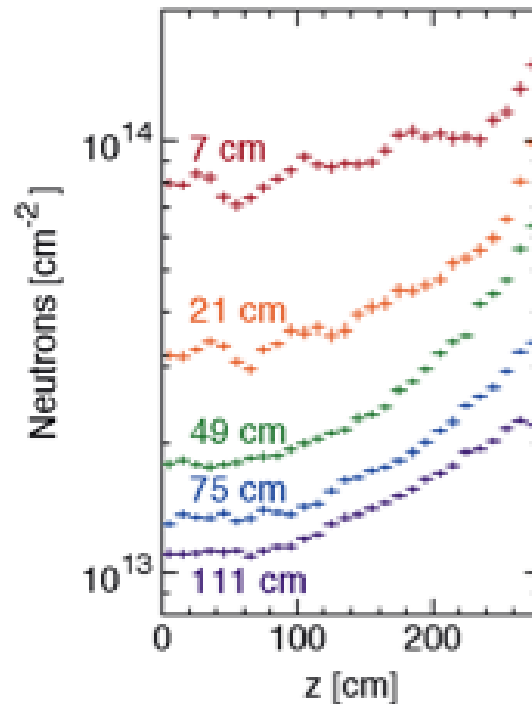
The event rate and as a consequence the irradiation load in experiments at hadron colliders is extreme (e.g. the pp collider LHC, collision energy 14 TeV, event rate = 10^9 /s).

Silicon detectors are the closest to the interaction point!

Expected particle rates for the silicon detector inner layers in CMS integrated over 10 years as a function of the distance from the vertex point and for various radii.

Left: neutrons

Right: charged hadrons



CERN/LHCC 98-6, CMS TDR 5, 20 April 1998

Radiation damage: introduction

- Particles (radiation) interact
 - with the electrons: used for particle detection and results in temporarily effects only.
 - with atoms of the detector material: may cause permanent changes (defects) in the detector bulk.
- One distinguishes between damage inside the detector bulk (**bulk damage**) and damage introduced in the surface layers (**surface damage**).

For the readout electronics (also silicon based!) inside the radiation field only surface damage is relevant.
- Defects may change with time. Therefore one distinguishes also between **primary defects and secondary defects**. The secondary defects appear with time caused by moving primary defects.

Radiation damage: introduction

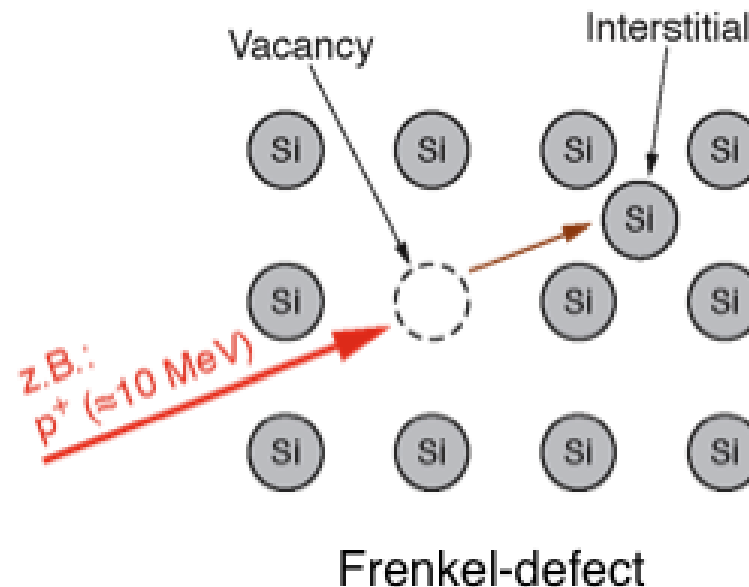
- Radiation induced damage in the semiconductor **bulk** are dislocated atoms from their position in the lattice. Such dislocations are caused by massive particles.
 - Bulk damage is primarily produced by **neutrons, protons and pions.**
- In the amorphous **oxide** such dislocations are not important. The radiation damage in the oxide is due to the charges generated in the oxide. Due to the isolating character of the oxide these charges cannot disappear and lead to local concentrations of these charges.
 - Radiation damage in the oxide is primarily produced by **photons and charged particles.**

Radiation damage: defects

Point defect

A displaced silicon atom produces an empty space in the lattice (**Vacancy, V**) and in another place an atom in an inter lattice space (**Interstitial, I**).

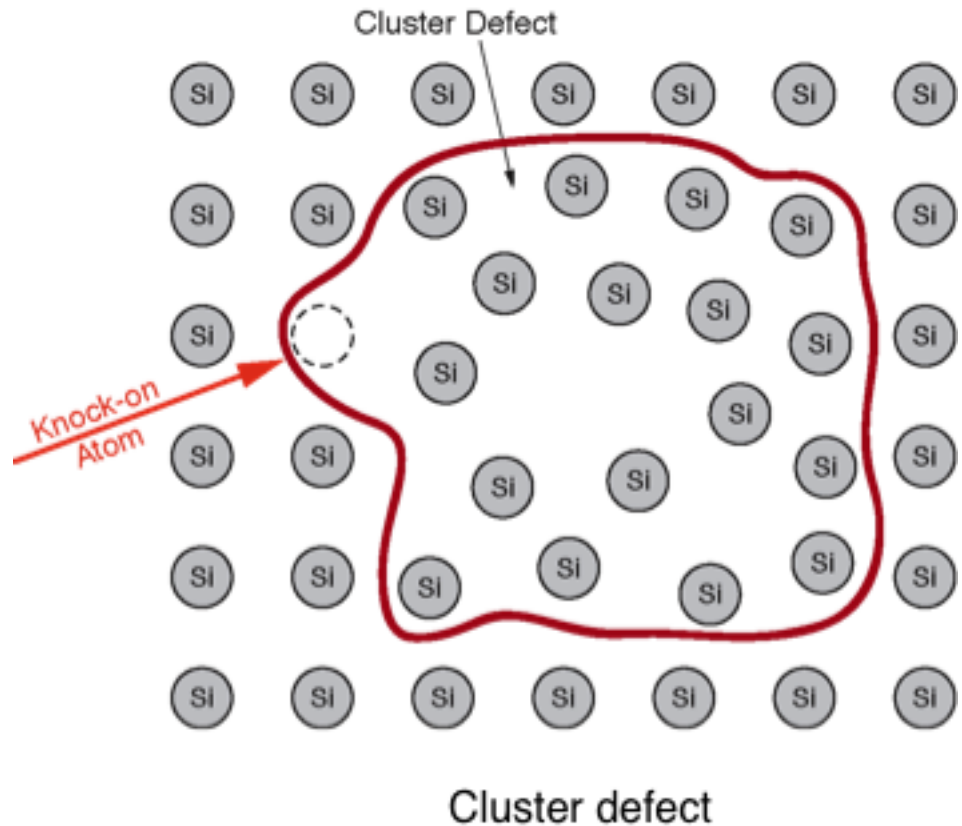
A vacancy-interstitial pair is called a **Frenkel-defect**.



Radiation damage: defects

Cluster defect

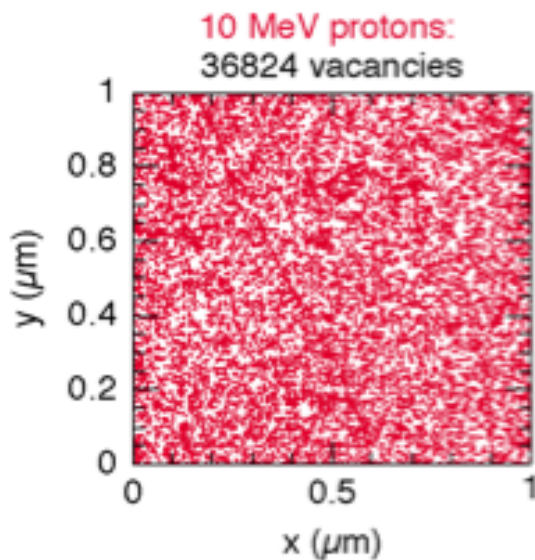
- In hard impacts the primary knock-on atom (PKA) displaces additional atoms. These defects are called cluster defects.
- The size of a cluster defect is approximately 5 nm and consists of about 100 dislocated atoms.
- For high energy PKA cluster defects appear at the end of the track when the atom loses the kinetic energy and the elastic cross section increases.



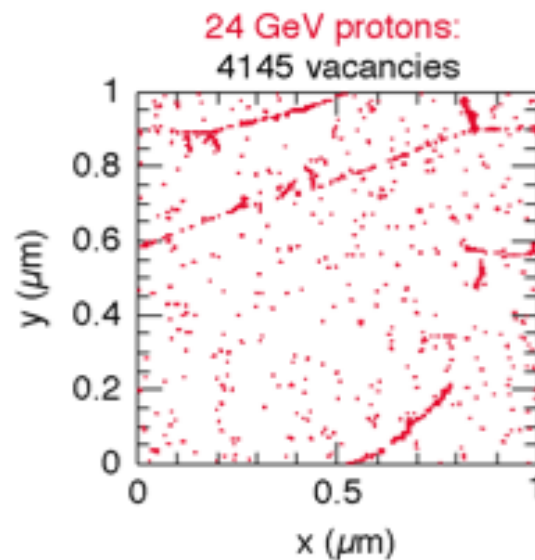
Radiation damage: defects

Type and frequency of defects depends on the particle type and the energy.

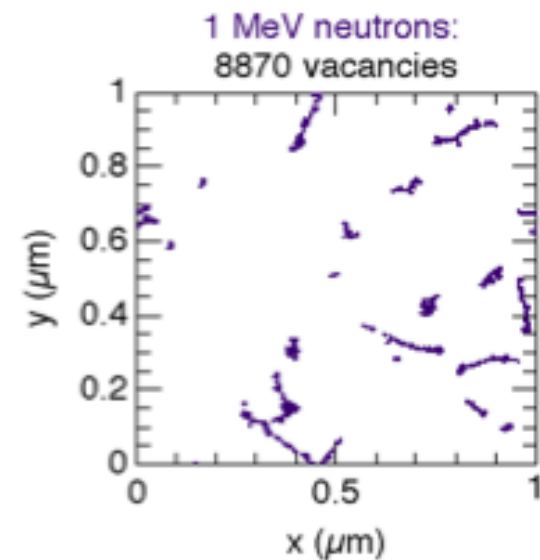
Plots below show a simulation of vacancies in 1 μm thick material after an integrated flux of 10^{14} particles / cm^2 :



Many vacancies produced



Less vacancies, a significant part of the energy is consumed to produce cluster defects



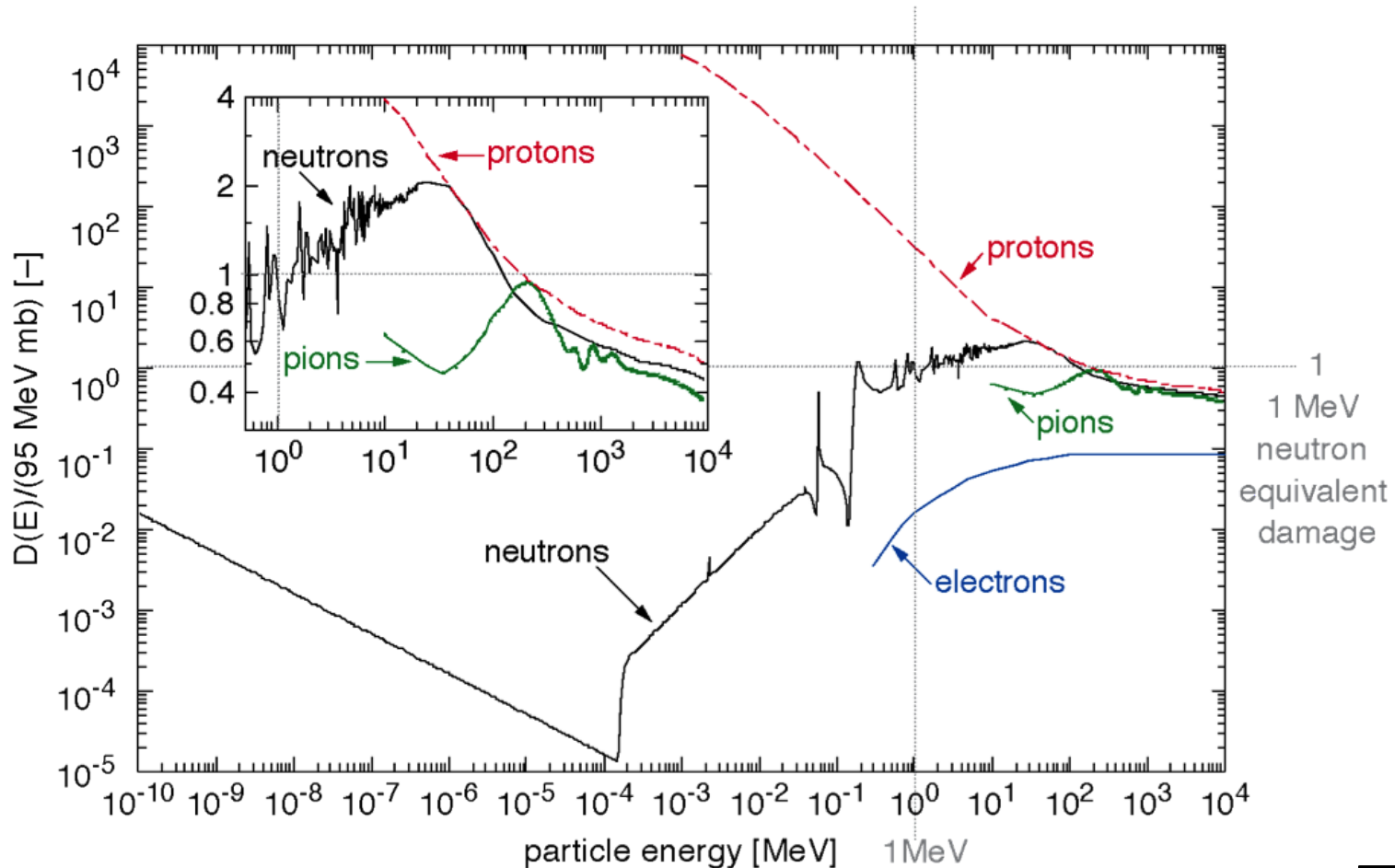
Very few vacancies, energy of the neutrons is used up to produce cluster defects.

M. Huhtinen, *Simulation of Non-Ionising Energy Loss and Defect Formation in Silicon*, Nucl. Instr. Meth. A **491**, 194 (2002)

Damage function

Displacement damage function (cross section) for various particles as function of their energy (Assumption: damage is proportional to the energy deposited into the displacement interaction)

$D(E)$ in the plot below is divided by 95 mb to be normalized to the damage caused by 1 MeV neutrons:

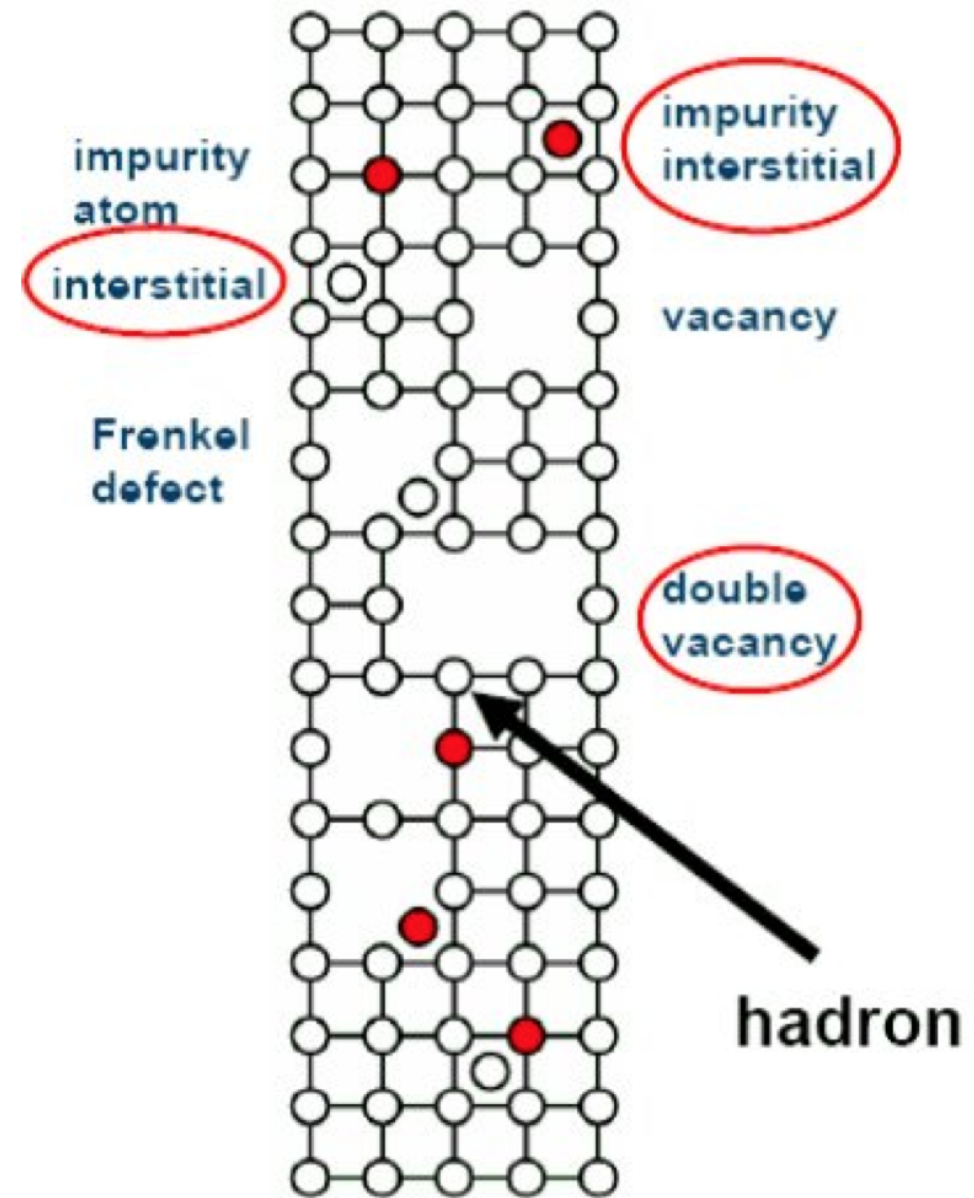


Annealing and secondary effects

- Interstitials and the position of vacancies are moving inside the crystal lattice and they are not stable defects.
- Some of the dislocated atoms may fall again into a regular lattice position. Both defects disappear! This effect is called annealing.

Annealing strongly depends on the temperature

- Some of these primary defects can combine with other defects to create immovable, stable **secondary defects**.

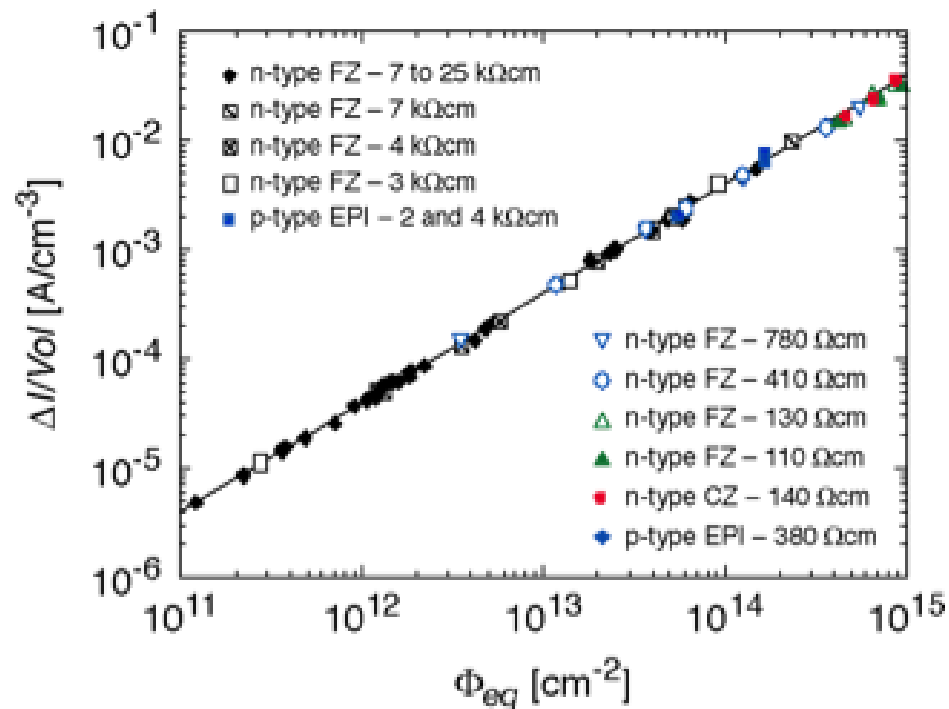


Leakage current

- Irradiation induced leakage current increases linearly with the integrated flux of radiation:

$$\frac{\Delta I}{Vol} = \alpha \cdot \phi_{eq}$$

- α is called the **current related damage rate**. It is largely independent of the material type. α depends on temperature, the time between exposure to radiation and measurement (annealing).



Increase of leakage current as function of irradiation fluence (different materials). Measurement after 80 minute annealing time at 60°C. The linear increase equals to $\alpha \approx 4 \cdot 10^{-17}$ A/cm.

In ten years of LHC operation the currents of the innermost layers increase by 3 orders of magnitude!

Change of effective doping concentration

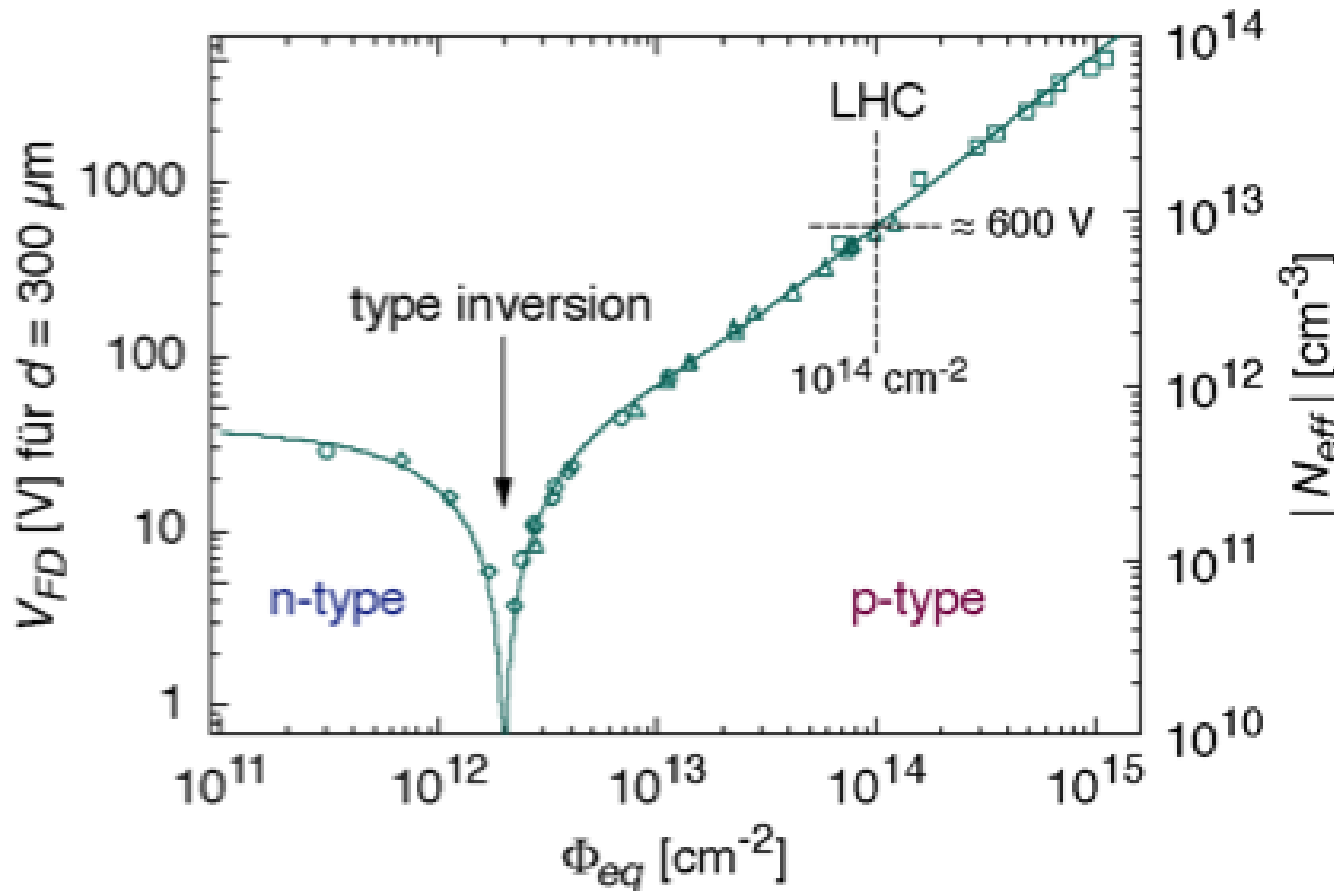
- The voltage needed to fully deplete the detector V_{FD} is directly related to the effective doping concentration:

$$V_{FD} = \frac{e}{2\epsilon_0\epsilon_r} |N_{eff}| d^2$$

- The irradiation produces mainly acceptor like defects and removes donor type defects. In a n type silicon the effective doping concentration N_{eff} decreases and after a point called **type inversion** (n type Si becomes p type Si) increases again.
 - The depletion voltage and consequently the minimum operation voltage decreases, and after the inversion point increases again.

Change of effective doping concentration

Full depletion voltage and effective doping concentration of an originally n type silicon detector as a function of the fluence Φ_{eq}

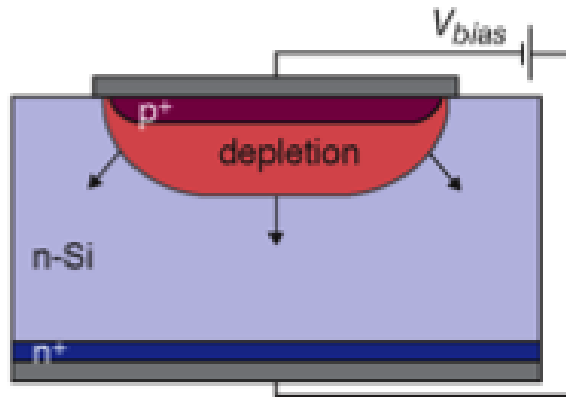


G. Lindström, *Radiation Damage in Silicon Detectors*, Nucl. Instr. Meth. A **512**, 30 (2003)

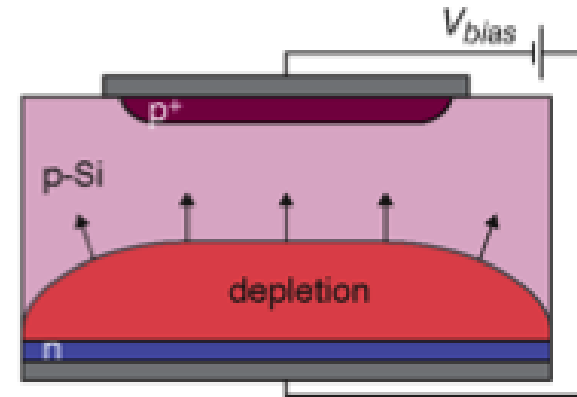
Operation before and after type inversion

- In n type sensors with p⁺ implants the depletion zone grows from the p⁺ implants to the backplane n⁺ implant. After type inversion the p⁺ bulk is now depleted from the backside → **polarity of bias voltage remains the same!**

Unirradiated detector:



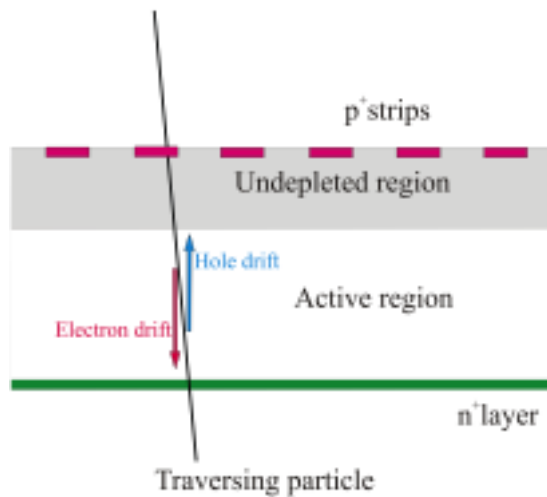
Detector after type inversion:



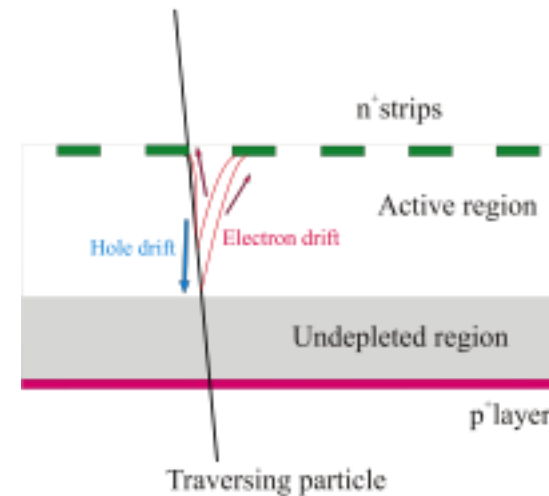
- n-type detectors before type inversion can be operated below full depletion. After type inversion, the depletion zone has to reach the strips. (A possible solution is to use n+p or n+n detectors)

Operation before and after type inversion

p⁺ n after high fluences
n-type silicon is type inverted



n⁺ p after high fluences
p-type silicon remains p-type



In case the detector has to be operated under-depleted:

- Charge spread – degraded resolution
- Charge loss – reduced CCE
- Limited loss in CCE
- Less degradation with under-depletion
- Collect electrons (faster than holes)

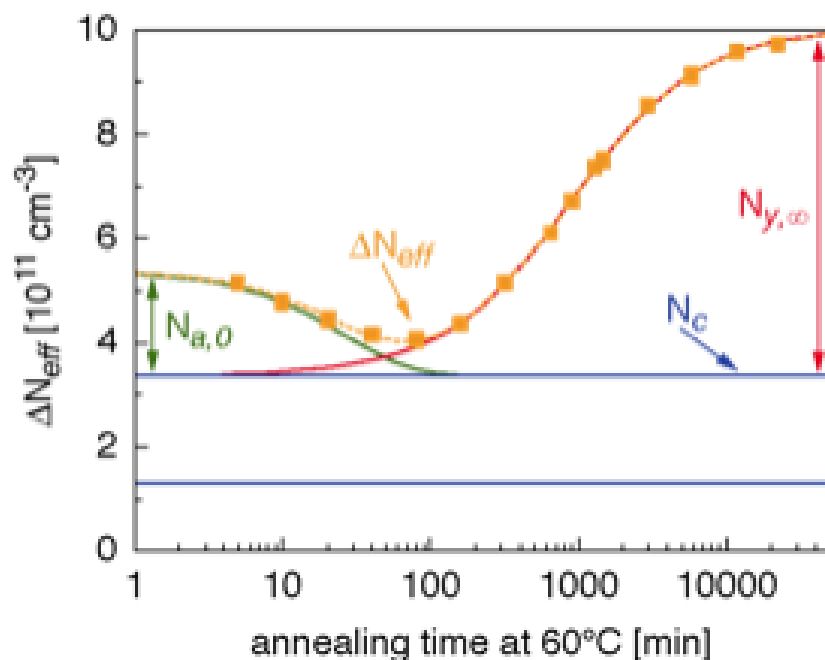
n⁺ p sensors baseline for ATLAS and CMS upgrade detectors.

Instead of n⁺ p also n⁺n devices could be used, but requires double sided processing.

Annealing and reverse annealing

- The effect of annealing is also seen in the development of the effective doping concentration and the full depletion voltages.
- After some time the annealing process inverts and secondary defects develop and worsen the radiation damage with time **reverse annealing**.

Long time dependence of $\Delta N_{eff}(t)$ of a silicon detector irradiated with a fluence of $\Phi_{eq} = 1.4 \cdot 10^{13} \text{ cm}^{-2}$ and storage at a temperature of $T = 60^\circ\text{C}$:



- N_c ... Contribution of stable primary defects
- N_a ... Defects disappearing with time – annealing.
- N_y ... Secondary defects developing with time – reverse annealing.

Operating temperature

- Annealing and reverse annealing are strongly depending on temperature. Both effects increase with temperature.
- Annealing and reverse annealing overlap in time and develop with different time constants.

In an operating experiment (detectors under radiation) the operating temperature of the silicon is a compromise between beneficial annealing and deteriorating reverse annealing.

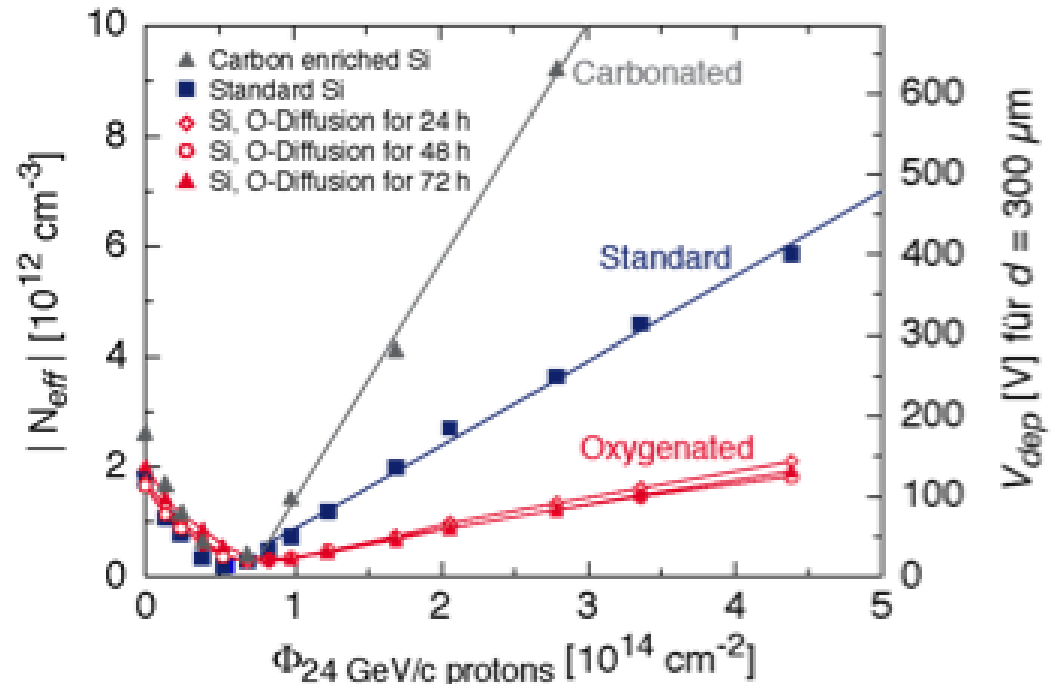
- N_{eff} is relatively stable below a temperature of -10°C .
- The CMS silicon tracker is operated at a temperature of -10°C .
- An irradiated detector has to remain cooled down even in non operating periods.

Material engineering

- Introduction of impurity atoms, initially electrically neutral, can combine to secondary defects and modify the radiation tolerance of the material.
- Silicon enriched with carbon makes the detector less radiation hard.
- **Oxygen enriched silicon** (e.g. Magnet Czochralski Si) has proven to be more radiation hard with respect to charged hadrons (no effect for neutrons)

Oxygen enriched Si used for pixel detectors in ATLAS and CMS.

Influence of C and O enriched silicon on the full depletion voltage and the effective doping concentration (Irradiation with 24 GeV protons, no annealing):



Surface defects

- In the amorphous oxide dislocation of atoms is not relevant. However, ionizing radiation creates charges in the oxide.
- Within the band gap of amorphous oxide (8.8 eV compared to 1.12 eV in Si) a large number of deep levels exist which trap charges for a long time.
- The mobility of electrons in SiO_2 is much larger than the mobility of holes
 - electrons diffuse out of the oxide, holes remain semi permanent fixed
 - the oxide becomes positively charged due to these fixed oxide charges.
- Consequences for the detector:
 - Reduced electrical separation between implants
 - Increase of interstrip capacitance
 - Increase of detector noise
 - Worsening of position resolution
 - Increase of surface leakage current

Surface defects

- The read out electronics is equally based on silicon and SiO_2 structures.
- Read out electronics is based on surface structures (e.g. MOS process) and hence very vulnerable to changes in the oxide.
- The front end electronics is mounted close to the detector and experiences equal radiation levels.

Radiation damage is a very critical issue also for the readout electronics!

Radiation damage: summary

- Silicon detectors are very radiation tolerant
- The defect introduced by radiation change significantly the properties of the detectors
- As long as the bias voltage can follow the development of the full depletion voltage (voltage remains below break down voltage) and the effect of increased leakage current can be controlled (cooling) the detector remains functional.
- Charge trapping, increase of capacitance and leakage current, etc. worsen the performance of the detector gradually.
- The radiation tolerance can be improved by the design of the detector structures, the use of oxygenated silicon, or the development of detectors based on alternative materials (diamond).